SPECTRAL STABILITY OF NONLINEAR WAVES

IN DYNAMICAL SYSTEMS

SPECTRAL STABILITY OF NONLINEAR WAVES IN DYNAMICAL SYSTEMS

BY
MARINA CHUGUNOVA, B.Sc., M.Sc.

A Thesis
Submitted to the School of Graduate Studies
in Partial Fulfillment of the Requirements
for the Degree
Doctor of Philosophy

McMaster University

DOCTOR OF PHILOSOPHY (2007)
(Mathematics)

McMaster University
Hamilton, Ontario

TITLE:	Spectral Stability of Nonlinear Waves in Dynamical Systems
AUTHOR:	Marina Chugunova B.Sc., M.Sc. (Moscow Institute of Physics and Technology , Russia)
SUPERVISOR:	Professor Dmitry Pelinovsky
NUMBER OF PAGES:	X, 129

Abstract

Partial differential equations that conserve energy can often be written as infinite-dimensional hamiltonian systems of the following general form: $\frac{du}{dt} = JE'(u(t)), \quad u(t) \in X$ where: $J : X \to X$ is a symplectic matrix and $E : X \to R$ is a C^2 functional defined on some Hilbert space X. A critical point of this equation is a point $\phi \in X$ such that $E'(\phi) = 0$.

We investigate the spectral stability of solutions in a neighborhood of the critical point by using the linearized Hamiltonian system $\frac{dv}{dt} = JE''(\phi)v$. The main objective of this thesis is to develop analysis of the spectral properties of the non-self-adjoint operator $JE''(\phi)$ using the Pontryagin space decomposition. We adopt parallel computations on Sharcnet clusters to study eigenvalues and eigenvectors of $JE''(\phi)$ numerically.

The structure of the thesis is as follows. The brief introduction to the spectral stability theory is given in Chapter 1. Count of spectrally unstable eigenvalues of the linearized Hamiltonian system using the indefinite metric approach is given in Chapter 2. This chapter with general theory is followed by case study of three particular problems where applications of analysis are interwinded with numerical approximations. In Chapter 3, we analyze spectral stability of double-hump solitary wave solutions of the fifth-th order Korteweg–de Vries equation. In Chapter 4, we deal with the coupled-mode system of the Dirac type, where the linearized operators can be block-diagonalized for analytical and numerical studies. In Chapter 5, we study the spectrum of the singular differential operator $L = \partial_\theta + \epsilon\partial_\theta(\sin\theta\partial_\theta)$ subject to the periodic boundary conditions on $\theta \in [-\pi, \pi]$. We prove that the set of linearly independent eigenfunctions for isolated simple purely imaginary eigenvalues is complete but does not form a basis in $H^1_{\rm per}([-\pi, \pi])$. In the concluding Chapter 6, we summarize all our results and formulate a list of open questions for further research.

Acknowledgements

I thank my advisor Dmitry Pelinovsky. From the day I became a graduate student in McMaster University, he has inspired and taught me the powerful tools of applied mathematics. He has provided me with invaluable physical insight and guidance. Being a spectral analysis theorist, I have been deeply impressed by the fact that physical reality provides such amazing, interesting, and infinite stream of problems.

I thank Bartosz Protas and Nicholas Kevlahan for their introduction to the parallel programming on Sharcnet clusters and suggestions on the choices of numerical methods. I have enjoyed physical and mathematical discussions with Walter Craig and Andrey Biryuk. They have informed much of my analytical results in the thesis. Special thanks is due to Tomas Azizov, who has made a number of helpful corrections in applications of the indefinite metric theory.

To all my friends, family, my life has been enriched by your presence. Thank you all for your help and support. I wish you all peace and happiness.

To my parents with deep respect and love

CONTENTS

List of Figures

CHAPTER 1

INTRODUCTION

1.1 The organization of the thesis

Chapter 1 gives a brief introduction to solitary wave solutions of nonlinear PDEs, to the spectral stability theory and a review of different numerical approaches.

Chapter 2 develops the count of isolated and embedded eigenvalues in a generalized eigenvalue problem defined by two self-adjoint operators with a positive essential spectrum and a finite number of isolated eigenvalues. This generalized eigenvalue problem determines spectral stability of nonlinear waves in a Hamiltonian dynamical system. The theory is based on Pontryagin's Invariant Subspace theorem in an indefinite inner product space but it extends beyond the scope of earlier papers of Pontryagin, Krein, Grillakis, and others. In particular, we prove the following three main original results:

(i) the number of unstable and potentially unstable eigenvalues of the generalized eigenvalue problem $Au = \gamma Ku$ *equals* the number of negative eigenvalues of the self-adjoint operators A and K^{-1},

(ii) the total number of isolated eigenvalues of the generalized eigenvalue problem $Au = \gamma Ku$ is *bounded from above* by the total number of isolated eigenvalues of the self-adjoint operators A and K^{-1},

(iii) the quadratic forms defined by the two self-adjoint operators A and K^{-1} are *strictly positive* on the subspace related to the continuous spectrum of the generalized eigenvalue problem $Au = \gamma Ku$.

Applications of general theory are developed for three examples: solitons and vortices of the nonlinear Schrödinger equations and solitons of the Korteweg–De Vries equations.

Chapter 3 deals with the existence and stability of two–pulse solutions in the fifth-order Korteweg–de Vries (KdV) equation. Two new results are obtained:

(i) the Petviashvili method of successive iterations is developed for numerical (spectral) approximations of the two-pulse solitons and convergence of the iterations is proved in a neighborhood of the solutions,

(ii) structural stability of embedded eigenvalues of negative Krein signature is proved in a context of a linearized KdV equation.

Combined with stability analysis in Pontryagin spaces from the second chapter, the new results complete the proof of spectral stability of the corresponding two-pulse solutions. Eigenvalues of the linearized problem are approximated numerically in exponentially weighted spaces where embedded eigenvalues are isolated from the continuous spectrum. Approximations of eigenvalues and full numerical simulations of the fifth-order KdV equation confirm stability of two-pulse solutions related to the minima of the effective interaction potential and instability of two-pulse solutions related to the maxima points.

Chapter 4 considers the Hamiltonian coupled-mode system that occur in nonlinear optics, photonics, atomic physics, and general relativity. Spectral stability of gap solitons is determined by eigenvalues of the linearized coupled-mode equations, which are equivalent to a four-by-four Dirac system with sign-indefinite metric. Our main result is:

(i) the block-diagonal representation of the linearized coupled-mode equations is constructed to reduce the spectral problem to two coupled two-by-two Dirac systems.

This block-diagonalization is used in numerical computations of eigenvalues that determine stability of gap solitons.

Chapter 5 studies the spectrum of the linear operator $L = -\partial_\theta - \epsilon\partial_\theta(\sin\theta\partial_\theta)$ subject to the periodic boundary conditions on $[-\pi, \pi]$. Our three main results are:

(i) the operator L admits the closure in $L^2([-\pi,\pi])$ with the domain in $H^1_{\rm per}([-\pi,\pi])$ for $|\epsilon| < 2$,

(ii) the spectrum of the operator L consists of an infinite sequence of isolated eigenvalues with accumulation point at infinity,

(iii) the set of eigenfunctions of the operator L is complete in $L^2_{\rm per}([-\pi,\pi])$.

By using numerical approximations of eigenvalues and eigenfunctions, we show that all eigenvalues are simple, located on the imaginary axis and the angle between two subsequent eigenfunctions tends to zero for larger eigenvalues. As a result, the complete set of linearly independent eigenfunctions does not form a basis in $L^2_{\rm per}([-\pi,\pi])$.

Chapter 6 summarizes the main results and states open questions for further research.

1.2 Nonlinear waves and solitons

Solitary waves or solitons are localized travelling wave solutions of nonlinear PDEs, resulting from a certain balance of dispersive and nonlinear effects. A variety of examples

exists in the natural science. A solitary wave was first observed by J. Scott Russell in 1834 while riding on horseback beside the narrow Union canal near Edinburgh, Scotland. He described his observation as follows:

"I was observing the motion of a boat which was rapidly drawn along a narrow channel by a pair of horses, when the boat suddenly stopped - not so the mass of water in the channel which it had put in motion; it accumulates round the prow of the vessel in a state of violent agitation, then suddenly leaving it behind, rolled forward with great velocity, assuming the form of a large solitary elevation, a rounded, smooth and well defined heap of water, which continued its course along the channel apparently without change of form or diminution of speed. I followed it on horseback, and overtook it still rolling on at a rate of some eight or nine miles an hour, preserving its original figure some thirty feet long and a foot to a foot and a half in height. Its height gradually diminished, and after a chase of one or two miles I lost it in the windings of the channel. Such, in month of August 1834, was my first chance interview with that rare and beautiful phenomenon which I have called the Wave of Translation... "

Further investigations were undertaken by G.B. Airy [1845], G.G. Stokes [1847], J.V. Boussinesq [1871] and B. Rayleigh [1876] in an attempt to understand this phenomenon. J.V. Boussinesq derived a one-dimensional nonlinear evolution equation, which now bears his name, in order to obtain an approximate description of the solitary wave.

Soliton collisions were studied by the computer experimentation in the 1960s by M. Kruskal and N. Zabusky [126]. The experiment can be described as follows. If we start with two solitons, the faster one will overtake the slower one and, after a complicated nonlinear interaction, the two solitons will emerge unchanged as they move, except for a slight delay. This kind of behaviour is expected for linear problems since each eigenfunction evolves separately, but that it could happen for a nonlinear problem was a complete surprise at that time.

The development of the mathematical theory of solitons started from the works of P. Lax [83], V. Zakharov and A. Shabat [127], M.J. Ablowitz, D.J. Kaup, A.C. Newell and H. Segur [1]. In parallel, optical solitons were independently predicted and experimentally realized in 1980 [90].

The easiest way to describe an optical soliton is using the spatial domain, where it is simply a self-guided wave. Consider an optical beam as narrow as 5 microns. If such a beam propagates in a linear medium it diffracts and broadens after even a short 1mm distance. In a nonlinear material light actually changes the index of refraction of the medium in which it propagates, leading to self-focusing. This self-focusing competes with diffractive effects, and at sufficient intensities can lead to the development of a structure for which diffraction and self-focusing exactly balance to create a soliton. The field of optical solitons has greatly developed over the past decade, and they have become a promising candidate for optical communication networks.

Typical examples of nonlinear partial differential equations that have soliton so-

lutions include the Korteweg-de Vries equation, the nonlinear Schrödinger equation, the coupled-mode Dirac equations, and the sine-Gordon equation. Soliton solutions of nonlinear partial differential equations have arisen in a number of physical contexts: water waves, collision-free hydromagnetic waves, plasma physics, non-linear optics, lattice dynamics, ion-acoustic waves (for details and further references see, for example: M.J. Ablowitz and H. Segur [2]; S.P. Novikov, S.V. Manakov, L.P. Pitaevskii and V.E. Zakharov [91])

1.3 Spectral stability problems

Partial differential equations that conserve energy can often be written as infinite-dimensional Hamiltonian systems. We investigate the spectral stability of critical points of such systems by using the linearization. We call the critical point spectrally stable if the whole spectrum of the linearized energy operator lies in the closed left complex half plane. Spectral stability is the necessary condition for the Lyapunov stability.

Spectral stability of solitary waves has been studied extensively in the recent past. The first stability instability theorem for a scalar NLS equation was proved by J. Shatah, W. Strauss [59] and M. Weinstein [122]. Their result was restricted to the case when the linearized energy operator had not more than one negative eigenvalue and method was based on the variational structure of the problem. More general approach (for the case of a finite number of negative eigenvalues) was developed in [60]. This work was followed by the work of M. Grillakis [62] who derived existence criteria of an eigenvalue of linearized energy operator with strictly positive real part in terms of the difference in the number of negative eigenvalues of two self-adjoint operators L_+ and L_- which diagonalize this operator.

In many problems, stability of equilibrium points in a finite–dimensional Hamiltonian system of finitely many interacting particles is determined by the eigenvalues of some generalized eigenvalue problem [49],

$$A\mathbf{u} = \gamma K\mathbf{u}, \qquad \mathbf{u} \in \mathbb{R}^n, \tag{1.1}$$

where A and K are symmetric matrices in $\mathbb{R}^{n\times n}$ which define the quadratic forms for potential and kinetic energies, respectively. The eigenvalue γ corresponds to the normal frequency $\lambda = i\omega$ of the normal mode of the linearized Hamiltonian system near the equilibrium point, such that $\gamma = -\lambda^2 = \omega^2$. The equilibrium point is unstable if there exists an eigenvalue γ such that $\gamma < 0$ or $\Im(\gamma) \neq 0$. Otherwise, the system is spectrally stable. Moreover, the equilibrium point is a minimizer of the Hamiltonian if all eigenvalues γ are positive and semi-simple and the quadratic forms for potential and kinetic energies evaluated at eigenvectors of $Au = \gamma Ku$ are strictly positive.

The eigenspace corresponding to a given eigenvalue is the vector space of all its eigenvectors. The geometric multiplicity of an eigenvalue is the dimension of the associated eigenspace. The generalized eigenspace is the vector space of all eigenvectors and

generalized eigenvectors corresponding to the eigenvalue. The algebraic multiplicity is the dimension of the associated generalized eigenspace. When the matrix K is positive definite, all eigenvalues γ are real and semi-simple (that is the geometric and algebraic multiplicities coincide). By the Sylvester's Inertia Law theorem [50], the numbers of positive, zero and negative eigenvalues of the generalized eigenvalue problem $Au = \gamma Ku$ *equal to* the numbers of positive, zero and negative eigenvalues of the matrix A.

In our context, the Hamiltonian system is infinite dimensional as it represents a nonlinear PDE, while the critical points of the system are solitary wave solutions. In many PDE problems, a linearization of the nonlinear system at the spatially localized solution results in the generalized eigenvalue problem of the form $Au = \gamma Ku$, where A and K^{-1} are self-adjoint operators on a complete infinite-dimensional metric space (Hilbert space). This generalized eigenvalue problem can be studied using the Pontryagin space Π_κ where the index κ equals to the number of negative eigenvalues of the operators A or K^{-1} .

The indefinite metric space Π_1 (that is with the index $\kappa = 1$) was first introduced by S.L. Sobolev in 1940's when he studied the rotating shallow water model. S.L. Sobolev sparked the interest of L.S. Pontryagin who wrote a pioneer article "Hermitian operators in spaces with indefinite metric" in 1944. This Pontryagin's result started the new branch of the functional analysis - theory of linear operators in indefinite metric space.

Most of fundamental results in this theory were obtained by M.G. Krein in 1960's: axiomatic approach to the Pontryagin space Π_κ, spectral theory of unitary and self-adjoint operators acting in Pontryagin space, sign definite invariant subspaces of these operators, bifurcation theory. M.G. Krein also described application of this indefinite matric spectral analysis to the problem of oscillations of heavy viscous fluid in the open motionless vessel (the most complete list of references can be found in [8, 67]). The spectral properties and sign definite invariant subspaces of dissipative and contractive operators acting in the spaces with indefinite metric were studied in 1980's by T. Azizov and I.S. Iohvidov [8].

There has been recently a rapidly growing sequence of publications on mathematical analysis of the spectral stability problem in the context of nonlinear Schrödinger equations [37, 70, 97]. Besides predictions of spectral stability or instability of spatially localized solutions in Hamiltonian dynamical systems, linearized Hamiltonian systems are important in analysis of orbital stability [59, 60, 33], asymptotic stability [105, 107, 36], stable manifolds [32, 112], and blow-up of solutions in nonlinear equations [104, 80].

1.4 Numerical methods in nonlinear PDEs.

Both spectral and nonlinear stability of a critical point in a dynamical system can be investigated numerically.

To solve a spectral stability problem, the eigenvalues of the operator $JE''(\phi)$ can be found by the Fourier basis decomposition and the Galerkin approximation. Although

this is a very robust numerical method it may also result in spurious unstable eigenvalues originated from the continuous spectrum as it was found for the coupled mode Dirac system in [9, 10]. A delicate but time-consuming implementation of the continuous Newton method was developed to identify the "right" unstable eigenvalues from the spurious ones [9, 10]. Similar problems were discovered in the variational method [76, 77] and in the numerical finite-difference method [114, 115]. To analyse the bifurcations from the edge of the continuous spectrum, however the more accurate method of the discretization should be applied. A new progress on computations of eigenvalues in the coupled-mode system was made with the use of exterior algebra in the numerical computations of the Evans function [41].

Another approach is the discretization of the linear differential operator $JE''(\phi)$ using approximation of derivatives by the differentiation matrices. It is a very useful tool to convert a two-point boundary eigenvalue problem to a matrix eigenvalue problem [22, 44]. Differentiation matrices are derived from a spectral collocation method. In this method, an unknown solution to the differential equation is expanded as a global interpolant, such as trigonometric or polynomial functions [45, 58]. In other methods, such as finite elements or finite differences, the underlying expansions involves local interpolants such as piecewise polynomials. In practice that means that the accuracy of the spectral methods is superior: for problems with smooth solutions convergence rates of $O(e^{-cn})$ or $O(e^{-c\sqrt{n}})$ are routinely achieved, where n is the number of grid nodes. In contrast, finite difference or finite elements yield convergence rates that are only algebraic in n, typically $O(n^{-2})$ or $O(n^{-4})$.

The negative side of using spectral methods instead of finite differences or finite elements is replacing sparse matrices by full matrices that leads to the significant increase of the computational time. Partially this long-computational-time problem can be solved by means of parallel software libraries (Scalapack) which were recently developed for computations of large eigenvalue problems [54]. Distribution of computations of eigenvalues for different parameter values between parallel processors can be implemented by using Message Passing Interface [30].

To solve a nonlinear stability problem, a slightly perturbed spectrally stable critical point ϕ can be used as an initial value of the nonlinear dynamical problem. A split-step method can be used to discretize the time variable of the partial differential equation and the finite-difference or Fourier methods can be used to discretize space variable [121]. Although this method is robust and widely used, it does not solve the stiffness problem, which arises in the higher-order weakly nonlinear partial differential equations such as the fifth-order KdV equation with cubic nonlinearity. The reason why the problem is stiff can be explained by different scales associated with linear and nonlinear components of the equation. The linear part involves a huge range of scales from the very slow to the very fast, while the effects of nonlinearity are significant only over long time intervals and couple the various linear modes. The problem can be eliminated by numerical pseudo-

spectral method which is described in details in [89]. The method is based on the explicit analytical integration of the linear part of the equation, through an integrating factor. The fourth-order Runge-Kutta method can be used to integrate the evolution equation in time. The greatest advantage of this numerical method is that no stability restriction arising from the linear part of the partial differential equation is posed on the timestep of the numerical integration scheme.

CHAPTER 2

SPECTRAL ANALYSIS OF LINEARIZED HAMILTONIAN SYSTEMS USING THE PONTRYAGIN SPACE DECOMPOSITION.

2.1 Introduction

Nonlinear partial differential equations that conserve energy can often be written as infinite-dimensional Hamiltonian systems in the following general form:

$$\frac{du}{dt} = JE'(u(t)), \quad u(t) \in \mathcal{X}, \tag{2.1.1}$$

where $J : \mathcal{X} \to \mathcal{X}$ is a symplectic operator with the property $J^* = -J$ and $E : \mathcal{X} \to \mathbb{R}$ is a C^2 functional defined on some Hilbert space $\mathcal{X}$. A critical point $\phi \in \mathcal{X}$ of the Hamiltonian functional E, such that $E'(\phi) = 0$, represents a localized solution of the nonlinear partial differential equation. The spectral stability of a localized solution ϕ is defined by the spectrum of the non-self-adjoint eigenvalue problem

$$JE''(\phi)v = \lambda v, \quad v \in \mathcal{X}, \tag{2.1.2}$$

which is obtained after a linearization of the Hamiltonian system (4.2.6). Although the operator $JE''(\phi)$ is non-self-adjoint, it is related to the self-adjoint operator $E''(\phi)$ by multiplication of the symplectic operator J. In many specific examples, such as the nonlinear Schrödinger and Korteweg–de Vries equations, the non-self-adjoint eigenvalue problem (2.1.2) can be rewritten as the generalized eigenvalue problem

$$Aw = \gamma Kw, \qquad w \in \mathcal{X}, \tag{2.1.3}$$

where A and K are self-adjoint operators in the Hilbert space $\mathcal{X}$ and $\gamma = -\lambda^2$. The critical point ϕ is said to have an unstable eigenvalue γ if $\gamma < 0$ or $\mathrm{Im}(\gamma) \neq 0$. Otherwise, the critical point is weakly spectrally stable. Moreover, it is a minimizer of the Hamiltonian functional $E(\phi)$ if all eigenvalues γ are positive and the quadratic forms $(A\cdot, \cdot)$ and $(K\cdot, \cdot)$ evaluated at the eigenvectors of the generalized eigenvalue problem (2.1.3), are strictly positive.

The main purpose of this chapter to develop analysis of the generalized eigenvalue problem 2.1.3 in infinite dimensions by using the Pontryagin space decomposition [106]. The theory of Pontryagin spaces was developed by M.D. Krein and his students (see books [8, 53, 67]) and partly used in the context of spectral stability of solitary waves by R. MacKay [86], M. Grillakis [62], and V. Buslaev & G. Perelman [21] (see also a recent application in [64]). We shall give an elegant geometric proof of the Pontryagin's Invariant Subspace theorem.We shall give an elegant geometric proof of Pontryagin's Invariant Subspace Theorem and then apply this theorem to establish our main results:

(i) the number of unstable and potentially unstable eigenvalues of the generalized eigenvalue problem (2.1.3) *equals* the number of negative eigenvalues of the self-adjoint operators A and K^{-1},

(ii) the total number of isolated eigenvalues of the generalized eigenvalue problem (2.1.3) is *bounded from above* by the total number of isolated eigenvalues of the self-adjoint operators A and K^{-1},

(iii) the quadratic forms defined by the two self-adjoint operators A and K^{-1} are *strictly positive* on the subspace related to the continuous spectrum of the generalized eigenvalue problem (2.1.3).

The first result is a remake of the main results obtained in [37, 70, 97], although the method of proof presented therein is quite different than that given here. The second result gives a new inequality on the number of isolated eigenvalues of the generalized eigenvalue problem (2.1.3), which can be useful to control the number of neutrally stable eigenvalues in the gap of the continuous spectrum of the linearized operator associated with the stable localized solutions. The third result has a technical significance since it establishes a similarity between Sylvester's Inertial Law used in [97] and Pontryagin's space decomposition used here. With this construction, one can bypass the topological theory developed in [62] and used in [70].

The structure of this chapter is as follows. Main formalism of the generalized eigenvalue problem is described in *Section 2.2.* The Pontryagin Invariant Subspace theorem is proved in *Section 2.3.* Spectral properties of self adjoint operators acting in the Pontryagin space are studied in the *Section 2.4.* Main results on eigenvalues of the generalized eigenvalue problem are formulated and proved in *Section 2.5. Sections 2.6, 2.7 and 2.8* contain applications of the main results to solitons and vortices of the nonlinear Schrodinger equations and solitons of the Korteweg–De Vries equations.

2.2 Formalism and review of results

Let L_+ and L_- be two real-valued self-adjoint operators defined on a Hilbert space $\mathcal{X}$ with the inner product $(\cdot,\cdot)$. Our two assumptions on operators L_+ and L_- are listed here:

P1 The essential spectrum $\sigma_e(L_\pm)$ includes the absolute continuous part bounded from below by $\omega_+ \geq 0$ and $\omega_- > 0$ and finitely many embedded eigenvalues of finite multiplicities.

P2 The discrete spectrum $\sigma_d(L_\pm)$ in $\mathcal{X}$ includes finitely many isolated eigenvalues of finite multiplicities with $p(L_\pm)$ positive, $z(L_\pm)$ zero, and $n(L_\pm)$ negative eigenvalues[1].

We consider the linear eigenvalue problem defined by the self-adjoint operators $L_\pm$ in the form

$$L_+u = -\lambda w, \quad L_-w = \lambda u, \qquad u, w \in \mathcal{X}, \tag{2.2.1}$$

where $\lambda \in \mathbb{C}$. Under the assumptions P1–P2 the kernel $\ker L_-$ of the operator L_- is finite dimensional, the eigenvalue $\lambda = 0$ of this operator is isolated. It follows from above that the range of the operator $\operatorname{ran} L_- =: \mathcal{H}$ is closed. Let $\mathcal{P}$ be the orthogonal projection from $\mathcal{X}$ to $\mathcal{H}$, where $\mathcal{H}$ is the constrained Hilbert space

$$\mathcal{H} = \{u \in \mathcal{X} : \ u \perp \operatorname{Ker}(L_-)\}. \tag{2.2.2}$$

Since $\mathcal{P}u \in \operatorname{range}(L_-)$, then $\mathcal{P}w = \lambda \mathcal{P}L_-^{-1}\mathcal{P}u$ and

$$\mathcal{P}L_+\mathcal{P}u = -\lambda^2 \mathcal{P}L_-^{-1}\mathcal{P}u, \qquad u \in \mathcal{H}.$$

Therefore, the linear eigenvalue problem (2.2.1) in the Hilbert space $\mathcal{X}$ is rewritten as the generalized eigenvalue problem in the constrained space $\mathcal{H}$ as follows

$$Au = \gamma Ku, \qquad u \in \mathcal{H}, \tag{2.2.3}$$

where $A = \mathcal{P}L_+\mathcal{P}$, $K = \mathcal{P}L_-^{-1}\mathcal{P}$, and $\gamma = -\lambda^2$. We note that K is a bounded invertible self-adjoint operator on $\mathcal{H}$, while A is a generally unbounded non-invertible self-adjoint operator on $\mathcal{H}$. Finitely many isolated eigenvalues of the operators A and K^{-1} in $\mathcal{H}$ are distributed between negative, zero and positive eigenvalues away from the essential spectrum. By the spectral theory of self-adjoint operators, the Hilbert space $\mathcal{H}$ can be equivalently

[1]These indices can be zero and the corresponding subspaces can be empty. For instance, if $\omega_+ = 0$, then $p(L_+) = z(L_+) = 0$.

decomposed into two orthogonal sums of subspaces which are invariant with respect to the operators K and A:

$$\mathcal{H} = \mathcal{H}_K^- \oplus \mathcal{H}_K^+ \oplus \mathcal{H}_K^{\sigma_e(K)}, \tag{2.2.4}$$

$$\mathcal{H} = \mathcal{H}_A^- \oplus \mathcal{H}_A^0 \oplus \mathcal{H}_A^+ \oplus \mathcal{H}_A^{\sigma_e(A)}, \tag{2.2.5}$$

where notation $-(+)$ stands for negative (positive) isolated eigenvalues, 0 for the isolated kernel, and σ_e for the essential spectrum that includes the absolute continuous part and embedded eigenvalues. The subspaces $\mathcal{H}_A^+$ and $\mathcal{H}_A^0$ are empty if $\omega_+ = 0$, while $\sigma_e(A)$ belongs to the interval $[\omega_+, \infty)$. Since $\mathcal{P}$ is a projection defined by eigenspaces of L_- while $K = \mathcal{P}L_-^{-1}\mathcal{P}$, it is obvious that $\dim(\mathcal{H}_K^-) = n(L_-)$, $\dim(\mathcal{H}_K^+) = p(L_-)$, and $\sigma_e(K)$ belongs to the interval $(0, \omega_-^{-1}]$. The eigenvalues of A are related to the eigenvalues of L_+ according to the standard variational theory in constrained Hilbert spaces [60, 37]. The main result of this theory is formulated in the following proposition.

Proposition 2.1 *Let $\omega_+ > 0$, $\mathrm{Ker}(L_-) = \mathrm{Span}\{v_1, v_2, ..., v_n\} \in \mathcal{X}$, and define the matrix-valued function $M(\mu)$:*

$$\forall \mu \notin \sigma(L_+): \quad M_{ij}(\mu) = ((\mu - L_+)^{-1}v_i, v_j), \qquad 1 \le i, j \le n. \tag{2.2.6}$$

Let n_0, z_0, and p_0 be the number of negative, zero and positive eigenvalues of $M_0 = \lim_{\mu \uparrow 0} M(\mu)$[2]. Then,

$$\dim(\mathcal{H}_A^-) = n(L_+) - p_0 - z_0, \quad \dim(\mathcal{H}_A^0) = z(A) + z_0,$$

$$\dim(\mathcal{H}_A^+) \le p(L_+) + p_0 + z(L_+) - z(A). \tag{2.2.7}$$

Proof. According to the results of [37], all n eigenvalues of $M(\mu)$ are strictly decreasing functions of μ on the intervals $(-\infty, \omega_+)\backslash\sigma_d(L_+)$. These functions may have infinite jump discontinuities from minus infinity to plus infinity across the points of $\sigma_d(L_+)$ and have a uniform limit to minus zero as $\mu \to -\infty$. The count of jumps of the eigenvalues of $M(\mu)$ gives the count of eigenvalues of the constrained variational problem

$$(\mu - L_+)v = \sum_{j=1}^{n} \nu_j v_j, \qquad v \in \mathcal{H},\ \mu \in (-\infty, \omega_+), \tag{2.2.8}$$

where $(\nu_1, \nu_2, ..., \nu_n)$ are Lagrange multipliers. The first two equalities (2.2.7) are proved in Lemma 3.4 of [37] for the case $z(L_+) = z(A) = 0$ and in Theorem 2.9 of [37] for the case $z(L_+) \neq 0$. The last inequality (2.2.7) follows from the count of positive eigenvalues of

[2]Since L_+ is generally non-invertible, some eigenvalues of M_0 can be infinite if $z(A) \neq z(L_+)$ that is if $\mathrm{Ker}(L_+) \notin \mathcal{H}$. The numbers n_0, z_0, and p_0 denote *finite* eigenvalues of M_0, such that $n_0 + z_+ + p_0 \le n$.

the constrained variational problem (2.2.8), which originate from jumps of eigenvalues of $M(\mu)$ on $0 < \mu < \omega$ at $p(L_+)$ positive eigenvalues of L_+, from p_0 positive eigenvalues of M_0, and from $(z(L_+)-z(A))$ eigenvalues of $M(\mu)$ which have infinite jump discontinuities across $\mu = 0$. The upper bound in the last inequality is achieved if all limiting eigenvalues of $M_+ = \lim_{\mu\uparrow\omega_+} M(\mu)$ are either negative or diverge to negative infinity. ∎

Since A has finitely many negative eigenvalues and K has no kernel in $\mathcal{H}$, there exists a small number $\delta > 0$ in the gap $0 < \delta < |\sigma_{-1}|$, where σ_{-1} is the smallest (in absolute value) negative eigenvalue of $K^{-1}A$. The operator $A + \delta K$ is continuously invertible in $\mathcal{H}$ and the generalized eigenvalue problem (2.2.3) is rewritten in the shifted form,

$$(A + \delta K)u = (\gamma + \delta)Ku, \qquad u \in \mathcal{H}. \tag{2.2.9}$$

By the spectral theory, an alternative decomposition of the Hilbert space $\mathcal{H}$ exists for $0 < \delta < |\sigma_{-1}|$:

$$\mathcal{H} = \mathcal{H}^-_{A+\delta K} \oplus \mathcal{H}^+_{A+\delta K} \oplus \mathcal{H}^{\sigma_e(A+\delta K)}_{A+\delta K}, \tag{2.2.10}$$

where $\sigma_e(A + \delta K)$ belongs to the interval $[\omega_{A+\delta K}, \infty)$ and $\omega_{A+\delta K}$ is the minimum of $\sigma_e(A + \delta K)$. If $\omega_+ > 0$, then $\omega_{A+\delta K} > 0$ for sufficiently small $\delta \neq 0$. If $\omega_+ = 0$, we shall add the following assumption:

P3 If $\omega_+ = 0$, then $\omega_{A+\delta K} > 0$ for sufficiently small $\delta > 0$[3]. Moreover, $\dim(\mathrm{Ker}(A)) \leq 1$ and there exists at most one small negative eigenvalue $\mu(\delta)$ of $A + \delta K$, such that $\lim_{\delta\uparrow 0} \mu(\delta) = 0$.

We shall now introduce notations for particular eigenvalues of the generalized eigenvalue problem (2.2.3) and formulate our main results proved in this chapter. Let N_p^- (N_n^-), N_p^0 (N_n^0), and N_p^+ (N_n^+) be respectively the numbers of negative, zero, and positive eigenvalues γ of the generalized eigenvalue problem (2.2.3) with the account of their algebraic multiplicities whose eigenvectors are associated to the non-negative (non-positive) values of the quadratic form $(K\cdot, \cdot)$. The positive eigenvalues γ with $\gamma \geq \omega_+\omega_-$ are embedded into the continuous spectrum of the generalized eigenvalue problem (2.2.3). Finally, let N_{c^+} (N_{c^-}) be the number of complex eigenvalues in the upper (lower) half-plane $\gamma \in \mathbb{C}$, $\mathrm{Im}(\gamma) > 0$ ($\mathrm{Im}(\gamma) < 0$). Because A and K are real-valued operators, it is obvious that $N_{c^+} = N_{c^-}$.

Theorem 1 *Let assumptions P1–P3 be satisfied. Eigenvalues of the generalized eigenvalue problem (2.2.3) satisfy the following two equalities:*

$$N_p^- + N_n^0 + N_n^+ + N_{c^+} = \dim(\mathcal{H}^-_{A+\delta K}) \tag{2.2.11}$$

$$N_n^- + N_n^0 + N_n^+ + N_{c^+} = \dim(\mathcal{H}^-_K) \tag{2.2.12}$$

[3]The first statement of assumption P3 was recently proved for abstract operators A and K in [7].

Proof. The theorem is proved in Section 5. ∎

Corollary 2.2 *Let* $N_{\text{neg}} = \dim(\mathcal{H}^-_{A+\delta K}) + \dim(\mathcal{H}^-_K)$ *be the total negative index of the shifted generalized eigenvalue problem (2.2.9). Let* $N_{\text{unst}} = N_p^- + N_n^- + 2N_{c^+}$ *be the total number of unstable eigenvalues that includes* $N^- = N_p^- + N_n^-$ *negative eigenvalues* $\gamma < 0$ *and* $N_c = N_{c^+} + N_{c^-}$ *complex eigenvalues with* $\text{Im}(\gamma) \neq 0$. *Then,*

$$\Delta N = N_{\text{neg}} - N_{\text{unst}} = 2N_n^+ + 2N_n^0 \geq 0. \tag{2.2.13}$$

Proof. The equality (2.2.13) follows by the sum of (2.2.11) and (2.2.12). ∎

Theorem 2 *Let assumptions P1–P2 be satisfied and* $\omega_+ > 0$. *Let* $N_A = \dim(\mathcal{H}^-_A \oplus \mathcal{H}^0_A \oplus \mathcal{H}^+_A)$ *be the total number of isolated eigenvalues of* A. *Let* $N_K = \dim(\mathcal{H}^-_K \oplus \mathcal{H}^+_K)$ *be the total number of isolated eigenvalues of* K. *Isolated eigenvalues of the generalized eigenvalue problem (2.2.3) satisfy the inequality:*

$$N_p^- + N_p^0 + N_p^+ + N_{c^+} \leq N_A + N_K, \tag{2.2.14}$$

where N_p^+ *is counted from isolated positive eigenvalues* $\gamma < \omega_+\omega_-$.

Proof. This theorem is proved in Section 5. ∎

Corollary 2.3 *Let* $N_{\text{total}} = N_A + N_K$ *be the total number of isolated eigenvalues of operators* A *and* K. *Let* $N_{\text{isol}} = N_p^- + N_n^- + N_p^0 + N_n^0 + N_p^+ + N_n^+ + N_{c^+} + N_{c^-}$ *be the total number of isolated eigenvalues of the generalized eigenvalue problem (2.2.3). Then,*

$$N_{\text{isol}} \leq N_{\text{total}} + \dim(\mathcal{H}^-_K), \tag{2.2.15}$$

where N_p^+ *and* N_n^+ *are counted from isolated positive eigenvalues* $\gamma < \omega_+\omega_-$.

Proof. The inequality (2.2.15) follows by the sum of (2.2.12) and (2.2.14). ∎

To prove Theorems 1 and 2, we shall prove Pontryagin's Invariant Subspace Theorem and apply this theorem to the count of isolated and embedded eigenvalues for the non-self-adjoint operator $K^{-1}A$.

2.3 Pontryagin's Invariant Subspace Theorem

We develop here an abstract theory of Pontryagin spaces with sign-indefinite metric, where the main result is Pontryagin's Invariant Subspace Theorem.

Definition 3.1 *Let $\mathcal{H}$ be a Hilbert space equipped with the inner product $(\cdot,\cdot)$ and the sesquilinear form $[\cdot,\cdot]$[4]. The Hilbert space $\mathcal{H}$ is called the Pontryagin space (denoted as Π_κ) if it can be decomposed into the sum, which is orthogonal with respect to $[\cdot,\cdot]$,*

$$\mathcal{H} \doteq \Pi_\kappa = \Pi_+ \oplus \Pi_-, \tag{2.3.1}$$

where Π_+ is a Hilbert space with the inner product $(\cdot,\cdot) = [\cdot,\cdot]$, Π_- is a Hilbert space with the inner product $(\cdot,\cdot) = -[\cdot,\cdot]$, and $\kappa = \dim(\Pi_-) < \infty$.

Remark 3.2 We shall write components of an element x in the Pontryagin space Π_κ as a vector $x = \{x_-, x_+\}$. The orthogonal sum (2.3.1) implies that any non-zero element $x \neq 0$ is represented by two terms,

$$\forall x \in \Pi_\kappa : \quad x = x_+ + x_-, \tag{2.3.2}$$

such that

$$[x_+, x_-] = 0, \quad [x_+, x_+] > 0, \quad [x_-, x_-] < 0, \tag{2.3.3}$$

and $\Pi_+ \cap \Pi_- = \varnothing$.

Definition 3.3 *We say that Π is a non-positive subspace of Π_κ if $[x,x] \leq 0\ \forall x \in \Pi$. We say that Π is a maximal non-positive subspace if any subspace of Π_κ of dimension higher than $\dim(\Pi)$ is not a non-positive subspace of Π_κ. Similarly, we say that Π is a non-negative (neutral) subspace of Π_κ if $[x,x] \geq 0$ ($[x,x] = 0$) $\forall x \in \Pi$.*

Lemma 3.4 *The dimension of the maximal non-positive subspace of Π_κ is κ.*

Proof. By contradiction, we assume that there exists a $(\kappa+1)$-dimensional non-positive subspace $\tilde{\Pi}$. Let $\{e_1, e_2, ..., e_\kappa\}$ be a basis in Π_- in the canonical decomposition (2.3.2). We fix two elements $y_1, y_2 \in \tilde{\Pi}$ with the same projections to $\{e_1, e_2, ..., e_\kappa\}$, such that

$$\begin{aligned} y_1 &= \alpha_1 e_1 + \alpha_2 e_2 + ... + \alpha_\kappa e_\kappa + y_{1p}, \\ y_2 &= \alpha_1 e_1 + \alpha_2 e_2 + ... + \alpha_\kappa e_\kappa + y_{2p}, \end{aligned}$$

where $y_{1p}, y_{2p} \in \Pi_+$. It is clear that $y_1 - y_2 = y_{1p} - y_{2p} \in \Pi_+$ such that $[y_{1p} - y_{2p}, y_{1p} - y_{2p}] > 0$. On the other hand, $y_1 - y_2 \in \tilde{\Pi}$, such that $[y_1 - y_2, y_1 - y_2] \leq 0$. Hence, we have a contradiction, which is resolved only if $y_{1p} = y_{2p} = 0$. Therefore, $\tilde{\Pi}$ is still a κ-dimensional non-positive subspace of Π_κ. ∎

[4]We say that a complex-valued form $[u,v]$ on the product space $\mathcal{H} \times \mathcal{H}$ is a sesquilinear form if it is linear in u for each fixed v and linear with complex conjugate in v for each fixed u.

Lemma 3.5 (Cauchy-Schwartz) *Let Π be either non-positive or non-negative subspace of Π_κ. Then,*

$$\forall f, g \in \Pi: \quad |[f,g]|^2 \leq [f,f][g,g]. \tag{2.3.4}$$

Proof. The proof resembles that of the standard Cauchy–Schwartz inequality. Let Π be a non-positive subspace of Π_κ, Then, for any $f, g \in \Pi$ and any $\alpha, \beta \in \mathbb{C}$, we have

$$0 \geq [\alpha f + \beta g, \alpha f + \beta g] = [f,f]|\alpha|^2 + [f,g]\alpha\bar{\beta} + [g,f]\bar{\alpha}\beta + [g,g]|\beta|^2. \tag{2.3.5}$$

If $[f,g] = 0$, then inequality (2.3.4) is satisfied since $[f,f] \leq 0$ and $[g,g] \leq 0$. If $[f,g] \neq 0$, then we choose

$$\alpha \in \mathbb{R}, \quad \beta = \frac{[f,g]}{|[f,g]|},$$

such that inequality (2.3.5) becomes

$$0 \geq [f,f]\alpha^2 + 2\alpha|[f,g]| + [g,g].$$

The inequality is satisfied if the discriminant of the quadratic equation is non-positive such that $4|[f,g]|^2 - 4[f,f][g,g] \leq 0$, that is inequality (2.3.4). Let Π be a non-negative subspace of Π_κ. Then, for any $f, g \in \Pi$ and any $\alpha, \beta \in \mathbb{C}$, we have $[\alpha f + \beta g, \alpha f + \beta g] \geq 0$ and the same arguments result in the same inequality (2.3.4). ∎

Corollary 3.6 *Let Π be either non-positive or non-negative subspace of Π_κ. Let $f \in \Pi$ such that $[f,f] = 0$. Then $[f,g] = 0$, $\forall g \in \Pi$.*

Proof. The proof follows from inequality (2.3.4) since $0 \leq |[f,g]|^2 \leq 0$. ∎

Lemma 3.7 *Let Π be an invariant subspace of Π_κ with respect to operator T and $\Pi^\perp$ be the orthogonal compliment of Π in Π_κ with respect to $[\cdot,\cdot]$. Then, $\Pi^\perp$ is also invariant with respect to T.*

Proof. For all $f \in \mathrm{Dom}(T) \cap \Pi$, we have $Tf \in \Pi$. Let $g \in \mathrm{Dom}(T) \cap \Pi^\perp$. Then $[g, Tf] = [Tg, f] = 0$. ∎

Theorem 3 (Pontryagin) *Let T be a self-adjoint bounded operator in Π_κ, such that $[T\cdot,\cdot] = [\cdot, T\cdot]$. There exists a κ-dimensional, maximal non-positive, T-invariant subspace of Π_κ.*

Remark 3.8 There are historically two completely different approaches to the proof of this theorem. A proof based on theory of analytic functions was given by L.S. Pontryagin [106] while a proof based on angular operators was given by M.G. Krein [53] and later developed by students of M.G. Krein [8, 67]. Theorem 3 was rediscovered by M. Grillakis [62] with the use of topology. We describe a geometric proof of Theorem 3 based on Shauder's

Fixed Point Theorem. The proof uses the Cayley transformation of a self-adjoint operator in Π_κ to a unitary operator in Π_κ (Lemma 3.9) and the Krein representation of the maximal non-positive subspace of Π_κ in terms of a graph of the contraction map (Lemma 3.11). While many statements of our analysis are available in the literature, details of the proofs are missing. Our presentation gives full details of the proof of Theorem 3 (see [64] for a similar treatment in the case of compact operators).

Lemma 3.9 *Let T be a linear operator in Π_κ and $z \in \mathbb{C}$, $\mathrm{Im}(z) > 0$ be a regular point of the operator T, such that $z \in \rho(T)$. Let U be the Cayley transform of T defined by $U = (T - \bar{z})(T - z)^{-1}$. The operators T and U have the same invariant subspaces in Π_κ.*

Proof. Let Π be a finite-dimensional invariant subspace of the operator T in Π_κ. It follows from $z \in \rho(T)$ that $(T - z)\Pi = \Pi$ then $(T - z)^{-1}\Pi = \Pi$ and $(T - \bar{z})(T - z)^{-1}\Pi \subseteq \Pi$, i.e $U\Pi \subseteq \Pi$. Conversely, let Π be an invariant subspace of the operator U. It follows from $U - I = (z - \bar{z})(T - z)^{-1}$ that $1 \in \rho(U)$ therefore $\Pi = (U - I)\Pi = (T - z)^{-1}\Pi$. From there, $\Pi \subseteq \mathrm{dom}(T)$ and $(T - z)\Pi = \Pi$ so $T\Pi \subseteq \Pi$. ∎

Corollary 3.10 *If T is a self-adjoint operator in Π_κ, then U is a unitary operator in Π_κ.*

Proof. We shall prove that $[Ug, Ug] = [g, g]$, where $g \in \mathrm{dom}(U)$, by the explicit computation:

$$[Ug, Ug] = [(T - \bar{z})f, (T - \bar{z})f] = [Tf, Tf] - \bar{z}[f, Tf] - z[Tf, f] + |z|^2[f, f],$$
$$[g, g] = [(T - z)f, (T - z)f] = [Tf, Tf] - \bar{z}[f, Tf] - z[Tf, f] + |z|^2[f, f],$$

where we have introduced $f \in \mathrm{dom}(T)$ such that $f = (T - z)^{-1}g$. ∎

Lemma 3.11 *A linear subspace $\Pi \subseteq \Pi_\kappa$ is a κ-dimensional non-positive subspace of Π_κ if and only if it is a graph of the contraction map $\mathcal{K} : \Pi_- \to \Pi_+$, such that $\Pi = \{x_-, \mathcal{K}x_-\}$ and $\|\mathcal{K}x_-\| \leq \|x_-\|$.*

Proof. Let $\Pi = \{x_-, x_+\}$ be a κ-dimensional non-positive subspace of Π_κ. We will show that there exist a contraction map $\mathcal{K} : \Pi_- \mapsto \Pi_+$ such that Π is a graph of $\mathcal{K}$. Indeed, the subspace Π is a graph of a linear operator $\mathcal{K}$ if and only if it follows from $\{0, x_+\} \in \Pi$ that $x_+ = 0$. Since Π is non-positive with respect to $[\cdot, \cdot]$, then $[x, x] = \|x_+\|^2 - \|x_-\|^2 \leq 0$, where $\|\cdot\|$ is a norm in $\mathcal{H}$. As a result, $0 \leq \|x_+\| \leq \|x_-\|$ and if $x_- = 0$ then $x_+ = 0$. Moreover, for any $x_- \in \Pi_-$, it is true that $\|\mathcal{K}x_-\| \leq \|x_-\|$ such that $\mathcal{K}$ is a contraction map. Conversely, let $\mathcal{K}$ be a contraction map $\mathcal{K} : \Pi_- \mapsto \Pi_+$. The graph of $\mathcal{K}$ belongs to the non-positive subspace of Π_κ as

$$[x, x] = \|x_+\|^2 - \|x_-\|^2 = \|\mathcal{K}x_-\|^2 - \|x_-\|^2 \leq 0.$$

Let $\Pi = \{x_-, \mathcal{K}x_-\}$. Since $\dim(\Pi_-) = \kappa$, then $\dim(\Pi) = \kappa$. [5] ∎

Proof of Theorem 3. Let $z \in \mathbb{C}$, $\mathrm{Im}(z) > 0$ be a regular point of the self-adjoint operator T in Π_κ. Let $U = (T - \bar{z})(T - z)^{-1}$ be the Cayley transform of T. By Corollary 3.10, U is a unitary operator in Π_κ. By Lemma 3.9, T and U have the same invariant subspaces in Π_κ. Therefore, the existence of the maximal non-positive invariant subspace for the self-adjoint operator T can be proved from the existence of such a subspace for the unitary operator U. Let $x = \{x_-, x_+\}$ and

$$U = \begin{bmatrix} U_{11} & U_{12} \\ U_{21} & U_{22} \end{bmatrix}$$

be the matrix representation of the operator U with respect to the decomposition (2.3.1). Let Π denote a κ-dimensional non-positive subspace in Π_κ. Since U has a trivial kernel in Π_κ and U is unitary in Π_κ such that $[Ux, Ux] = [x, x] \leq 0$, then $\tilde{\Pi} = U\Pi$ is also a κ-dimensional non-positive subspace of Π_κ. By Lemma 3.11, there exist two contraction mappings $\mathcal{K}$ and $\tilde{\mathcal{K}}$ for subspaces Π and $\tilde{\Pi}$, respectively. Therefore, the assignment $\tilde{\Pi} = U\Pi$ is equivalent to the system,

$$\begin{pmatrix} \tilde{x}_- \\ \tilde{\mathcal{K}}\tilde{x}_- \end{pmatrix} = \begin{bmatrix} U_{11} & U_{12} \\ U_{21} & U_{22} \end{bmatrix} \begin{pmatrix} x_- \\ \mathcal{K}x_- \end{pmatrix} = \begin{pmatrix} (U_{11} + U_{12}\mathcal{K})x_- \\ (U_{21} + U_{22}\mathcal{K})x_- \end{pmatrix},$$

and it follows from the mapping $\Pi_- \mapsto \Pi_-$ that

$$U_{21} + U_{22}\mathcal{K} = \tilde{\mathcal{K}}(U_{11} + U_{12}\mathcal{K}).$$

We shall prove that the operator $(U_{11} + U_{12}\mathcal{K})$ is invertible. By contradiction, we assume that there exists $x_- \neq 0$ such that $\tilde{x}_- = (U_{11} + U_{12}\mathcal{K})x_- = 0$. Since $\tilde{x}_- = 0$ implies that $\tilde{x}_+ = \tilde{\mathcal{K}}\tilde{x}_- = 0$, we obtain that $\{x_-, \mathcal{K}x_-\}$ is an eigenvector in the kernel of U. However, U has a trivial kernel in Π_κ so that $x_- = 0$. Let $F(\mathcal{K})$ be an operator-valued function in the form,

$$F(\mathcal{K}) = (U_{21} + U_{22}\mathcal{K})(U_{11} + U_{12}\mathcal{K})^{-1},$$

such that $\tilde{\mathcal{K}} = F(\mathcal{K})$. This function is defined for any contraction operator K. By Lemma 3.11, the operator $F(\mathcal{K})$ maps the operator unit ball $\|\mathcal{K}\| \leq 1$ to itself. Since U is a continuous operator and U_{12} is a finite-dimensional operator, then U_{12} is a compact operator. Hence the operator ball $\|\mathcal{K}\| \leq 1$ is a weakly compact set and the function $F(\mathcal{K})$ is continuous with respect to weak topology. By Schauder's Fixed-Point Principle, there exists a fixed point $\mathcal{K}_0$ such that $F(\mathcal{K}_0) = \mathcal{K}_0$ and $\|\mathcal{K}_0\| \leq 1$. By Lemma 3.11, the graph of $\mathcal{K}_0$ defines the κ-dimensional non-positive subspace Π, which is invariant with respect to U. By Lemma 3.4, the κ-dimensional non-positive subspace Π is a maximal non-positive subspace of Π_κ. ∎

[5] Extending arguments of Lemma 3.11, one can prove that the subspace Π is strictly negative with respect to $[\cdot, \cdot]$ if and only if it is a graph of the strictly contraction map $\mathcal{K} : \Pi_- \mapsto \Pi_+$, such that $\Pi = \{x_-, \mathcal{K}x_-\}$ and $\|\mathcal{K}x_-\| < \|x_-\|$.

2.4 Spectrum of a self-adjoint operator in Pontryagin space

We apply here Pontryagin's Invariant Subspace Theorem (Theorem 3) to the product of two bounded invertible self-adjoint operators $T = BC$ in Pontryagin space Π_κ, where $\kappa = \dim(\mathcal{H}_C^-)$. In the context of the shifted generalized eigenvalue problem (2.2.9), we shall consider two operators T in two different Pontryagin spaces Π_κ. In the first setting, $B = (A + \delta K)^{-1}$ and $C = K$ with $\kappa = \dim(\mathcal{H}_K^-)$, while in the second setting, $B = K$ and $C = (A + \delta K)^{-1}$ with $\kappa = \dim(\mathcal{H}_{A+\delta K}^-)$. With a slight abuse of notations, we shall denote eigenvalues of the operator $T = BC$ by λ[6]. In the context of the shifted generalized eigenvalue problem (2.2.9), $\lambda = (\gamma + \delta)^{-1}$ in the first setting and $\lambda = (\gamma + \delta)$ in the second setting.

Lemma 4.1 *Let $\mathcal{H}$ be a Hilbert space with the inner product $(\cdot, \cdot)$ and $B, C : \mathcal{H} \to \mathcal{H}$ be bounded invertible self-adjoint operators in $\mathcal{H}$. Define the sesquilinear form*

$$[\cdot, \cdot] = (C\cdot, \cdot) \tag{2.4.1}$$

and extend $\mathcal{H}$ to the Pontryagin space Π_κ, where κ is the finite number of negative eigenvalues of C counted with their algebraic multiplicities. The operator $T = BC$ is self-adjoint in Π_κ and there exists a κ-dimensional maximal non-positive subspace of Π_κ which is invariant with respect to T.

Proof. It follows from the orthogonal sum decomposition in the Hilbert space $\mathcal{H}$ that the quadratic form $(C\cdot, \cdot)$ is strictly negative on the κ-dimensional subspace $\mathcal{H}_C^-$ and strictly positive on the infinite-dimensional subspace $\mathcal{H}_C^+ \oplus \mathcal{H}_C^{\sigma_e(C)}$. By continuity and Gram–Schmidt orthogonalization, the Hilbert space $\mathcal{H}$ is extended to the Pontryagin space Π_κ with respect to the sesquilinear form (2.4.1). The bounded operator $T = BC$ is self-adjoint in Π_κ, since B and C are self-adjoint in $\mathcal{H}$ and

$$[T\cdot, \cdot] = (CBC\cdot, \cdot) = (C\cdot, BC\cdot) = [\cdot, T\cdot].$$

Existence of the κ-dimensional maximal non-positive T-invariant subspace of Π_κ follows from Pontryagin's Invariant Subspace Theorem (Theorem 3). ∎

Remark 4.2 The decomposition (2.3.1) of the Pontryagin space Π_κ is canonical in the sense that $\Pi_+ \cap \Pi_- = \varnothing$. We consider now various sign-definite subspaces of Π_κ which are invariant with respect to the operator $T = BC$. In general, these invariant sign-definite subspaces do not provide a canonical decomposition of Π_κ.

[6]Spectral parameter λ here does not correspond to parameter λ used in the linear eigenvalue problem (2.2.1).

Let $\mathcal{H}_{c^+}$ ($\mathcal{H}_{c^-}$) denote the T-invariant subspace associated with complex eigenvalues λ in the upper (lower) half-plane and $\mathcal{H}_n(\mathcal{H}_p)$ denote the non-positive (non-negative) T-invariant subspace associated with real eigenvalues λ. Spectrum of T consists of three disjoint sets: isolated and embedded eigenvalues, continuous spectrum, and residual spectrum (see Definitions 4.3 and 4.4). We will show that the maximal non-positive T-invariant subspace in Lemma 4.1 does not include the residual and continuous spectra but may include isolated and embedded eigenvalues of finite multiplicities.

Definition 4.3 *We say that λ is a point of the residual spectrum of T if*

$$\mathrm{Ker}(T-\lambda I)=\varnothing,\quad \overline{\mathrm{Range}(T-\lambda I)}\neq\Pi_\kappa$$

and λ is a point of the continuous spectrum of T if

$$\mathrm{Ker}(T-\lambda I)=\varnothing,\quad \mathrm{Range}(T-\lambda I)\neq\overline{\mathrm{Range}(T-\lambda I)}=\Pi_\kappa.$$

Definition 4.4 *We say that λ is a point of the discrete spectrum of T (an eigenvalue) if* $\mathrm{Ker}(T-\lambda I)\neq\varnothing$. *The eigenvalue is said to be multiple if*

$$\dim\left(\cap_{k\in\mathbb{N}}\mathrm{Ker}(T-\lambda I)^k\right)>1.$$

Let λ_0 be a multiple eigenvalue with

$$\dim\left(\mathrm{Ker}(T-\lambda I)\right)=1,\quad \dim\left(\cap_{k\in\mathbb{N}}\mathrm{Ker}(T-\lambda I)^k\right)=n<\infty.$$

The canonical basis for the corresponding eigenspace is defined by the Jordan block of generalized eigenvectors

$$f_j\in\Pi_\kappa:\quad Tf_j=\lambda_0 f_j+f_{j-1},\qquad j=1,...,n, \tag{2.4.2}$$

where $f_0=0$. If $n=\infty$, the eigenvalue λ_0 is said to have an infinite multiplicity. If $\dim\left(\mathrm{Ker}(T-\lambda_0 I)\right)>1$, *the eigenspace associated with the eigenvalue λ_0 can be represented by the union of the Jordan blocks.*

Lemma 4.5 *The residual spectrum of T is empty.*

Proof. By a contradiction, assume that λ belongs to the residual part of the spectrum of T such that $\mathrm{Ker}(T-\lambda I)=\varnothing$ but $\mathrm{Range}(T-\lambda I)$ is not dense in Π_κ. Let $g\in\Pi_\kappa$ be orthogonal to $\mathrm{Range}(T-\lambda I)$, such that

$$\forall f\in\Pi_\kappa:\quad 0=[(T-\lambda I)f,g]=[f,(T-\bar{\lambda}I)g].$$

Therefore, $(T-\bar{\lambda}I)g=0$, that is $\bar{\lambda}$ is an eigenvalue of T. Since T is real-valued operator, λ is also an eigenvalue of T and hence it can not be in the residual part of the spectrum of T. ∎

Lemma 4.6 *The continuous spectrum of T is real.*

Proof. Let P^+ and P^- be orthogonal projectors to Π^+ and Π^- respectively, such that $I = P^+ + P^-$. Since $\Pi^\pm$ are defined by the quadratic form (2.4.1), the self-adjoint operator C admits the polar decomposition $C = J|C|$, where $J = P^+ - P^-$ and $|C|$ is a positive operator. Since $J^2 = I$ and C is self-adjoint, we have $J|C|J = |C|$. As a result, $J|C|^{1/2}J = |C|^{1/2}$ and the operator $T = BC$ is similar to the operator

$$|C|^{1/2}BJ|C|^{1/2} = |C|^{1/2}BJ|C|^{1/2}(J + 2P^-) = |C|^{1/2}B|C|^{1/2} + 2|C|^{1/2}BJ|C|^{1/2}P^-.$$

Since P^- is a projection to a finite-dimensional subspace, the operator $|C|^{1/2}BJ|C|^{1/2}$ is a finite-rank perturbation of the self-adjoint operator $|C|^{1/2}B|C|^{1/2}$. By Theorem 18 on p.22 in [51], the continuous part of the self-adjoint operator $|C|^{1/2}B|C|^{1/2}$ is the same as that of $|C|^{1/2}BJ|C|^{1/2}$. By similarity transformation, it is the same as that of T. ∎

Theorem 4 *Let Π_c be an invariant subspace associated with the continuous spectrum of T. Then, $[f, f] > 0$, $\forall f \in \Pi_c$.*

Proof. By Lemma 4.1, the operator T has a κ-dimensional maximal non-positive invariant subspace of Π_κ. Let us denote this subspace by Π. Because spectrum of T is decomposed into disjoint sets of eigenvalues and the continuous spectrum, any finite-dimensional invariant subspace of T cannot be a part of Π_c. Therefore, Π and Π_c do not intersect. Assume now that there exists $f_0 \in \Pi_c$ such that $[f_0, f_0] \leq 0$. Since $f_0 \notin \Pi$, the subspace spanned by f_0 and the basis vectors in Π is a $(\kappa + 1)$-dimensional non-positive subspace of Π_κ. However, by Lemma 3.4, the maximal dimension of any non-positive subspace of Π_κ is κ. Therefore, $[f_0, f_0] > 0$ for any $f_0 \in \Pi_c$. ∎

2.5 Eigenvalues of the generalized eigenvalue problem

We count here isolated and embedded eigenvalues for the product operator $T = BC$. This operator is self-adjoint in the Pontryagin space Π_κ, which is defined by the sesquilinear form (2.4.1) with $\kappa = \dim(\mathcal{H}_C^-)$. This count is used in the proofs of our main Theorems 1 and 2. We assume that the eigenspaces associated with eigenvalues of T are represented by the union of the Jordan blocks, according to Definition 4.4. Each Jordan block of generalized eigenvectors (2.4.2) is associated with a single eigenvector of T. We start with an elementary result about the generalization of the Fredholm theory in the Hilbert space $\mathcal{H}$ to that in the Pontryagin space Π_κ.

Proposition 5.1 *Let λ_0 be an isolated eigenvalue of $T = BC$ associated with a one-dimensional eigenspace $\mathcal{H}_{\lambda_0} = \mathrm{Span}\{f_0\}$. Then, $\lambda_0 = \bar{\lambda}_0$ is algebraically simple if and only if $[f_0, f_0] \neq 0$, while $\lambda_0 \neq \bar{\lambda}_0$ is algebraically simple if and only if $[f_0, \bar{f}_0] \neq 0$.*

Proof. Since B and C are bounded invertible self-adjoint operators in the Hilbert space $\mathcal{H}$, the eigenvalue problem $Tf = \lambda f$ in the Pontryagin space Π_κ is rewritten as the generalized eigenvalue problem $Cf = \lambda B^{-1} f$ in the Hilbert space $\mathcal{H}$. Since λ_0 is an isolated eigenvalue, the Fredholm theory for the generalized eigenvalue problem implies that $\lambda_0 = \bar{\lambda}_0$ is algebraically simple if and only if $(B^{-1} f_0, f_0) \neq 0$, while $\lambda_0 \neq \bar{\lambda}_0$ is algebraically simple if and only if $(B^{-1} f_0, \bar{f}_0) \neq 0$. Since $\lambda_0 \neq 0$ (otherwise, C would not be invertible), the condition of the Fredholm theory is equivalent to the condition that $(Cf_0, f_0) \neq 0$ and $(Cf_0, \bar{f}_0) \neq 0$, respectively. The assertion is proved due to definition (2.4.1) of the sesquilinear form. ∎

Lemma 5.2 ***(Pontryagin)*** *Let $\mathcal{H}_\lambda$ and $\mathcal{H}_\mu$ be eigenspaces associated with eigenvalues λ and μ of the operator T in Π_κ and $\lambda \neq \bar{\mu}$. Then $\mathcal{H}_\lambda$ is orthogonal to $\mathcal{H}_\mu$ with respect to $[\cdot, \cdot]$.*

Proof. Let n and m be dimensions of $\mathcal{H}_\lambda$ and $\mathcal{H}_\mu$, respectively, such that $n \geq 1$ and $m \geq 1$. By Definition 4.4, it is clear that

$$f \in \mathcal{H}_\lambda \Longleftrightarrow (T - \lambda I)^n f = 0, \tag{2.5.1}$$

$$g \in \mathcal{H}_\mu \Longleftrightarrow (T - \mu I)^m g = 0. \tag{2.5.2}$$

We should prove that $[f, g] = 0$ by induction for $n + m \geq 2$. If $n + m = 2$ ($n = m = 1$), then it follows from system (2.5.1)–(2.5.2) that

$$(\lambda - \bar{\mu})[f, g] = 0, \qquad f \in \mathcal{H}_\lambda, \quad g \in \mathcal{H}_\mu,$$

such that $[f, g] = 0$ for $\lambda \neq \bar{\mu}$. Let us assume that subspaces $\mathcal{H}_\lambda$ and $\mathcal{H}_\mu$ are orthogonal for $2 \leq n + m \leq k$ and prove that an extended subspace $\tilde{\mathcal{H}}_\lambda$ with $\tilde{n} = n + 1$ remains orthogonal to $\mathcal{H}_\mu$. To do so, we define $\tilde{f} = (T - \lambda I) f$ and verify that

$$f \in \tilde{\mathcal{H}}_\lambda \Longleftrightarrow (T - \lambda I)^{\tilde{n}} f = (T - \lambda I)^n \tilde{f} = 0.$$

By the inductive assumption, we have $[\tilde{f}, g] = 0$, such that

$$[(T - \lambda I) f, g] = 0. \tag{2.5.3}$$

By using system (2.5.1)–(2.5.2) and relation (2.5.3), we obtain that

$$(\lambda - \bar{\mu})[f, g] = 0, \qquad f \in \tilde{\mathcal{H}}_\lambda, \quad g \in \mathcal{H}_\mu.$$

Using the same analysis, one can prove that an extended subspace $\tilde{\mathcal{H}}_\mu$ with $\tilde{m} = m + 1$ remains orthogonal to $\mathcal{H}_\lambda$. As a result, the assertion of the lemma follows by the induction method. ∎

Lemma 5.3 *Let $\mathcal{H}_{\lambda_0}$ be an eigenspace associated with a multiple real isolated eigenvalue λ_0 of T in Π_κ and $\{f_1, f_2, ...f_n\}$ be the Jordan chain of eigenvectors. Let $\mathcal{H}_0 = \mathrm{Span}\{f_1, f_2, ..., f_k\} \subset \mathcal{H}_{\lambda_0}$, where $k = \frac{n}{2}$ if n is even and $k = \frac{n-1}{2}$ if n is odd, and $\tilde{\mathcal{H}}_0 = \mathrm{Span}\{f_1, f_2, ..., f_k, f_{k+1}\} \subset \mathcal{H}_{\lambda_0}$.*

- *If n is even ($n = 2k$), the neutral subspace $\mathcal{H}_0$ is the maximal sign-definite subspace of $\mathcal{H}_{\lambda_0}$.*
- *If n is odd ($n = 2k+1$), the subspace $\tilde{\mathcal{H}}_0$ is the maximal non-negative subspace of $\mathcal{H}_{\lambda_0}$ if $[f_1, f_n] > 0$ and the maximal non-positive subspace of $\mathcal{H}_{\lambda_0}$ if $[f_1, f_n] < 0$, while the neutral subspace $\mathcal{H}_0$ is the maximal non-positive subspace of $\mathcal{H}_{\lambda_0}$ if $[f_1, f_n] > 0$ and the maximal non-negative subspace of $\mathcal{H}_{\lambda_0}$ if $[f_1, f_n] < 0$.*

Proof. Without loss of generality we will consider the case $\lambda_0 = 0$ (if $\lambda_0 \neq 0$ the same argument is applied to the shifted self-adjoint operator $\tilde{T} = T - \lambda_0 I$). We will show that $[f, f] = 0, \forall f \in \mathcal{H}_0$. By a decomposition over the basis in $\mathcal{H}_0$, we obtain

$$\forall f = \sum_{i=1}^{k} \alpha_i f_i : \quad [f, f] = \sum_{i=1}^{k} \sum_{j=1}^{k} \alpha_i \bar{\alpha}_j [f_i, f_j]. \tag{2.5.4}$$

We use that

$$[f_i, f_j] = [Tf_{i+1}, Tf_{j+1}] = ... = \left[T^k f_{i+k}, T^k f_{j+k}\right] = \left[T^{2k} f_{i+k}, f_{j+k}\right],$$

for any $1 \leq i, j \leq k$. In the case of even $n = 2k$, we have $[f_i, f_j] = [T^n f_{i+k}, f_{j+k}] = 0$ for all $1 \leq i, j \leq k$. In the case of odd $n = 2k+1$, we have $[f_i, f_j] = [T^{n+1} f_{i+k+1}, f_{j+k+1}] = 0$ for all $1 \leq i, j \leq k$. Therefore, $\mathcal{H}_0$ is a neutral subspace of $\mathcal{H}_{\lambda_0}$. To show that it is the maximal neutral subspace of $\mathcal{H}_{\lambda_0}$, let $\mathcal{H}'_0 = \mathrm{Span}\{f_1, f_2, ..., f_k, f_{k_0}\}$, where $k+1 \leq k_0 \leq n$. Since f_{n+1} does not exist in the Jordan chain (2.4.2) (otherwise, the algebraic multiplicity is $n+1$) and λ_0 is an isolated eigenvalue, then $[f_1, f_n] \neq 0$ by Proposition 5.1. It follows from the Jordan chain (2.4.2) that

$$[f_1, f_n] = [T^{m-1} f_m, f_n] = [f_m, T^{m-1} f_n] = [f_m, f_{n-m+1}] \neq 0. \tag{2.5.5}$$

When $n = 2k$, we have $1 \leq n - k_0 + 1 \leq k$, such that $[f_{k_0}, f_{n-k_0+1}] \neq 0$ and the subspace $\mathcal{H}'_0$ is sign-indefinite in the decomposition (2.5.4). When $n = 2k+1$, we have $1 \leq n - k_0 + 1 \leq k$ for $k_0 \geq k+2$ and $n - k_0 + 1 = k+1$ for $k_0 = k+1$. In either case, $[f_{k_0}, f_{n-k_0+1}] \neq 0$ and the subspace $\mathcal{H}'_0$ is sign-indefinite in the decomposition (2.5.4) unless $k_0 = k+1$. In the latter case, we have $[f_{k+1}, f_{k+1}] = [f_1, f_n] \neq 0$ and $[f_j, f_{k+1}] = [T^{2k} f_{j+k}, f_n] = 0$ for $1 \leq j \leq k$, such that this subspace $\tilde{\mathcal{H}}_0 \equiv \mathcal{H}'_0$ with $k_0 = k+1$ is non-negative for $[f_1, f_n] > 0$ and non-positive for $[f_1, f_n] < 0$. ∎

Remark 5.4 If λ_0 is a real embedded eigenvalue of T, the Jordan chain (2.4.2) can be truncated at f_n even if $[f_1, f_n] = 0$. Indeed, the Fredholm theory for the generalized eigenvalue problem (used in Proposition 5.1) gives a necessary but not a sufficient condition for existence of the solution f_{n+1} in the Jordan chain (2.4.2) if the eigenvalue λ_0 is embedded into the continuous spectrum. If $[f_1, f_n] = 0$ but f_{n+1} does not exist in Π_κ, the neutral subspaces $\mathcal{H}_0$ for $n = 2k$ and $\tilde{\mathcal{H}}_0$ for $n = 2k+1$ in Lemma 5.3 do not have to be the maximal non-positive or non-negative subspaces. The construction of a maximal non-positive subspace for embedded eigenvalues depends on the computations of the projection matrix $[f_i, f_j]$ in the eigenspace $\mathcal{H}_\lambda = \mathrm{Span}\{f_1, ..., f_n\}$. For instance, if λ_0 is an algebraically simple embedded eigenvalue, then the corresponding eigenspace $\mathcal{H}_{\lambda_0} = \mathrm{Span}\{f_1\}$ is either positive or negative or neutral depending on the value of $[f_1, f_1]$.

Lemma 5.5 *Let $\lambda_0 \in \mathbb{C}$, $\mathrm{Im}(\lambda_0) > 0$ be an eigenvalue of T in Π_κ, $\mathcal{H}_{\lambda_0}$ be the corresponding eigenspace, and $\tilde{\mathcal{H}}_{\lambda_0} = \{\mathcal{H}_{\lambda_0}, \mathcal{H}_{\bar{\lambda}_0}\} \subset \Pi_\kappa$. Then, the neutral subspace $\mathcal{H}_{\lambda_0}$ is the maximal sign-definite subspace of $\tilde{\mathcal{H}}_{\lambda_0}$, such that $[f, f] = 0$, $\forall f \in \mathcal{H}_{\lambda_0}$.*

Proof. By Lemma 5.2 with $\lambda = \mu = \lambda_0$, the eigenspace $\mathcal{H}_{\lambda_0}$ is orthogonal to itself with respect to $[\cdot, \cdot]$, such that $\mathcal{H}_{\lambda_0}$ is a neutral subspace of $\tilde{\mathcal{H}}_{\lambda_0}$. It remains to prove that $\mathcal{H}_{\lambda_0}$ is the maximal sign-definite subspace in $\tilde{\mathcal{H}}_\lambda$. Let $\mathcal{H}_{\lambda_0} = \mathrm{Span}\{f_1, f_2, ..., f_n\}$, where $\{f_1, f_2, ..., f_n\}$ is the Jordan chain of eigenvectors (2.4.2). Consider a subspace $\tilde{\mathcal{H}}'_{\lambda_0} = \mathrm{Span}\{f_1, f_2, ..., f_n, \bar{f}_j\}$ for any $1 \le j \le n$ and construct a linear combination of f_{n+1-j} and $\bar{f}_j$:

$$\forall \alpha \in \mathbb{C}: \quad [f_{n+1-j} + \alpha \bar{f}_j, f_{n+1-j} + \alpha \bar{f}_j] = 2\mathrm{Re}\left(\alpha [\bar{f}_j, f_{n+1-j}]\right). \tag{2.5.6}$$

By Proposition 5.1, we have $[f_n, \bar{f}_1] \neq 0$ and, by virtue of the chain (2.5.5), we obtain $[\bar{f}_j, f_{n+1-j}] \neq 0$. As a result, the linear combination $f_{n+1-j} + \alpha \bar{f}_j$ in equality (2.5.6) is sign-indefinite with respect to $[\cdot, \cdot]$. ∎

We shall summarize the count of the dimensions of the maximal non-positive and non-negative subspaces associated with eigenspaces of T in Π_κ. Let $N_n(\lambda_0)$ ($N_p(\lambda_0)$) denote the dimension of the maximal non-positive (non-negative) subspace of Π_κ corresponding to the eigenvalue λ_0. By Lemma 5.3, if λ_0 is a real isolated eigenvalue, then the sum of dimensions of the maximal non-positive and non-negative subspaces of $\mathcal{H}_{\lambda_0}$ equals the dimension of $\mathcal{H}_{\lambda_0}$ (although the intersection of the two subspaces can be non-empty). For each Jordan block of generalized eigenvectors, we have

(i) If $n = 2k$, then $N_p(\lambda_0) = N_n(\lambda_0) = k$.

(ii) If $n = 2k+1$ and $[f_1, f_n] > 0$, then $N_p(\lambda_0) = k+1$ and $N_n(\lambda_0) = k$.

(iii) If $n = 2k+1$ and $[f_1, f_n] < 0$, then $N_p(\lambda_0) = k$ and $N_n(\lambda_0) = k+1$.

By Remark 5.4, if λ_0 is a simple embedded eigenvalue, then

(i) If $[f_1, f_1] > 0$, then $N_p(\lambda_0) = 1$, $N_n(\lambda_0) = 0$.

(ii) If $[f_1, f_1] < 0$, then $N_p(\lambda_0) = 0$, $N_n(\lambda_0) = 1$.

(iii) If $[f_1, f_1] = 0$, then $N_p(\lambda_0) = N_n(\lambda_0) = 1$.

We note that the sum of dimensions of the maximal non-positive and non-negative subspaces of $\mathcal{H}_{\lambda_0}$, that is $N_p(\lambda_0) + N_n(\lambda_0)$, exceeds the dimension of $\mathcal{H}_{\lambda_0}$ in the case (iii). If λ_0 is a multiple embedded eigenvalue, computations of the projection matrix $[f_i, f_j]$ is needed to find the dimensions $N_p(\lambda_0)$ and $N_n(\lambda_0)$. Finally, by Lemma 5.5, if λ_0 is a complex eigenvalue, then $N_p(\lambda_0) = N_n(\lambda_0) = \dim(\mathcal{H}_{\lambda_0}) = \frac{1}{2}\dim(\tilde{\mathcal{H}}_{\lambda_0})$.

Before proofs of Theorems 1 and 2, we have to deal with one more complication, which is the presence of zero eigenvalues of operator A. Operator A determines either B or C in the product operator $T = BC$. Since we shift A to $A + \delta K$ for sufficiently small $\delta > 0$, all zero eigenvalues of A become small non-zero eigenvalues of $A + \delta K$, where K is a bounded invertible self-adjoint operator that also determines either B or C. Therefore, we need to know how many zero eigenvalues of A becomes small positive and negative eigenvalues of $A + \delta K$. This splitting is described by the following result.

Lemma 5.6 *Let $\mathcal{H}_0$ be an eigenspace associated with a multiple zero eigenvalue of operator $K^{-1}A$ in $\mathcal{H}$ and $\{f_1, ..., f_n\}$ be the Jordan chain of eigenvectors, such that $f_1 \in \mathrm{Ker}(A)$. Let $\omega_+ > 0$ and $0 < \delta < |\sigma_{-1}|$, where σ_{-1} is the smallest negative eigenvalue of $K^{-1}A$. Then $(Kf_1, f_n) \neq 0$ and*

- *If n is odd, the subspace $\mathcal{H}_0$ corresponds to a positive eigenvalue of the operator $(A + \delta K)$ if $(Kf_1, f_n) > 0$ and to a negative eigenvalue if $(Kf_1, f_n) < 0$.*
- *If n is even, the subspace $\mathcal{H}_0$ corresponds to a positive eigenvalue of the operator $(A + \delta K)$ if $(Kf_1, f_n) < 0$ and to a negative eigenvalue if $(Kf_1, f_n) > 0$.*

Proof. Let $\mu(\delta)$ be an eigenvalue of the self-adjoint operator $A+\delta K$ related to the subspace $\mathcal{H}_0$. By analytic perturbation theory for isolated eigenvalues of self-adjoint operators (see Chapters VII.3 in [75]), eigenvalue $\mu_j(\delta)$ is a continuous function of δ and

$$\lim_{\delta \to 0+} \frac{\mu(\delta)}{\delta^n} = (-1)^{n+1} \frac{(Kf_1, f_n)}{(f_1, f_1)}. \tag{2.5.7}$$

Since $\omega_+ > 0$, the zero eigenvalue of A is isolated from the continuous spectrum of $K^{-1}A$, such that $(Kf_1, f_n) \neq 0$ by the Fredholm theory for the generalized eigenvalue problem (2.2.3). The assertion of the lemma follows from the limiting relation (2.5.7). Since no eigenvalues of $K^{-1}A$ exists in $(-|\sigma_{-1}|, 0)$, the eigenvalue $\mu(\delta)$ remains sign-definite for $0 < \delta < |\sigma_{-1}|$. ∎

Remark 5.7 If $\omega_+ = 0$ and assumption P3 is satisfied with $\mathrm{Ker}(A) = \mathrm{Span}\{f_1\}$, then the eigenvalue $\mu(\delta)$ is negative only if $(Kf_1, f_1) \leq 0$. If $(Kf_1, f_1) > 0$, the eigenvalue $\mu(\delta)$ is either positive or does not exist[7]. All other small eigenvalues, which may bifurcate from the end points of the essential spectrum of A by means of the edge bifurcations [74], are positive, according to assumption P3.

Proof of Theorem 1. We use the shifted generalized eigenvalue problem (2.2.9) for sufficiently small $\delta > 0$ and consider the bounded operator $T = (A + \delta K)^{-1}K$, that is $B = (A+\delta K)^{-1}$ and $C = K$. By Lemma 4.1, the operator T is self-adjoint with respect to $[\cdot,\cdot] = (K\cdot,\cdot)$ and it has a κ-dimensional maximal non-positive invariant subspace, where $\kappa = \dim(\mathcal{H}_K^-)$. Counting all eigenvalues of the shifted generalized eigenvalue problem (2.2.9) with the use of notations of Section 2, we establish equality (2.2.12).
Now, let $B = K$ and $C = (A + \delta K)^{-1}$ and consider the bounded operator $\tilde{T} = K(A + \delta K)^{-1}$ which is self-adjoint with respect to $[\cdot,\cdot] = ((A + \delta K)^{-1}\cdot,\cdot)$. The self-adjoint operator $(A + \delta K)^{-1}$ defines the indefinite metric in the Pontryagin space $\tilde{\Pi}_{\tilde{\kappa}}$, where $\tilde{\kappa} = \dim(\mathcal{H}^-_{A+\delta K})$. For any simple eigenvalue γ_0 of the shifted eigenvalue problem (2.2.9), we have

$$\forall f, g \in \mathcal{H}_{\gamma_0}: \quad ((A + \delta K)f, g) = (\gamma_0 + \delta)(Kf, g).$$

If $\gamma_0 \geq 0$ or $\mathrm{Im}(\gamma_0) \neq 0$, the maximal non-positive eigenspace of $\tilde{T}$ in $\tilde{\Pi}_{\tilde{\kappa}}$ associated with γ_0 coincides with the maximal non-positive eigenspace of T in Π_κ. If $\gamma_0 < 0$, the maximal non-positive eigenspace of $\tilde{T}$ in $\tilde{\Pi}_{\tilde{\kappa}}$ coincides with the maximal non-negative eigenspace of T in Π_κ. The same statement can be proved for the case of multiple eigenvalues γ_0. Threrefore, the dimension of the maximal non-positive eigenspace of $\tilde{T}$ in $\tilde{\Pi}_{\tilde{\kappa}}$ is $N_p^- + N_n^0 + N_n^+ + N_{c+}$, such that equality (2.2.11) follows by Lemma 4.1. ∎

Proof of Theorem 2. We prove this theorem by contradiction and explicit computations. First, we introduce T and Π_κ according to the choice $B = (A + \delta K)^{-1}$ and $C = K$. Let Π be a non-negative invariant subspace in Π_κ, which is spanned by eigenvectors of the generalized eigenvalue problem (2.2.3) for N_p^- negative eigenvalues $\gamma < 0$, N_p^0 zero eigenvalues $\gamma = 0$, N_p^+ positive isolated eigenvalues $\gamma > 0$, and N_{c+} complex eigenvalues with $\mathrm{Im}(\gamma) > 0$. Let us assume that $N_p^- + N_p^0 + N_p^+ + N_{c+} > N_A + N_K$ and derive a contradiction.

By Gram–Schmidt orthogonalization with respect to the inner product in the Hilbert space $\mathcal{H}$, if $N_p^- + N_p^0 + N_p^+ + N_{c+} > N_A + N_K$, then there exist a vector $h \in \Pi$ such that $(h, f) = 0$ and $(h, g) = 0$ for any $f \in \mathcal{H}_A^- \oplus \mathcal{H}_A^0 \oplus \mathcal{H}_A^+$ and $g \in \mathcal{H}_K^- \oplus \mathcal{H}_K^+$. Therefore, $h \in \mathcal{H}_A^{\sigma_e(A)} \cap \mathcal{H}_K^{\sigma_e(K)}$, such that

$$(Ah, h) \geq \omega_+(h, h), \qquad (Kh, h) \leq \omega_-^{-1}(h, h),$$

[7]Positive eigenvalues can disappear in the essential spectrum of $A + \delta K$ if $\mu(\delta) > \omega_{A+\delta K}$ for sufficiently small $\delta > 0$.

and

$$(Ah, h) \geq \omega_+\omega_-(Kh, h).$$

On the other hand, since $h \in \Pi$, then it can be represented by $h = \sum_{i=1}^{N_p^- + N_p^0 + N_p^+ + N_{c^+}} \alpha_i h_i$, where $(h_1, h_2, ..., h_{N_p^- + N_p^0 + N_p^+ + N_{c^+}})$ is a basis in Π associated with the eigenspaces of the generalized eigenvalue problem (2.2.3). By Lemmas 5.2 and 5.5, we obtain

$$\begin{aligned}(Ah, h) &= \sum_{i,j} \alpha_i \bar{\alpha}_j (Ah_i, h_j) \\ &= \sum_{\gamma_i = \gamma_j < 0} \alpha_i \bar{\alpha}_j (Ah_i, h_j) + \sum_{\gamma_i = \gamma_j = 0} \alpha_i \bar{\alpha}_j (Ah_i, h_j) + \sum_{\gamma_i = \gamma_j > 0} \alpha_i \bar{\alpha}_j (Ah_i, h_j).\end{aligned}$$

By Lemma 5.3, the non-zero values in (Ah_i, h_j) for isolated eigenvalues occur only for (Af_{k+1}, f_{k+1}), where f_{k+1} is the generalized eigenvector for a multiple eigenvalue with odd algebraic multiplicity $n = 2k + 1$. Since all these cases are similar to the case of simple eigenvalues, we can write the representation above in the simplified form

$$\begin{aligned}(Ah, h) &= \sum_{\gamma_j < 0} |\alpha_j|^2 (Ah_j, h_j) + \sum_{\gamma_j = 0} |\alpha_j|^2 (Ah_j, h_j) + \sum_{\gamma_j > 0} |\alpha_j|^2 (Ah_j, h_j) \\ &= \sum_{\gamma_j < 0} \gamma_j |\alpha_j|^2 (Kh_j, h_j) + \sum_{\gamma_j > 0} \gamma_j |\alpha_j|^2 (Kh_j, h_j) \\ &< \omega_+\omega_- \sum_{\gamma_j > 0} |\alpha_j|^2 (Kh_j, h_j),\end{aligned}$$

where we have used the fact that $(Kh_j, h_j) \geq 0$ for any eigenvector $h_j \in \Pi$ and that $\gamma_j < \omega_+\omega_-$ for any isolated eigenvalue γ_j. On the other hand,

$$\begin{aligned}(Kh, h) &= \sum_{i,j} \alpha_i \bar{\alpha}_j (Kh_i, h_j) \\ &= \sum_{\gamma_j < 0} |\alpha_j|^2 (Kh_j, h_j) + \sum_{\gamma_j = 0} |\alpha_j|^2 (Kh_j, h_j) + \sum_{\gamma_j > 0} |\alpha_j|^2 (Kh_j, h_j) \\ &\geq \sum_{\gamma_j > 0} |\alpha_j|^2 (Kh_j, h_j).\end{aligned}$$

Therefore, $(Ah, h) < \omega_+\omega_-(Kh, h)$, which is a contradiction. As a result, $N_p^- + N_p^0 + N_p^+ + N_{c^+} \leq N_A + N_K$. ∎

Remark 5.8 Isolated eigenvalues of infinite multiplicities are excluded by the counts of Theorems 1 and 2. Embedded eigenvalues of infinite multiplicity are possible but they may only correspond to finitely many Jordan blocks of finite length, according to Theorem 1. In the Jordan block decomposition, one can not exclude an infinite number of simple Jordan blocks corresponding to the same embedded eigenvalue with infinitely many eigenvectors in the positive invariant subspace of Π_κ.

2.6 Application: NLS solitons

Consider a nonlinear Schrödinger (NLS) equation in multi dimensions,

$$i\psi_t = -\Delta\psi + F(|\psi|^2)\psi, \qquad \Delta = \partial^2_{x_1x_1} + ... + \partial^2_{x_dx_d}, \tag{2.6.1}$$

where $(x,t) \in \mathbb{R}^d \times \mathbb{R}$ and $\psi \in \mathbb{C}$. For a suitable nonlinear function $F(|\psi|^2)$, where F is C^∞ and $F(0) = 0$, the NLS equation (2.6.1) possesses a solitary wave solution $\psi = \phi(x)e^{i\omega t}$, where $\omega > 0$ and $\phi : \mathbb{R}^d \to \mathbb{R}$ is an exponentially decaying C^∞ function. See [88] for existence and uniqueness of ground state solutions to the NLS equation (2.6.1). Linearization of the NLS equation (2.6.1) with the ansatz,

$$\psi = \left(\phi(x) + [u(x) + iw(x)]e^{\lambda t} + [\bar{u}(x) + i\bar{w}(x)]e^{\bar{\lambda}t}\right)e^{i\omega t}, \tag{2.6.2}$$

where $\lambda \in \mathbb{C}$ and $(u(x), w(x)) \in \mathbb{C}^2$, results in the linear eigenvalue problem (2.2.1)(after neglecting all terms with u and w with the order higher than one), where $L_\pm$ are Schrödinger operators given by

$$L_+ = -\Delta + \omega + F(\phi^2) + 2\phi^2 F'(\phi^2), \tag{2.6.3}$$
$$L_- = -\Delta + \omega + F(\phi^2). \tag{2.6.4}$$

We note that $L_\pm$ are unbounded operators and $\sigma_e(L_\pm) = [\omega_\pm, \infty)$ with $\omega_+ = \omega_- = \omega > 0$. The kernel of L_- includes at least one eigenvector $\phi(x)$ and the kernel of L_+ includes at least d eigenvectors $\partial_{x_j}\phi(x)$, $j = 1, ..., d$. The Hilbert space is defined as $\mathcal{X} = L^2(\mathbb{R}^d, \mathbb{C})$ and the main assumptions P1-P2 are satisfied due to the exponential decay of the functions $F(\phi^2)$ and $\phi^2 F'(\phi^2)$. Theorems 1 and 2 give precise count of eigenvalues of the stability problem $L_-L_+u = -\lambda^2 u$, provided that the numbers $\dim(\mathcal{H}^-_K)$, $\dim(\mathcal{H}^-_{A+\delta K})$, N_K and N_A can be computed from the count of isolated eigenvalues of $A = \mathcal{P}L_+\mathcal{P}$ and $K = \mathcal{P}L_-^{-1}\mathcal{P}$, where $\mathcal{P}$ is the orthogonal projection to the complement of $\mathrm{Ker}(L_-)$. We illustrate these computations with two examples.

Example 1. Let $\phi(x)$ be the ground state solution such that $\phi(x) > 0$ on $x \in \mathbb{R}^d$. By spectral theory, $\mathrm{Ker}(L_-) = \{\phi\}$ is one-dimensional and the subspace $\mathcal{H}^-_K$ is empty.

- It follows by equality (2.2.12) that $N^-_n = N^0_n = N^+_n = N_{c^+} = 0$. Therefore, the spectrum of the generalized eigenvalue problem (2.2.3) is real-valued and all eigenvalues γ are semi-simple.
- Since $\mathrm{Ker}(L_-) \notin \mathrm{Ker}(L_+)$ and $\mathcal{H}^-_K$ is empty, eigenvectors of $\mathrm{Ker}(A)$ are in the positive subspace of K, such that $N^0_p = z(L_+)$. By Lemma 5.6, zero eigenvalues of A become positive eigenvalues of $A + \delta K$ for any $\delta > 0$, such that $\dim(\mathcal{H}^-_{A+\delta K}) = \dim(\mathcal{H}^-_A)$.

- It follows by equality (2.2.11) that $N_p^- = \dim(\mathcal{H}^-_{A+\delta K})$. By Proposition 2.1, we have $\dim(\mathcal{H}_A^-) = n(L_+) - p_0 - z_0$, where p_0 and z_0 are the number of positive and zero values of a scalar function $M_0 = -(L_+^{-1}\phi, \phi)$. Since $L_+\partial_\omega\phi(x) = -\phi(x)$, we have $M_0 = \frac{1}{2}\frac{d}{d\omega}\|\phi\|^2_{L^2}$.

- It follows by inequality (2.2.14) that $N_p^- + N_p^0 + N_p^+ \leq \dim(\mathcal{H}_A^-) + \dim(\mathcal{H}_A^0) + \dim(\mathcal{H}_A^+) + \dim(\mathcal{H}_K^+)$. By Proposition 2.1 and the previous counts, we obtain $N_p^+ \leq p(L_+) + p(L_-) + p_0 + z_0$.

Remark 6.1 If $n(L_+) = n \in \mathbb{N}$ and $\frac{d}{d\omega}\|\phi\|^2_{L^2} > 0$, the count above gives $N_p^- = n(L_+) - 1$, which coincides with Theorem 2.1 of [61] (the case $n = 1$ is known as the Stability Theorem in [59]). If $n(L_+) = 1$, $z(L_+) = d$, $p(L_+) = p(L_-) = 0$ and $\frac{d}{d\omega}\|\phi\|^2_{L^2} < 0$, the count above gives $N_p^- = 1$, $N_p^0 = d$, and $N_p^+ = 0$, which is proved, with a direct variational method, in Proposition 2.1.2 [104] and Proposition 9.2 [80] for $d = 1$ and in Lemma 1.8 [112] for $d = 3$, in the context of the super-critical power NLS equation with $F = |\psi|^q$ and $q > \frac{2}{d}$.

Remark 6.2 Stability of vector solitons in the coupled NLS equations, which generalize the scalar NLS equation (2.6.1), is defined by the same linear eigenvalue problem (2.2.1), where $L_\pm$ are matrix Schrödinger operators. General results for non-ground state solutions are obtained in [70, 97] for $d = 1$ and in [37] for $d = 3$. Multiple and embedded eigenvalues were either excluded from analysis by an assumption [97, 37] or were treated implicitly [70]. The present work generalizes these results with a precise count of multiple and embedded eigenvalues.

Example 2. Let the cubic NLS equation (2.6.1) with $F = |\psi|^2$ be discretized so that $\Delta \equiv \epsilon\Delta_{\text{disc}}$, where Δ_{disc} is the second-order discrete Laplacian and ϵ is a small parameter. We note that Δ_{disc} is a bounded operator and $\sigma_c(-\Delta_{\text{disc}}) \in [0, 4d]$. The Hilbert space is defined as $\mathcal{X} = l^2(\mathbb{Z}^d, \mathbb{C})$. By the Lyapunov–Schmidt reduction method, the solution $\psi = \phi e^{i\omega t}$ with $\omega > 0$ and $\phi \in l^2(\mathbb{Z}^d)$ bifurcates from the limiting solution with N non-zero lattice nodes at $\epsilon = 0$. It is proved in [98] for $d = 1$ and [99] for $d = 2$ that $\frac{d}{d\omega}\|\phi\|^2_{l^2} > 0$, $\text{Ker}(L_+) = \varnothing$, and $\text{Ker}(L_-) = \{\phi\}$ for sufficiently small $\epsilon \neq 0$. It follows by equalities (2.2.11) and (2.2.12) that

$$\begin{aligned} N_p^- + N_n^+ + N_{c^+} &= n(L_+) - 1, \\ N_n^- + N_n^+ + N_{c^+} &= n(L_-), \end{aligned}$$

where it is found in [98, 99] that $n(L_+) = N$ and $n(L_-) \leq N - 1$. Lyapunov–Schmidt reductions give, however, more precise information than the general count above, since Corollary 3.5 in [98] for $d = 1$ predicts that $N_n^+ = n(L_-)$, $N_n^- = N_{c^+} = 0$, and $N_p^- =$

$N - 1 - n(L_-)$[8]. Similarly, it follows by inequality (2.2.14) and the above count that

$$N_p^+ \leq 2n(L_-) + \dim(\mathcal{H}_A^+) + \dim(\mathcal{H}_K^+).$$

If the solution ϕ is a ground state, then $N = 1$ and $n(L_-) = 0$. In this case, the above inequality shows that the number of edge bifurcations from the continuous spectrum of $K^{-1}A$ (given by N_p^+) is bounded from above by the number of edge bifurcations from the essential spectrum of A (given by $\dim(\mathcal{H}_A^+)$) and the numbers of edge bifurcations from the essential spectrum of K^{-1} (given by $\dim(\mathcal{H}_K^+)$). The bound above becomes less useful if $N > 1$ and $n(L_-) \neq 0$.

Remark 6.3 The Lyapunov–Schmidt reduction method was also used for continuous coupled NLS equations with and without external potentials. See [71, 103] for various results on the count of unstable eigenvalues in parameter continuations of the NLS equations.

2.7 Application: NLS vortices

Consider the two-dimensional NLS equation (2.6.1) in polar coordinates (r, θ):

$$i\psi_t = -\Delta\psi + F(|\psi|^2)\psi, \qquad \Delta = \partial_{rr}^2 + \frac{1}{r}\partial_r + \frac{1}{r^2}\partial_{\theta\theta}^2, \tag{2.7.1}$$

where $r > 0$ and $\theta \in [0, 2\pi]$. Assume that the NLS equation (2.7.1) possesses a charge-m vortex solution $\psi = \phi(r)e^{im\theta + i\omega t}$, where $\omega > 0$, $m \in \mathbb{N}$, and $\phi : \mathbb{R}_+ \to \mathbb{R}$ is an exponentially decaying C^∞ function with $\phi(0) = 0$. See [94] for existence results of charge-m vortices in the cubic-quintic NLS equation with $F = -|\psi|^2 + |\psi|^4$. Linearization of the NLS equation (2.7.1) with the ansatz,

$$\psi = \left(\phi(r)e^{im\theta} + \varphi_+(r,\theta)e^{\lambda t} + \bar{\varphi}_-(r,\theta)e^{\bar{\lambda}t}\right)e^{i\omega t}, \tag{2.7.2}$$

where $\lambda \in \mathbb{C}$ and $(\varphi_+(r,\theta), \varphi_-(r,\theta)) \in \mathbb{C}^2$, results in the stability problem,

$$\sigma_3 H\boldsymbol{\varphi} = i\lambda\boldsymbol{\varphi}, \tag{2.7.3}$$

where $\boldsymbol{\varphi} = (\varphi_+, \varphi_-)^T$, $\sigma_3 = \mathrm{diag}(1, -1)$, and

$$H = \begin{pmatrix} -\Delta + \omega + F(\phi^2) + \phi^2 F'(\phi^2) & \phi^2 F'(\phi^2)e^{2im\theta} \\ \phi^2 F'(\phi^2)e^{-2im\theta} & -\Delta + \omega + F(\phi^2) + \phi^2 F'(\phi^2) \end{pmatrix}.$$

[8]Corollary 3.5 in [98] is valid only when small positive eigenvalues of L_- are simple. It is shown in [99] for $d = 2$ that the case of multiple small positive eigenvalues of L_- leads to splitting of real eigenvalues N_p^- of the generalized eigenvalue problem (2.2.3) to complex eigenvalues N_{c+} beyond the leading-order Lyapunov–Schmidt reduction.

Expand $\varphi(r,\theta)$ in the Fourier series

$$\varphi = \sum_{n\in\mathbb{Z}} \varphi^{(n)}(r)e^{in\theta}$$

and reduce the problem to a sequence of spectral problems for ODEs:

$$\sigma_3 H_n \varphi_n = i\lambda\varphi_n, \qquad n\in\mathbb{Z}, \tag{2.7.4}$$

where $\varphi_n = (\varphi_+^{(n+m)}, \varphi_-^{(n-m)})^T$, and

$$H_n = \begin{pmatrix} A_r + \omega + F(\phi^2) + \phi^2F'(\phi^2) & \phi^2F'(\phi^2) \\ \phi^2F'(\phi^2) & A_r + \omega + F(\phi^2) + \phi^2F'(\phi^2) \end{pmatrix}.$$

The operator A_r is given by expression

$$A_r = -\partial_{rr}^2 - \frac{1}{r}\partial_r + \frac{(n+m)^2}{r^2}.$$

When $n = 0$, the stability problem (2.7.4) transforms to the linear eigenvalue problem (2.2.1), where $L_\pm$ is given by (2.6.3)–(2.6.4) with $\Delta = \partial_{rr}^2 + \frac{1}{r}\partial_r - \frac{m^2}{r^2}$ and (u,w) are given by $u = \varphi_+^{(m)} + \varphi_-^{(-m)}$ and $w = -i(\varphi_+^{(m)} - \varphi_-^{(-m)})$. When $n\in\mathbb{N}$, the stability problem (2.7.4) transforms to the linear eigenvalue problem (2.2.1) with $L_+ = H_n$ and $L_- = \sigma_3 H_n \sigma_3$, where

$$L_+ = L_- + 2\phi^2F'(\phi^2)\sigma_1, \qquad \sigma_1 = \begin{pmatrix} 0 & 1 \\ 1 & 0 \end{pmatrix},$$

and (u,w) are given by $u = \varphi_n$ and $w = -i\sigma_3\varphi_n$. When $-n\in\mathbb{N}$, the stability problem (2.7.4) admits a transformation with $H_{-n} = \sigma_1 H_n \sigma_1$ and $\sigma_3\sigma_1 = -\sigma_1\sigma_3$ to the stability problem with $n\in\mathbb{N}$. Let us introduce the weighted inner product for functions on $r\geq 0$:

$$(f,g)_r = \int_0^\infty f(r)g(r)rdr.$$

In all cases $n = 0$, $n\in\mathbb{N}$ and $-n\in\mathbb{N}$, $L_\pm$ are unbounded self-adjoint differential operators and $\sigma_e(L_\pm) = [\omega_\pm,\infty)$ with $\omega_+ = \omega_- = \omega > 0$. The kernel of the linearized operators includes at least three eigenvectors:

$$n = \pm 1: \quad \phi_{\pm 1} = \phi'(r)\mathbf{1} \mp \frac{m}{r}\phi(r)\sigma_3\mathbf{1}, \qquad n = 0: \quad \phi_0 = \phi(r)\sigma_3\mathbf{1},$$

where $\mathbf{1} = (1,1)^T$. The Hilbert space is defined as $\mathcal{X} = L_r^2(\mathbb{R}_+,\mathbb{C})$ for $n = 0$ and $\mathcal{X} = L_r^2(\mathbb{R}_+,\mathbb{C}^2)$ for $\pm n\in\mathbb{N}$. In all cases, the main assumptions P1-P2 are satisfied due to exponential decay of the functions $F(\phi^2)$ and $\phi^2F'(\phi^2)$.

The case $n = 0$ is the same as for solitons (see Section 5.1). We shall hence consider adjustments in the count of eigenvalues in the case $\pm n \in \mathbb{N}$, when the stability problem (2.7.4) is rewritten in the form,

$$\begin{cases} \sigma_3 H_n \varphi_n = i\lambda \varphi_n \\ \sigma_3 H_{-n} \varphi_{-n} = i\lambda \varphi_{-n} \end{cases} \qquad n \in \mathbb{N}. \tag{2.7.5}$$

Let $L_+ = \mathrm{diag}(H_n, H_{-n})$ and $L_- = \mathrm{diag}(\sigma_3 H_n \sigma_3, \sigma_3 H_{-n} \sigma_3)$.

Lemma 7.1 *Let λ be an eigenvalue of the stability problem (2.7.5) with the eigenvector $(\varphi_n, \mathbf{0})$. Then there exists another eigenvalue $-\lambda$ with the linearly independent eigenvector $(\mathbf{0}, \sigma_1 \varphi_n)$. If $\mathrm{Re}(\lambda) > 0$, there exist two more eigenvalues $\bar{\lambda}, -\bar{\lambda}$ with the linearly independent eigenvectors $(\mathbf{0}, \sigma_1 \bar{\varphi}_n)$, $(\bar{\varphi}_n, \mathbf{0})$.*

Proof. We note that $\sigma_1 \sigma_3 = -\sigma_3 \sigma_1$ and $\sigma_1^2 = \sigma_3^2 = \sigma_0$, where $\sigma_0 = \mathrm{diag}(1, 1)$. Therefore, each eigenvalue λ of H_n with the eigenvector φ_n generates eigenvalue $-\lambda$ of H_{-n} with the eigenvector $\varphi_{-n} = \sigma_1 \varphi_n$. When $\mathrm{Re}(\lambda) \neq 0$, each eigenvalue λ of H_n generates also eigenvalue $-\bar{\lambda}$ of H_n with the eigenvector $\bar{\varphi}_n$ and eigenvalue $\bar{\lambda}$ of H_{-n} with the eigenvector $\varphi_{-n} = \sigma_1 \bar{\varphi}_n$. ∎

Theorem 5 *Let N_{real} be the number of real eigenvalues in the stability problem (2.7.5) with $\mathrm{Re}(\lambda) > 0$, N_{comp} be the number of complex eigenvalues with $\mathrm{Re}(\lambda) > 0$ and $\mathrm{Im}(\lambda) > 0$, N^-_{imag} be the number of purely imaginary eigenvalues with $\mathrm{Im}(\lambda) > 0$ and $(\varphi_n, H_n \varphi_n) \leq 0$, and N^-_{zero} be the algebraic multiplicity of the zero eigenvalue of $\sigma_3 H_n \varphi_n = i\lambda \varphi_n$ with $(\varphi_n, H_n \varphi_n) \leq 0$. Then,*

$$\frac{1}{2} N_{\mathrm{real}} + N_{\mathrm{comp}} = n(H_n) - N^-_{\mathrm{zero}} - N^-_{\mathrm{imag}}, \tag{2.7.6}$$

where N_{real} is even.

Proof. By Lemma 7.1, a pair of real eigenvalues of $\sigma_3 H_n \varphi_n = i\lambda \varphi_n$ corresponds to two linearly independent eigenvectors φ_n and $\bar{\varphi}_n$. Because $(H_n \varphi_n, \varphi_n)$ is real-valued and hence zero for $\lambda \in \mathbb{R}$, we have

$$(H_n(\varphi_n \pm \bar{\varphi}_n), (\varphi_n \pm \bar{\varphi}_n)) = \pm 2\mathrm{Re}(H_n \varphi_n, \bar{\varphi}_n).$$

By counting multiplicities of the real negative and complex eigenvalues of the generalized eigenvalue problem (2.2.3) associated with the stability problem (2.7.5), we have $N_n^- = N_p^- = N_{\mathrm{real}}$ and $N_{c+} = 2N_{\mathrm{comp}}$. By Lemma 7.1, a pair of purely imaginary and zero eigenvalues of the stability problem (2.7.5) corresponds to two linearly independent eigenvectors $(\varphi_n, \mathbf{0})$ and $(\mathbf{0}, \varphi_{-n})$, where $\varphi_{-n} = \sigma_1 \varphi_n$ and $(H_{-n} \varphi_{-n}, \varphi_{-n}) = (H_n \varphi_n, \varphi_n)$. By

counting multiplicities of the real positive and zero eigenvalues of the generalized eigenvalue problem (2.2.3) associated with the stability problem (2.7.5), we have $N_n^0 = 2N_{\text{zero}}^-$ and $N_n^+ = 2N_{\text{imag}}^-$. Since the spectra of H_n, $\sigma_1 H_n \sigma_1$, and $\sigma_3 H_n \sigma_3$ coincide, we have $n(L_-) = 2n(H_n)$. As a result, equality (2.7.6) follows by equality (2.2.12) of Theorem 1. By Lemma 7.1, the multiplicity of N_{real} is even in the stability problem (2.7.5). ∎

Corollary 7.2 *Let $A = \mathcal{P}L_+\mathcal{P}$ and $K = \mathcal{P}L_-^{-1}\mathcal{P}$, where $\mathcal{P}$ is an orthogonal projection to the complement of* $\text{Ker}(L_-) = \text{Span}\{v_1, ..., v_n\}$. *The number of small negative eigenvalues of $A + \delta K$ for sufficiently small $\delta > 0$ equals the number of non-negative eigenvalues of $M_0 = \lim_{\mu \uparrow 0} M(\mu)$, where $M_{ij}(\mu) = ((\mu - L_+)^{-1} v_i, v_j)$.*

Proof. The same count (2.7.6) follows by equality (2.2.11) of Theorem 1 if and only if $\dim(\mathcal{H}^-_{A+\delta K}) = \dim(\mathcal{H}^-_K) = n(L_-)$. Since the zero eigenvalue of A is isolated from the essential spectrum and $n(L_+) = n(L_-)$, the number of small negative eigenvalues of $A + \delta K$ for sufficiently small $\delta \neq 0$ must be equal to

$$\dim(\mathcal{H}^-_{A+\delta K}) - \dim(\mathcal{H}^-_A) = n(L_+) - \dim(\mathcal{H}^-_A).$$

By Proposition 2.1, this number is given by the number $p_0 + z_0$ of non-negative eigenvalues of matrix M_0. ∎

Example 3. Let $\phi(r)$ be the fundamental charge-m vortex solution such that $\phi(r) > 0$ for $r > 0$ and $\phi(0) = 0$. By spectral theory, $\text{Ker}(H_0) = \text{Span}\{\boldsymbol{\phi}_0\}$ and the analysis for $n = 0$ becomes similar to Example 1. In the case $n \in \mathbb{N}$, let us assume that $\text{Ker}(H_1) = \text{Span}\{\boldsymbol{\phi}_1\}$ and $\text{Ker}(H_n) = \varnothing$ for $n \geq 2$.

- By direct computation, we obtain $(\sigma_3 H_1 \sigma_3)^{-1} \boldsymbol{\phi}_1 = -\frac{1}{2} r\phi(r)\mathbf{1}$ and

$$((\sigma_3 H_1 \sigma_3)^{-1} \boldsymbol{\phi}_1, \boldsymbol{\phi}_1) = \int_0^\infty r\phi^2(r) dr > 0.$$

  By Lemma 5.6, we have $N_n^0 = 0$ for $n = 1$ ($N_n^0 = 0$ holds also for $n \geq 2$). By Proposition 2.1, we have then $M_0 < 0$ such that $p_0 = z_0 = 0$ for all $n \in \mathbb{N}$. Corollary 7.2 is hence confirmed.

- Since $(\sigma_3 \boldsymbol{\phi}_1, \boldsymbol{\phi}_1) = 0$ and $\text{Ker}(\sigma_3 H_1 \sigma_3) = \{\sigma_3 \boldsymbol{\phi}_1\}$, then $\boldsymbol{\phi}_1 \perp \text{Ker}(\sigma_3 H_1 \sigma_3)$. By Proposition 2.1, we have $z(A) = z(L_+) = 1$ for $n = 1$ and $z(A) = z(L_+) = 0$ for $n \geq 2$.

- By Theorem 5, we have

$$N_{\text{real}} + 2N_{\text{comp}} = 2n(H_n) - 2N_{\text{imag}}^-, \tag{2.7.7}$$

  where N_{imag}^- gives the total number of eigenvalues in the stability problem (2.7.5) with $\text{Re}(\lambda) = 0$, $\text{Im}(\lambda) > 0$, and $(H_n \boldsymbol{\varphi}_n, \boldsymbol{\varphi}_n) < 0$, while $N_{\text{zero}}^- = N_n^0 = 0$.

Remark 7.3 Stability of vortices was considered numerically in [94], where Lemma 7.1 was also obtained. The closure relation (2.7.7) was also discussed in [70] in a more general context. Vortices in the discretized scalar NLS equation were considered with the Lyapunov–Schmidt reduction method in [99]. Although the reduced eigenvalue problems were found in a much more complicated form compared to the reduced eigenvalue problem for solitons, equality (2.7.7) was confirmed for all vortex configurations considered in [99].

2.8 Application: KdV solitons

Consider a general fifth-order KdV equation,

$$v_t = a_1 v_x - a_2 v_{xxx} + a_3 v_{xxxxx} + 3b_1 v v_x - b_2 \left(v v_{xxx} + 2 v_x v_{xx}\right) + 6 b_3 v^2 v_x, \qquad (2.8.1)$$

where (a_1, a_2, a_3) and (b_1, b_2, b_3) are real-valued coefficients for linear and nonlinear terms, respectively. Without loss of generality, we assume that $a_3 > 0$ and

$$c_{\text{wave}}(k) = a_1 + a_2 k^2 + a_3 k^4 \geq 0, \qquad k \in \mathbb{R}. \qquad (2.8.2)$$

For suitable values of parameters, there exists a traveling wave solution $v(x,t) = \phi(x - ct)$, where $c > 0$ and $\phi : \mathbb{R} \mapsto \mathbb{R}$ is an even and exponentially decaying function. Existence of traveling waves was established in [128, 65, 5] for $b_2 = b_3 = 0$, in [25] for $b_3 = 0$, in [68] for $b_1 = -b_2 = b_3 = 1$, and in [84] for $b_3 = 0$ or $b_1 = b_2 = 0$. Linearization of the fifth-order KdV equation (2.8.1) with the ansatz

$$v(x,t) = \phi(x - ct) + w(x - ct) e^{\lambda t}$$

results in the stability problem

$$\partial_x L_- w = \lambda w, \qquad (2.8.3)$$

where L_- is an unbounded fourth-order operator,

$$L_- = a_3 \frac{d^4}{dx^4} - a_2 \frac{d^2}{dx^2} + a_1 + c + 3b_1 \phi(x) - b_2 \frac{d}{dx} \phi(x) \frac{d}{dx} - b_2 \phi''(x) + 6 b_3 \phi^2(x). \qquad (2.8.4)$$

Due to the condition (2.8.2), we have $\sigma_e(L_-) \in [c, \infty)$, such that $\omega_- = c > 0$. The kernel of L_- includes at least one eigenvector $\phi'(x)$. Since the image of L_- is in $L^2(\mathbb{R})$, the eigenfunction $w(x) \in L^1(\mathbb{R})$ for $\lambda \neq 0$ satisfies the constraint:

$$(1, w) = \int_{\mathbb{R}} w(x) dx = 0. \qquad (2.8.5)$$

Let $w = u'(x)$, where $u(x) \to 0$ as $|x| \to \infty$ and define $L_+ = -\partial_x L_- \partial_x$. The essential spectrum of L_+ is located at $\sigma_e(L_+) \in [0, \infty)$, such that $\omega_+ = 0$. The kernel of L_+ includes at least one eigenvector $\phi(x)$.

Let the Hilbert space $\mathcal{X}$ be defined as $\mathcal{X} = L^2(\mathbb{R}, \mathbb{C})$. The main assumptions P1-P2 for L_- and L_+ are satisfied due to exponential decay of the function $\phi(x)$. Since $\omega_+ = 0$, the kernel of L_+ is embedded into the endpoint of the essential spectrum of L_+. This introduces a technical complication in computations of the inverse of L_+ [79], which we avoid here with the use of the shifted generalized eigenvalue problem (2.2.9) with $\delta > 0$. We still need to check assumption P3. It is easy to see that

$$\omega_{A+\delta K} = \inf_{k\in\mathbb{R}} \left[k^2(c + c_{\text{wave}}(k)) + \frac{\delta}{c + c_{\text{wave}}(k)} \right] \geq \frac{\delta}{c} > 0,$$

such that the first part of assumption P3 is satisfied. Since new eigenvalues of $A+\delta K$ bifurcating from the end points of the essential spectrum of $A + \delta K$ with the edge bifurcations are quadratic with respect to δ [74], while the end points are linear with respect to δ, all new eigenvalues are positive for sufficiently small $\delta > 0$. Therefore, assumption P3 is satisfied if we assume that the kernel of L_+ is one-dimensional, that is $\text{Ker}(L_+) = \text{Span}\{\phi\}$.

We shall apply Theorem 1 after the count of isolated and embedded eigenvalues in the stability problem (2.8.3). Since $\omega_+ = 0$, the continuous spectrum of $\partial_x L_-$ covers the entire imaginary axis of λ. Therefore, all real and complex eigenvalues are isolated, while all purely imaginary eigenvalues including the zero eigenvalue are embedded.

Lemma 8.1 *Let λ_j be a real eigenvalue of the stability problem (2.8.3) with the real-valued eigenvector $w_j(x)$, such that $\text{Re}(\lambda_j) > 0$ and $\text{Im}(\lambda_j) = 0$. Then there exists another eigenvalue $-\lambda_j$ in problem (2.8.3) with the linearly independent eigenvector $w_j(-x)$. The linear combinations $w_j^{\pm}(x) = w_j(x) \pm w_j(-x)$ are orthogonal with respect to the operator L_-,*

$$\left(L_- w_j^{\pm}, w_j^{\pm}\right) = \pm 2 \left(L_- w_j(-x), w_j(x)\right), \qquad \left(L_- w_j^{\mp}, w_j^{\pm}\right) = 0. \tag{2.8.6}$$

Proof. Since $\phi(-x) = \phi(x)$, the self-adjoint operator L_- is invariant with respect to the transformation $x \mapsto -x$. The functions $w_j(x)$ and $w_j(-x)$ are linearly independent since $w_j(x)$ has both symmetric and anti-symmetric parts provided that $\lambda_j \neq 0$. Under the same constraint,

$$\left(L_- w_j(\pm x), w_j(\pm x)\right) = \pm \lambda_j^{-1} \left(L_- w_j(\pm x), \partial_x L_- w_j(\pm x)\right) = 0,$$

and the orthogonality relations (2.8.6) hold by direct computations. ∎

Corollary 8.2 *Let λ_j be a complex eigenvalue of the stability problem (2.8.3) with the complex-valued eigenvector $w_j(x)$, such that $\text{Re}(\lambda_j) > 0$ and $\text{Im}(\lambda_j) > 0$. Then there exist eigenvalues $\bar{\lambda}_j$, $-\lambda_j$, and $-\bar{\lambda}_j$ in problem (2.8.3) with the linearly independent eigenvectors $\bar{w}_j(x)$, $w_j(-x)$, and $\bar{w}_j(-x)$, respectively.*

Lemma 8.3 *Let λ_j be a purely imaginary embedded eigenvalue of the stability problem (2.8.3) with the complex-valued eigenvector $w_j(x)$, such that* $\mathrm{Re}(\lambda_j) = 0$ *and* $\mathrm{Im}(\lambda_j) > 0$. *Then there exists another eigenvalue $-\lambda_j = \bar{\lambda}_j$ in problem (2.8.3) with the linearly independent eigenvector $w_j(-x) = \bar{w}_j(x)$. The linear combinations $w_j^{\pm}(x) = w_j(x) \pm \bar{w}_j(x)$ are orthogonal with respect to the operator L_-,*

$$\left(L_- w_j^{\pm}, w_j^{\pm}\right) = 2\mathrm{Re}\left(L_- w_j(x), w_j(x)\right), \qquad \left(L_- w_j^{\mp}, w_j^{\pm}\right) = 0. \tag{2.8.7}$$

Proof. Since operator L_- is real-valued, the eigenvector $w_j(x)$ of problem (2.8.3) with $\mathrm{Im}(\lambda_j) > 0$ has both real and imaginary parts, which are linearly independent. Under the constraint $\lambda_j \neq 0$,

$$(L_- w_j, \bar{w}_j) = \lambda_j^{-1}\left(L_- w_j, \partial_x L_- \bar{w}_j\right) = 0,$$

and the orthogonality equations (2.8.7) follow by direct computations. ∎

Theorem 6 *Let N_{real} be the number of real eigenvalues of the stability problem (2.8.3) with* $\mathrm{Re}(\lambda) > 0$, *N_{comp} be the number of complex eigenvalues with* $\mathrm{Re}(\lambda) > 0$ *and* $\mathrm{Im}(\lambda) > 0$, *and N_{imag}^- be the number of imaginary eigenvalues with* $\mathrm{Im}(\lambda) > 0$ *and* $\mathrm{Re}\left(L_- w_j(x), w_j(x)\right) \leq 0$ *for the corresponding eigenvectors w_j. Assume that* $\mathrm{Ker}(L_+) = \mathrm{Span}\{\phi\} \in \mathcal{H}$ *and* $\frac{d}{dc}\|\phi\|_{L^2}^2 \neq 0$. *Then,*

$$N_{\mathrm{real}} + 2N_{\mathrm{comp}} + 2N_{\mathrm{imag}}^- = n(L_-) - p_0, \tag{2.8.8}$$

where $p_0 = 1$ if $\frac{d}{dc}\|\phi\|_{L^2}^2 > 0$ and $p_0 = 0$ if $\frac{d}{dc}\|\phi\|_{L^2}^2 < 0$.

Proof. Each isolated and embedded eigenvalue $\gamma_j = -\lambda_j^2$ of the generalized eigenvalue problem (2.2.3) is at least double with two linearly independent eigenvectors $u_j^{\pm}(x)$ defined by $w_j^{\pm} = \partial_x u_j^{\pm}$. By Lemma 8.1 and Corollary 8.2, the dimension of the maximal non-positive invariant eigenspace for isolated (real and complex) eigenvalues coincide with the algebraic multiplicities of isolated eigenvalues, such that $N_n^- = N_p^- = N_{\mathrm{real}}$ and $N_{c^+} = 2N_{\mathrm{comp}}$. By Lemma 8.3 and the relation for eigenvectors of the stability problem (2.8.3),

$$(L_+ u, u) = (L_- u', u') = (L_- w, w), \tag{2.8.9}$$

we have $N_n^+ = 2N_{\mathrm{imag}}^-$. By Remark 5.7 and the assumption that $\mathrm{Ker}(L_+) = \mathrm{Span}\{\phi\} \in \mathcal{H}$ and $\frac{d}{dc}\|\phi\|_{L^2}^2 \neq 0$, we have $N_n^0 = p_0$, where $p_0 = 1$ if $(L_-^{-1}\phi, \phi) \leq 0$ and $p_0 = 0$ if $(L_-^{-1}\phi, \phi) < 0$. Since $L_- \partial_c \phi(x) = -\phi(x)$, we obtain that $(L_-^{-1}\phi, \phi) = -(\partial_c \phi, \phi) = -\frac{1}{2}\frac{d}{dc}\|\phi\|_{L^2}^2$. The count (2.8.8) follows by equality (2.2.12) of Theorem 1. ∎

Remark 8.4 Since $\dim(\mathcal{H}_{A+\delta K}^-) = \dim(\mathcal{H}_A^-) + N_n^0$ and $N_p^- = N_{\mathrm{real}}$, the same count (2.8.8) also follows by equality (2.2.11) of Theorem 1:

$$N_{\mathrm{real}} + 2N_{\mathrm{comp}} + 2N_{\mathrm{imag}}^- = \dim(\mathcal{H}_{A+\delta K}^-) - N_n^0 = \dim(\mathcal{H}_A^-), \tag{2.8.10}$$

provided that $\dim(\mathcal{H}_A^-) = m(L_-) - p_0$. By Proposition 2.1, we have $z_0 = 0$ (since $\frac{d}{dc}\|\phi\|_{L^2}^2 \neq 0$ by assumption) and $\dim(\mathcal{H}_A^-) = n(L_+) - p_0$, where p_0 is the same as in Theorem 6 since $(L_+^{-1}\phi', \phi') = (L_-^{-1}\phi, \phi)$. Similarly, because of relation (2.8.9), we have $n(L_+) = n(L_-)$ and equality (2.8.10) is identical to equality (2.8.8).

Remark 8.5 If $n(L_-) = 1$, Theorem 6 predicts stability for $\frac{d}{dc}\|\phi\|_{L^2}^2 > 0$ and instability with $N_{\text{real}} = 1$ and $N_{\text{comp}} = 0$ for $\frac{d}{dc}\|\phi\|_{L^2}^2 < 0$. This result coincides with the Stability–Instability Theorems in [13, 116]. By a different method, Lyapunov stability of positive traveling waves $\phi(x)$ was considered in [122]. Specific studies of stability for the fifth-order KdV equation (2.8.1) were reported in [66, 42] with the energy-momentum methods. Extension of the Stability–Instability Theorems of [13, 122] with no assumption on a simple negative eigenvalue of L_- was developed in [84, 93] with a variational method. The variational theory is limited however to the case of homogeneous nonlinearities, e.g. $b_3 = 0$ or $b_1 = b_2 = 0$. Our treatment of stability in the fifth-order KdV equation (2.8.1) is novel as it exploits a similarity between stability problems for KdV and NLS equations. The first application of this theory to stability of N-solitons in the KdV hierarchy was reported in [79]. Another treatment of the coupled Klein–Gordon–Boussinesq system, which satisfies properties $\omega_+ = 0$ and $n(L_-) = 1$, is reported in [81]. The case $\frac{d}{dc}\|\phi\|_{L^2}^2 = 0$ was recently considered in [32] for the generalized KdV equation.

Remark 8.6 Theorem 6 can be generalized to any KdV-type evolution equation, when the linearized operator L_- is invariant with respect to the transformation $x \mapsto -x$. When $N_{\text{imag}}^- = 0$, the relation (2.8.8) extends the Morse index theory from gradient dynamical systems to the KdV-type Hamiltonian systems. For gradient dynamical systems, all negative eigenvalues of L_- are related to real unstable eigenvalues of the stability problem. For the KdV-type Hamiltonian system, negative eigenvalues of L_- may generate both real and complex unstable eigenvalues in the stability problem (2.8.3).

CHAPTER 3

SPECTRAL STABILITY OF TWO-PULSE SOLUTIONS IN THE FIFTH-ORDER KDV EQUATION.

3.1 Introduction

One-pulse solutions (solitons) are commonly met in many nonlinear evolution equations where dispersive terms (represented by unbounded differential operators) and nonlinear terms (represented by power functions) are taken in a certain balance. Typical examples of such nonlinear evolution equations with one-pulse solutions are given by the NLS (nonlinear Schrödinger) equation, the Klein-Gordon (nonlinear wave) equation and the KdV (Korteweg-de Vries) equation, as well as their countless generalizations.

One-pulse solutions are the only stationary (traveling) localized solutions of the simplest nonlinear evolution equations. However, uniqueness is not a generic property and bound states of spatially separated pulses can represent other stationary (traveling) localized solutions of the same evolution equation. For instance, two-pulse, three-pulse, and generally N-pulse solutions exist in nonlinear evolution equations with a higher-order dispersion (represented by a higher-order differential operator). The prototypical example of such situation is the fifth-order KdV equation in the form,

$$u_t + u_{xxx} - u_{xxxxx} + 2uu_x = 0, \qquad x \in \mathbb{R}, \quad t \in \mathbb{R}_+, \tag{3.1.1}$$

where $u : \mathbb{R} \times \mathbb{R}_+ \mapsto \mathbb{R}$ and all coefficients of the nonlinear PDE are normalized by a scaling transformation. The more general 5th order KdV equation has been used by W. Craig and M. Groves [35] to describe weakly nonlinear long waves on the surface of a fluid with surface tension. See T.J. Bridges & G. Derks [16] for a review of history and applications of the fifth-order KdV equation (3.1.1) to magneto-acoustic waves in plasma and capillary-gravity water waves.

Traveling localized solutions $u(x,t) = \phi(x - ct)$ of the fifth-order KdV equation (3.1.1) satisfies the fourth-order ODE

$$\phi^{(\mathrm{iv})} - \phi'' + c\phi = \phi^2, \qquad z \in \mathbb{R}, \tag{3.1.2}$$

where $z = x - ct$ is the traveling coordinate and one integration of the fifth-order ODE in z is performed subject to zero boundary conditions on $\phi(z)$ and its derivatives as $|z| \to \infty$.

Existence of localized solutions (homoclinic orbits) to the fourth-order ODE (3.1.2) was considered by methods of the dynamical system theory. See A.R. Champneys [24] for a review of various results on existence of homoclinic orbits in the ODE (3.1.2).

In particular, it is proved with the variational method by B. Buffoni & E. Sere [19] and M. Groves [63] (see references to earlier works in [24]) that the fourth-order ODE (3.1.2) has the one-pulse solution $\phi(z)$ for $c > 0$, which is the only localized solution of the ODE (3.1.2) for $0 < c < \frac{1}{4}$ up to the translation $\phi(z - s)$ for any $s \in \mathbb{R}$. The analytical expression for the one-pulse solution is only available for $c = \frac{36}{169} < \frac{1}{4}$ with

$$\phi(z) = \frac{105}{338} \operatorname{sech}^4\left(\frac{z}{2\sqrt{13}}\right). \tag{3.1.3}$$

For $c > \frac{1}{4}$, the fourth-order ODE (3.1.2) has infinitely many multi-pulse solutions in addition to the one-pulse solution [19, 63]. The multi-pulse solutions look like multiple copies of the one-pulse solutions separated by finitely many oscillations close to the zero equilibrium $\phi = 0$. Stability and evolution of multi-pulse solutions are beyond the framework of the fourth-order ODE (3.1.2) and these questions were considered by two theories in the recent past.

The pioneer work of K.A. Gorshkov & L.A. Ostrovsky explains multi-pulse solutions of the fifth-order KdV equation (3.1.1) from the effective interaction potential computed from the one-pulse solution [56, 57]. When the interaction potential has an alternating sequence of maxima and minima (which corresponds to the case when the one-pulse solution $\phi(z)$ has oscillatory decaying tails at infinity), an infinite countable sequence of two-pulse solutions emerge with the property that the distance between the pulses occurs near the extremal points of the interaction potential. Three-pulse solutions can be constructed as a bi-infinite countable sequence of three one-pulse solutions where each pair of two adjacent pulses is located approximately at a distance defined by the two-pulse solution. Similarly, N-pulse solutions can be formed by a $(N-1)$-infinite countable sequence of N copies of one-pulse solutions. The perturbative procedure in [56] has the advantages that both the linear and nonlinear stability of multi-pulse solutions can be predicted from analysis of the approximate ODE system derived for distances between the individual pulses. Numerical evidences of validity of this procedure in the context of the fifth-order KdV equation are reported in [20].

A different theory was developed by B. Sandstede [110] who extended the X.B. Lin's work on the Lyapunov–Schmidt reductions for nonlinear evolution equations [85]. In this method, a linear superposition of N one-pulse solutions $\phi(z) = \sum_{j=1}^{N} \Phi(z - s_j)$ is a solution of the ODE (3.1.2) in the case when the distances between pulses are infinite (i.e. $|s_{j+1} - s_j| = \infty$, $\forall j$). The Jacobian of the nonlinear ODE (3.1.2) defines a linear self-adjoint operator from $H^4(\mathbb{R})$ to $L^2(\mathbb{R})$:

$$\mathcal{H} = c - \partial_z^2 + \partial_z^4 - 2\phi(z), \qquad c > 0, \tag{3.1.4}$$

where the unbounded differential part $c - \partial_z^2 + \partial_z^4$ is positive and bounded away from zero while the exponentially decaying potential term $-2\phi(z)$ is a relatively compact perturbation. When $\phi(z)$ is a linear superposition of N infinitely-separated one-pulse solutions $\Phi(z - s_j)$, the Jacobian $\mathcal{H}$ has N zero eigenvalues related to the eigenfunctions $\Phi'(z - s_j)$ due to the translational invariance of the ODE (3.1.2). The Lyapunov–Schmidt method leads to a system of bifurcation equations for the distances between individual pulses. When $\phi(z)$ is the N-pulse solution with finitely separated pulses (i.e. $|s_{j+1} - s_j| < \infty$, $\forall j$), one zero eigenvalue of the Jacobian operator $\mathcal{H}$ survives beyond the reductive procedure due to the translational invariance of the N-pulse solution $\phi(z)$, while $N - 1$ real eigenvalues bifurcate from zero. The reduction method may give not only information about existence of multi-pulse solutions but also prediction of their spectral stability in the linearized time-evolution problem [110]. The linearized problem for the fifth-order KdV equation takes the form

$$\partial_z \mathcal{H} v = \lambda v, \qquad z \in \mathbb{R}, \tag{3.1.5}$$

where $v : \mathbb{R} \mapsto \mathbb{C}$ is an eigenfunction for a small perturbation of $\phi(z)$ in the reference frame $z = x - ct$ and $\lambda \in \mathbb{C}$ is an eigenvalue. We say that the eigenvalue λ is *unstable* if $\mathrm{Re}(\lambda) > 0$. We say that the eigenvalue λ is of *negative Krein signature* if $\mathrm{Re}(\lambda) = 0$, $\mathrm{Im}(\lambda) > 0$, $v \in H^2(\mathbb{R})$ and $(\mathcal{H}v, v) < 0$.

Our interest to this well-studied problem is revived by the recent progress in the spectral theory of non-self-adjoint operators arising from linearizations of nonlinear evolution equations [29]. These operators can be defined as self-adjoint operators into Pontryagin space where they have a finite-dimensional negative invariant subspace. Two physically relevant problems for the fifth-order KdV equation (3.1.1) have been solved recently by using the formalism of operators in Pontryagin spaces. First, convergence of the numerical iteration method (known as the Petviashvili method) for one-pulse solutions of the ODE (3.1.2) was proved using the contraction mapping principle in a weighted Hilbert space (which is equivalent to Pontryagin space with zero index) [101]. Second, eigenvalues of the spectral stability problem in a linearization of the fifth-order KdV equation (3.1.1) were characterized in Pontryagin space with a non-zero index defined by the finite number of negative eigenvalues of $\mathcal{H}$ using the invariant subspace theorem [79, 29].

Both recent works rise some open problems when the methods are applied to the N-pulse solutions in the fifth-order KdV equation (3.1.1), even in the case of two-pulse solutions ($N = 2$). The successive iterations of the Petviashvili's method do not converge for two-pulse solutions. The iterative sequence with two pulses leads either to a single pulse or to a spurious solution with two pulses located at an arbitrary distance (see Remark 6.5 in [101]). This numerical problem arises due to the presence of small and negative eigenvalues of $\mathcal{H}$. A modification of the Petviashvili's method is needed to suppress these eigenvalues similarly to the work of L. Demanet & W. Schlag [40] where the zero eigenvalue associated to the translational invariance of the three-dimensional NLS equation is suppressed. We

shall present the modification of the iterative Petviashvili's method in this chapter. See also [26, 92] and [14, 15] for alternative numerical techniques for approximations of multi-pulse solutions of the fifth-order KdV equation.

Another open question arises when spectral stability of multi-pulse solutions is considered within the linear eigenvalue problem (3.1.5). By either the Gorshkov–Ostrovsky perturbative procedure or the Sandstede–Lin reduction method, the small eigenvalues of the Jacobian operator $\mathcal{H}$ result in small eigenvalues of the linearized operator $\partial_z \mathcal{H}$, which are either pairs of real eigenvalues (one of which is unstable) or pairs of purely imaginary eigenvalues of negative Krein signature (which are neutrally stable but potentially unstable). Both cases are possible in the fifth-order KdV equation in agreement with the count of unstable eigenvalues in Pontryagin spaces (see Theorem 6 in [29]). (Similar count of unstable eigenvalues and eigenvalues of negative Krein signatures was developed for the NLS equations in recent papers [70, 97].) Since the real eigenvalues are isolated from the continuous spectrum of the eigenvalue problem (3.1.5), they are structurally stable and persist with respect to parameter continuations. However, the purely imaginary eigenvalues are embedded into the continuous spectrum of the eigenvalue problem (3.1.5) and their destiny remains unclear within the reduction methods. It is well known for the NLS-type and Klein–Gordon-type equations that embedded eigenvalues are structurally unstable to the parameter continuations [62]. If a certain Fermi golden rule related to the perturbation term is nonzero, the embedded eigenvalues of negative Krein signature bifurcate off the imaginary axis to complex eigenvalues inducing instabilities of pulse solutions [37]. (The embedded eigenvalues of positive Krein signature simply disappear upon a generic perturbation [37].) This bifurcation does not contradict the count of unstable eigenvalues [70, 97] and it is indeed observed in numerical approximations of various pulse solutions of the coupled NLS equations [103].

From a heuristic point of view, we would expect that the time evolution of an energetically stable superposition of stable one-pulse solutions remains stable. (Stability of one-pulse solutions in the fifth-order KdV equation (3.1.1) was established with the variational theory [84] and the multi-symplectic Evans function method [16, 17].) According to the Gorshkov-Ostrovsky perturbative procedure, dynamics of well-separated pulses is represented by the Newton law for particle dynamics which describes nonlinear stability of oscillations near the minima of the effective interaction potential [57]. Therefore, we would rather expect (on the contrary to embedded eigenvalues in the linearized NLS and Klein–Gordon equations) that the embedded eigenvalues of negative Krein signature are structurally stable in the linear eigenvalue problem (3.1.5) and persist beyond the leading order of the perturbative procedure. (Multi-pulse solutions of the NLS and Klein–Gordon equations with well-separated individual pulses are always linearly stable since the small purely imaginary eigenvalues of the Lyapunov–Schmidt reductions are isolated from the continuous spectrum of the corresponding linearized problems [124].)

Since the count of unstable eigenvalues in [29] does not allow us to prove structural

stability of embedded eigenvalues of negative Krein signature, we address this problem separately by using different analytical and numerical techniques. In particular, we present an analytical proof of persistence (structural stability) of embedded eigenvalues of negative Krein signature in the linearized problem (3.1.5). We also apply the Fourier spectral method and illustrate the linearized stability of the corresponding two-pulse solutions numerically. Our analytical and numerical methods are based on the construction of exponentially weighted spaces for the linear eigenvalue problem (3.1.5). (See [96] for analysis of exponentially weighted spaces in the context of the generalized KdV equation.) See [28] for computations of the Maslov index for two-pulse solutions of the fifth-order KdV equation (3.1.1) and [123] for stability analysis of two-pulse solutions of the coupled KdV equations.

This chapter is structured as follows. *Section 3.2* contains a summary of available results on existence and stability of one-pulse and two-pulse solutions of the fifth-order KdV equation (3.1.1). *Section 3.3* presents a modification of the iterative Petviashvili method for convergent numerical approximations of the two-pulse solutions in the fourth-order ODE (3.1.2). *Section 3.4* develops the proof of structural stability of embedded eigenvalues in the eigenvalue problem (3.1.5) and numerical approximations of unstable and stable eigenvalues in an exponentially weighted space. *Section 3.5* describes full numerical simulations of the fifth-order KdV equation (3.1.1) to study nonlinear dynamics of two-pulse solutions.

3.2 Review of available results

Linearization of the ODE (3.1.2) at the critical point $(0,0,0,0)$ leads to the eigenvalues κ given by roots of the quartic equation,

$$\kappa^4 - \kappa^2 + c = 0. \tag{3.2.1}$$

When $c < 0$, one pair of roots κ is purely imaginary and the other pair is purely real. When $0 < c < \frac{1}{4}$, two pairs of roots κ are real-valued. When $c > \frac{1}{4}$, the four complex-valued roots κ are located symmetric about the axes. We will use notations $k_0 = \text{Im}(\kappa) > 0$ and $\kappa_0 = \text{Re}(\kappa) > 0$ for a complex root of (3.2.1) in the first quadrant for $c > \frac{1}{4}$. The following two theorems summarize known results on existence of one-pulse and two-pulse solutions of the ODE (3.1.2).

Theorem 3.2.1 (One-pulse solutions)

(i) There exists a one-pulse solution $\phi(z)$ of the ODE (3.1.2) for $c > 0$ such that $\phi \in H^2(\mathbb{R}) \cap C^5(\mathbb{R})$, $\phi(-z) = \phi(z)$, and $\phi(z) \to 0$ exponentially as $|z| \to \infty$. Moreover, $\phi(z)$ is $C^m(\mathbb{R})$ for any $m \geq 0$.

(ii) The Jacobian operator $\mathcal{H}$ in (3.1.4) associated with the one-pulse solution $\phi(z)$ has exactly one negative eigenvalue with an even eigenfunction and a simple kernel with the odd eigenfunction $\phi'(z)$.

(iii) Assume that the map $\phi(z)$ from $c > 0$ to $H^2(\mathbb{R})$ is $C^1(\mathbb{R}_+)$ and that $P'(c) > 0$, where $P(c) = \|\phi\|_{L^2}^2$. The linearized operator $\partial_z\mathcal{H}$ has a two-dimensional algebraic kernel in $L^2(\mathbb{R})$ and no unstable eigenvalues with $\mathrm{Re}(\lambda) > 0$.

Proof. (i) Existence of a symmetric solution $\phi(z)$ in $H^2(\mathbb{R})$ follows by the mountain-pass lemma and the concentration-compactness principle (see Theorem 8 in [63] and Theorem 2.3 in [84]). The equivalence between weak solutions of the variational theory and strong solutions of the ODE (3.1.2) is established in Lemma 1 of [63] and Lemma 2.4 of [84]. The exponential decay of $\phi(z)$ follows from the Stable Manifold Theorem in Appendix A of [19]. Finally, the smoothness of the function $\phi(z)$ is proved from the ODE (3.1.2) by the bootstrapping principle [32].

(ii) The Jacobian operator $\mathcal{H}$ coincides with the Hessian of the energy functional $J(u)$ used in the constrained variational problem in [63]. By Proposition 16 in [63], the one-pulse solution $\phi(z)$ is a global minimizer of $J(u)$ subject to the constraint $K(u) = K_0$, where $K(u) = \int_{\mathbb{R}} u^3 dx$. By Lemma 2.3 in [101], ϕ is a minimizer of the constrained variational problem if $\mathcal{H}$ has exactly one negative eigenvalue. Since the negative eigenvalue corresponds to the ground state of $\mathcal{H}$, the corresponding eigenfunction is even. The kernel of $\mathcal{H}$ includes an eigenvalue with the odd eigenfunction $\phi'(z)$ due to the space translation. The one-pulse solution is isolated, and the kernel of $\mathcal{H}$ is hence simple, due to the duality principle in Theorem 4.1 of [19]. If it is not simple, then global two-dimensional stable and unstable manifolds coincide and the time for a homoclinic orbit to go from the local unstable manifold to the local stable manifold is uniformly bounded. However, a sequence of homoclinic solutions $\{u_n\}_{n\in\mathbb{N}}$ was constructed in [18] such that the time between local manifolds grows linearly in n. By the duality principle, no second even eigenfunction exists in the kernel of $\mathcal{H}$.

(iii) Smoothness of the map $\phi(z)$ from $c > 0$ to $H^2(\mathbb{R})$ is a standard assumption (see Assumption 5.1 in [84]). If $P'(c) > 0$, the one-pulse solution is stable, according to Theorem 4.1 of [84] and Theorem 8.1 of [16]. Therefore, no eigenvalues of $\partial_z\mathcal{H}$ with $\mathrm{Re}(\lambda) > 0$ exist. The two-dimensional algebraic kernel of $\partial_z\mathcal{H}$ follows from the derivatives of the ODE (3.1.2) in z and c:

$$\mathcal{H}\phi'(z) = 0, \qquad \mathcal{H}\partial_c\phi(z) = -\phi(z). \tag{3.2.2}$$

The algebraic kernel of $\partial_z\mathcal{H}$ is exactly two-dimensional under the condition $P'(c) \neq 0$ [95]. □

Theorem 3.2.2 (Two-pulse solutions) *There exists an infinite countable set of two-pulse solutions $\phi(z)$ of the ODE (3.1.2) for $c > \frac{1}{4}$ such that $\phi \in H^2(\mathbb{R}) \cap C^5(\mathbb{R})$, $\phi(-z) = \phi(z)$, $\phi(z) \to 0$ exponentially as $|x| \to \infty$, and $\phi(z)$ resembles two copies of the one-pulse solutions described in Theorem 3.2.1 which are separated by small-amplitude oscillatory tails. The members of the set are distinguished by the distance L between individual pulses which takes the discrete values $\{L_n\}_{n\in\mathbb{N}}$. Moreover, for any small $\delta > 0$ there exists $\gamma > 0$ such that*

$$\left| L_n - \frac{2\pi n}{k_0} - \gamma \right| < \delta, \qquad n \in \mathbb{N}. \tag{3.2.3}$$

Proof. Existence of an infinite sequence of geometrically distinct two-pulse solutions with the distances distributed by (3.2.3) follows by the variational theory in Theorem 1.1 of [19] under the assumption that the single-pulse solution $\phi(z)$ is isolated (up to the space translations). This assumption is satisfied by Theorem 3.2.1(ii). □

The following theorem describes an asymptotic construction of the two-pulse solutions, which is used in the rest of this chapter.

Theorem 3.2.3 *Let $c > \frac{1}{4}$ and $\Phi(z)$ denote the one-pulse solution described by Theorem 3.2.1. Let $L = 2s$ be the distance between two copies of the one-pulse solutions of the ODE (3.1.2) in the decomposition*

$$\phi(z) = \Phi(z - s) + \Phi(z + s) + \varphi(z), \tag{3.2.4}$$

where $\varphi(z)$ is a remainder term. Let $W(L)$ be $C^2(\mathbb{R}_+)$ function defined by

$$W(L) = \int_{\mathbb{R}} \Phi^2(z)\Phi(z + L)dz. \tag{3.2.5}$$

There exists an infinite countable set of extrema of $W(L)$, which is denoted by $\{L_n\}_{n\in\mathbb{N}}$.

(i) Assume that $W''(L_n) \neq 0$ for a given $n \in \mathbb{N}$. There exists a unique symmetric two-pulse solution $\phi(z)$ described by Theorem 3.2.2, such that

$$|L - L_n| \leq C_n e^{-\kappa_0 L}, \qquad \|\varphi\|_{H^2(\mathbb{R})} \leq \tilde{C}_n e^{-\kappa_0 L}, \tag{3.2.6}$$

for some $C_n, \tilde{C}_n > 0$.

(ii) The Jacobian $\mathcal{H}$ associated with the two-pulse solution $\phi(z)$ has exactly two finite negative eigenvalues with even and odd eigenfunctions, a simple kernel with the odd eigenfunction $\phi'(z)$ and a small eigenvalue μ with an even eigenfunction, such that

$$\left| \mu + \frac{2W''(L_n)}{Q(c)} \right| \leq D_n e^{-2\kappa_0 L} \tag{3.2.7}$$

for some $D_n > 0$, where $Q(c) = \|\Phi'\|_{L^2}^2 > 0$. In particular, the small eigenvalue μ is negative when $W''(L_n) > 0$ and positive when $W''(L_n) < 0$.

(iii) There exists a pair of small eigenvalues λ of the linearized operator $\partial_z \mathcal{H}$ associated with the two-pulse solution $\phi(z)$, such that

$$\left|\lambda^2 + \frac{4W''(L_n)}{P'(c)}\right| \leq \tilde{D}_n e^{-2\kappa_0 L}, \tag{3.2.8}$$

for some $\tilde{D}_n > 0$, where $P(c) = \|\Phi\|_{L^2}^2$ and $P'(c) > 0$. In particular, the pair is real when $W''(L_n) < 0$ and purely imaginary (up to the leading order) with negative Krein signature when $W''(L_n) > 0$.

Proof. When the tails of the one-pulse solution $\Phi(z)$ are decaying and oscillatory (i.e. when $c > \frac{1}{4}$), the function $W(L)$ in (3.2.5) is decaying and oscillatory in L and an infinite set of extrema $\{L_n\}_{n\in\mathbb{N}}$ exists. Let us pick L_n for a fixed value of $n \in \mathbb{N}$ such that $W'(L_n) = 0$ and $W''(L_n) \neq 0$.

(i) When the decomposition (3.2.4) is substituted into the ODE (3.1.2), we find the ODE for $\varphi(z)$:

$$\big(c - \partial_z^2 + \partial_z^4 - 2\Phi(z-s) - 2\Phi(z+s)\big)\,\varphi - \varphi^2 = 2\Phi(z-s)\Phi(z+s). \tag{3.2.9}$$

Let $\epsilon = e^{-\kappa_0 L}$ be a small parameter that measures the L^∞-norm of the overlapping term $\Phi(z-s)\Phi(z+s)$ in the sense that for each $\epsilon > 0$ there exist constants $C_0, s_0 > 0$ such that

$$\|\Phi(z-s)\Phi(z+s)\|_{L^\infty} \leq C_0\epsilon \qquad \forall s \geq s_0. \tag{3.2.10}$$

Denote $L = 2s$ and $\epsilon\Psi(z;L) = 2\Phi(z)\Phi(z+L)$ and rewrite the ODE (3.2.9) for $\tilde{\varphi}(z) = \varphi(z+s)$:

$$\big(c - \partial_z^2 + \partial_z^4 - 2\Phi(z)\big)\,\tilde{\varphi} - 2\Phi(z+L)\tilde{\varphi} - \tilde{\varphi}^2 = \epsilon\Psi(z;L). \tag{3.2.11}$$

The vector field of the ODE (3.2.11) is closed in function space $H^2(\mathbb{R})$, while the Jacobian for the one-pulse solution

$$\mathcal{H} = c - \partial_z^2 + \partial_z^4 - 2\Phi(z)$$

has a simple kernel with the odd eigenfunction $\Phi'(z)$ by Theorem 3.2.1(ii). By the Lyapunov–Schmidt reduction method (see [55]), there exists a unique solution $\tilde{\varphi} = \tilde{\varphi}_\epsilon(z;L) \in H^2(\mathbb{R}) : (\Phi', \tilde{\varphi}) = 0$, such that $\tilde{\varphi}_0(z;L) = 0$ and $\tilde{\varphi}_\epsilon(z;L)$ is smooth in ϵ, provided L solves the bifurcation equation $F_\epsilon(L) = 0$, where

$$\begin{aligned} F_\epsilon(L) &= \epsilon\,(\Phi'(z), \Psi(z;L)) + 2\,(\Phi'(z), \Phi(z+L)\tilde{\varphi}_\epsilon(z;L)) + \big(\Phi'(z), \tilde{\varphi}_\epsilon^2(z;L)\big) \\ &= \epsilon\,(\Phi'(z), \Psi(z;L)) - \epsilon\,(\partial_L\Psi(z;L), \tilde{\varphi}_\epsilon(z;L)) - \epsilon\,(\Psi(z;L), \partial_z\tilde{\varphi}_\epsilon(z;L)) \\ &\quad + \big(\Phi'(z), \tilde{\varphi}_\epsilon^2(z;L)\big)\,. \end{aligned}$$

Since $\tilde{\varphi}_\epsilon(z;L)$ is smooth in ϵ and $\tilde{\varphi}_0(z;L) = 0$, then $\|\tilde{\varphi}_\epsilon(z;L)\|_{H^2(\mathbb{R})} \leq C\epsilon$ for some $C > 0$ such that

$$F_\epsilon(L) = -W'(L) + \tilde{F}_\epsilon(L),$$

where $|W'(L)| \leq C_1\epsilon$ and $|\tilde{F}_\epsilon(L)| \leq C_2\epsilon^2$ for some $C_1, C_2 > 0$. The statement follows by the Implicit Function Theorem applied to the scalar equation $\frac{1}{\epsilon}F_\epsilon(L) = 0$ under the assumption that the root L_n of $W'(L)$ is simple.

(ii) The Jacobian $\mathcal{H}$ associated with the two-pulse solution $\phi(z)$ in (3.2.4) has the form:

$$\mathcal{H} = c - \partial_z^2 + \partial_z^4 - 2\Phi(z-s) - 2\Phi(z+s) - 2\varphi(z).$$

In the limit $s \to \infty$, the Jacobian $\mathcal{H}$ has a double negative eigenvalue and a double zero eigenvalue. By a linear combination of eigenfunctions, one can construct one even and one odd eigenfunctions for each of the double eigenvalues. By continuity of eigenvalues of self-adjoint operators, the double negative eigenvalue splits and the two simple eigenvalues remain negative for sufficiently large s. By reversibility of the system, eigenfunctions for simple eigenvalues are either even or odd and by continuity of eigenfunctions, there is exactly one even and one odd eigenfunctions for the two negative eigenvalues. By the translation invariance, the double zero eigenvalue splits into a simple zero eigenvalue which corresponds to the odd eigenfunction $\phi'(z)$ and a small non-zero eigenvalue that corresponds to an even eigenfunction. The splitting of the double zero eigenvalue in the problem $\mathcal{H}v = \mu v$ is considered by the perturbation theory,

$$v(z) = \alpha_1\Phi'(z-s) + \alpha_2\Phi'(z+s) + V(z), \tag{3.2.12}$$

where (α_1, α_2) are coordinates of the projections to the kernel of $\mathcal{H}$ in the limit $s \to \infty$ and $V(z)$ is the remainder term. By projecting the eigenvalue problem $\mathcal{H}v = \mu v$ to the kernel of $\mathcal{H}$ and neglecting the higher-order terms, we obtain a reduced eigenvalue problem:

$$\mu Q(c)\alpha_1 = -\tilde{W}\alpha_1 + W''(L_n)\alpha_2, \qquad \mu Q(c)\alpha_2 = W''(L_n)\alpha_1 - \tilde{W}\alpha_2,$$

where $Q(c) = \|\Phi'\|_{L^2}^2 > 0$, $W''(L_n)$ is computed from (3.2.5) and

$$\tilde{W} = 2\left([\Phi'(z-s)]^2, \varphi(z) + \Phi(z+s)\right) = 2\left([\Phi'(z)]^2, \tilde{\varphi}(z) + \Phi(z+L)\right).$$

Since one eigenvalue must be zero with the odd eigenfunction $\phi'(z)$, the zero eigenvalue corresponds to the eigenfunction (3.2.12) with $\alpha_1 = \alpha_2$ up to the leading order. By looking at the linear system, we find that the zero eigenvalue corresponding to $\alpha_1 = \alpha_2$ exists only if $\tilde{W} = W''(L_n)$. The other eigenvalue at the leading order is $\mu = -2W''(L_n)/Q(c)$ and it corresponds to the even eigenfunction (3.2.12) with $\alpha_1 = -\alpha_2$. By continuity of isolated eigenvalues $\mathcal{H}$ with respect to perturbation terms and estimates of Theorem 2.3(i), we obtain the result (3.2.7).

(iii) In the limit $s \to \infty$, the linearized operator $\partial_z \mathcal{H}$ for the two-pulse solution $\phi(z)$ has a four-dimensional algebraic kernel according to the two-dimensional kernel of the one-pulse solution (3.2.2). By the translation invariance, the two-dimensional algebraic kernel survives for any s with the eigenfunctions $\{\phi'(z), \partial_c \phi(z)\}$. Two eigenvalues λ of the operator $\partial_z \mathcal{H}$ may bifurcate from the zero eigenvalue. The splitting of the zero eigenvalue in the problem $\partial_z \mathcal{H} v = \lambda v$ is considered by the perturbation theory,

$$v(z) = -\alpha_1 \Phi'(z-s) - \alpha_2 \Phi'(z+s) + \beta_1 \partial_c \Phi(z-s) + \beta_2 \partial_c \Phi(z+s) + V(z), \quad (3.2.13)$$

where $(\alpha_1, \alpha_2, \beta_1, \beta_2)$ are coordinates of the projections to the algebraic kernel of $\partial_z \mathcal{H}$ in the limit $s \to \infty$ and $V(z)$ is the remainder term. By projecting the eigenvalue problem $\partial_z \mathcal{H} v = \lambda v$ to the algebraic kernel of the adjoint operator $-\mathcal{H} \partial_z$ and neglecting the higher-order terms, we find at the leading order that $\beta_j = \lambda \alpha_j$, $j = 1, 2$ and (α_1, α_2) satisfy a reduced eigenvalue problem:

$$\frac{1}{2}\lambda^2 P'(c)\alpha_1 = -\tilde{W}\alpha_1 + W''(L_n)\alpha_2, \qquad \frac{1}{2}\lambda^2 P'(c)\alpha_2 = W''(L_n)\alpha_1 - \tilde{W}\alpha_2,$$

where $P(c) = \|\Phi\|_{L^2}^2$ and $\tilde{W} = W''(L_n)$. The non-zero squared eigenvalue λ^2 at the leading order is

$$\lambda^2 = \frac{2Q(c)\mu}{P'(c)} = -\frac{4W''(L_n)}{P'(c)}.$$

Isolated eigenvalues $\partial_z \mathcal{H}$ are continuous with respect to perturbation terms, so that we immediately obtain the result (3.2.8) for $\lambda \in \mathbb{R}$ when $W''(L_n) < 0$. In order to prove (3.2.8) for $\lambda \in i\mathbb{R}$ when $W''(L_n) > 0$, we compute the energy quadratic form at the leading order

$$(\mathcal{H} v, v) = -4W''(L_n) - P'(c)|\lambda|^2,$$

where $v(z)$ is given by the eigenfunction (3.2.13) with $\alpha_1 = -\alpha_2 = 1$ and $\beta_j = \lambda \alpha_j$, $j = 1, 2$. When $\lambda \in i\mathbb{R}$ and $W''(L_n) > 0$, we have $(\mathcal{H} v, v) < 0$ up to the leading order, such that $\lambda \in i\mathbb{R}$ is an eigenvalue of negative Krein signature. Persistence of the eigenvalues of negative Krein signature (even although the eigenvalues $\lambda \in i\mathbb{R}$ are embedded into the continuous spectrum of $\partial_z \mathcal{H}$) follows from the invariant subspace theorem (Theorem 1 in [29]). In the exponentially weighted spaces [96], the eigenvalues of negative Krein signature are isolated and hence continuous, such that they satisfy the bound (3.2.8). □

Remark 3.2.4 Theorem 3.2.3 is a modification of more general Theorems 1 and 2 in [110] (see also [85]). We note that the persistence of eigenvalues (3.2.8) on the imaginary axis for $W''(L_n) > 0$ cannot be proved with the Lyapunov–Schmidt reduction method since the essential spectrum of $\partial_z \mathcal{H}$ occurs on the imaginary axis (contrary to the standard assumption of Theorem 2 in [110] that the essential spectrum is located in the left half-plane.)

The following conjecture from the Gorshkov–Ostrovsky perturbative procedure [56, 57] illustrates the role of $W(L)$ as the effective interaction potential for the slow dynamics of a two-pulse solution:

Conjecture: *Let C_1, C_2 be some positive constants. For the initial time interval $0 \leq t \leq C_1 e^{\kappa_0 L/2}$ and up to the leading order $\mathrm{O}(e^{-\kappa_0 L})$, the two-pulse solutions of the fifth-order KdV equation (3.1.1) can be written as the decomposition*

$$u(x,t) = \Phi(x - ct - s(t)) + \Phi(x - ct + s(t)) + U(x,t),$$

where $\|U\|_{L^\infty} \leq C_2 e^{-\kappa_0 L}$ and the slow dynamics of $L(t) = 2s(t)$ is represented by the Newton law:

$$P'(c)\ddot{L} = -4W'(L). \tag{3.2.14}$$

Although rigorous bounds on the time interval and the truncation error of the Newton law were recently found in the context of NLS solitons in external potentials (see [47]), the above conjecture was not proved yet in the context of two-pulse solutions of the fifth-order KdV equation (3.1.1). We note that perturbation analysis that leads to the Newton law (3.2.14) cannot be used to claim persistence and topological equivalence of dynamics of the second-order ODE (3.2.14) to the full dynamics of two-pulse solutions in the fifth-order KdV equation (3.1.1).

According to Theorem 3.2.3, an infinite set of extrema of $W(L)$ generates a sequence of equilibrium configurations for the two-pulse solutions in Theorem 3.2.2. Since $P'(c) > 0$ by Theorem 3.2.1(iii), the maxima points of $W(L)$ correspond to a pair of real eigenvalues λ of the spectral problem (3.1.5), while the minima points of $W(L)$ correspond to a pair of purely imaginary eigenvalues λ. The two-pulse solutions at the maxima points are thus expected to be linearly and nonlinearly unstable. The two-pulse solutions at the minima points are stable within the leading-order approximation (3.2.8) and within the Newton law (3.2.14) (a particle with the coordinate $L(t)$ performs a periodic oscillation in the potential well). Correspondence of these predictions to the original PDE (3.1.1) is a subject of the present chapter. We will compute the interaction potential $W(L)$ and the sequence of its extrema points $\{L_n\}_{n\in\mathbb{N}}$, as well as the numerical approximations of the two-pulse solutions of the ODE (3.1.2) and of the eigenvalues of the operator $\partial_z \mathcal{H}$ in (3.1.5).

3.3 Modification of the Petviashvili method

We address the Petviashvili method for numerical approximations of solutions of the fourth-order ODE (3.1.2) with $c > 0$. See review of literature on the Petviashvili's method in

[101]. By using the standard Fourier transform

$$\hat{\phi}(k) = \int_{\mathbb{R}} \phi(z) e^{-\imath k z} dz, \qquad k \in \mathbb{R},$$

we reformulate the ODE (3.1.2) as a fixed-point problem in the Sobolev space $H^2(\mathbb{R})$:

$$\hat{\phi}(k) = \frac{\widehat{\phi^2}(k)}{(c + k^2 + k^4)}, \qquad k \in \mathbb{R}, \tag{3.3.1}$$

where $\widehat{\phi^2}(k)$ can be represented by the convolution integral of $\hat{\phi}(k)$ to itself. An even real-valued solution $\phi(-z) = \phi(z)$ of the ODE (3.1.2) in $H^2(\mathbb{R})$ is equivalent to the even real-valued solution $\hat{\phi}(-k) = \hat{\phi}(k)$ of the fixed-point problem (3.3.1). Let us denote the space of all even functions in $H^2(\mathbb{R})$ by $H^2_{\text{ev}}(\mathbb{R})$ and consider solutions of the fixed-point problem (3.3.1) in $H^2_{\text{ev}}(\mathbb{R})$.

Let $\{\hat{u}_n(k)\}_{n=0}^{\infty}$ be a sequence of Fourier transforms in $H^2_{\text{ev}}(\mathbb{R})$ defined recursively by

$$\hat{u}_{n+1}(k) = M_n^2 \frac{\widehat{u_n^2}(k)}{(c + k^2 + k^4)}, \tag{3.3.2}$$

where $\hat{u}_0(k) \in H^2_{\text{ev}}(\mathbb{R})$ is a starting approximation and $M_n \equiv M[\hat{u}_n]$ is the Petviashvili factor defined by

$$M[\hat{u}] = \frac{\int_{\mathbb{R}} (c + k^2 + k^4) \left[\hat{u}(k)\right]^2 dk}{\int_{\mathbb{R}} \hat{u}(k) \widehat{u^2}(k) dk}. \tag{3.3.3}$$

If $u_n \in H^2(\mathbb{R})$, then $u \in L^3(\mathbb{R})$ due to the Sovolev embedding theorem, and both the nominator and denominator of $M[\hat{u}]$ are bounded. It follows from the fixed-point problem (3.3.1) that $M[\hat{\phi}] = 1$ for any solution $\hat{\phi} \in H^2_{\text{ev}}(\mathbb{R})$. The following theorem was proved in [101] and reviewed in [40].

Theorem 3.3.1 *Let $\hat{\phi}(k)$ be a solution of the fixed-point problem (3.3.1) in $H^2_{\text{ev}}(\mathbb{R})$. Let $\mathcal{H}$ be the Jacobian operator (3.1.4) evaluated at the corresponding solution $\phi(z)$ of the ODE (3.1.2). If $\mathcal{H}$ has exactly one negative eigenvalue and a simple zero eigenvalue and if*

$$\text{either} \quad \phi(z) \geq 0 \qquad \text{or} \quad \left| \inf_{z \in \mathbb{R}} \phi(z) \right| < \frac{c}{2}, \tag{3.3.4}$$

then there exists an open neighborhood of $\hat{\phi}$ in $H^2_{\text{ev}}(\mathbb{R})$, in which $\hat{\phi}$ is the unique fixed point and the sequence of iterations $\{\hat{u}_n(k)\}_{n=0}^{\infty}$ in (3.3.2)–(3.3.3) converges to $\hat{\phi}$.

Proof. We review the basic steps of the proof, which is based on the contraction mapping principle in a local neighborhood of $\hat{\phi}$ in $H^2_{\text{ev}}(\mathbb{R})$. The linearization of the iteration map (3.3.2) at the solution ϕ is rewritten in the physical space $z \in \mathbb{R}$ as follows:

$$v_{n+1}(z) = -2\alpha_n \phi(z) + v_n(z) - (c - \partial_z^2 + \partial_z^4)^{-1} \mathcal{H} v_n(z), \tag{3.3.5}$$

where α_n is a projection of v_n onto ϕ^2 in $L^2(\mathbb{R})$:

$$\alpha_n = \frac{(\phi^2, v_n)}{(\phi^2, \phi)},$$

such that $u_n = \phi + v_n$ and $M_n = 1 - \alpha_n$ to the linear order. The operator $\mathcal{T} = (c - \partial_z^2 + \partial_z^4)^{-1}\mathcal{H}$ is a self-adjoint operator in Pontryagin space Π_0 defined by the inner product

$$\forall f, g \in \Pi_0 : \quad [f, g] = ((c - \partial_z^2 + \partial_z^4)f, g).$$

See [29] for review of Pontryagin spaces and the invariant subspace theorem. Since $c > 0$, the Pontryagin space Π_0 has zero index and, by the invariant subspace theorem, the operator $\mathcal{T}$ in Π_0 has exactly one negative eigenvalue, a simple kernel and infinitely many positive eigenvalues. (Since $\mathcal{T}$ is an identity operator with a compact perturbation, the spectrum of $\mathcal{T}$ is purely discrete.) The eigenfunctions for the negative and zero eigenvalues are known exactly as

$$\mathcal{T}\phi = -\phi, \qquad \mathcal{T}\phi'(z) = 0.$$

Due to orthogonality of the eigenfunctions in the Pontryagin space Π_0 and the relation

$$\phi^2 = (c - \partial_z^2 + \partial_z^4)\phi,$$

we observe that α_n is a projection of v_n to ϕ in Π_0, which satisfies the trivial iteration map:

$$\alpha_{n+1} = 0, \qquad n \geq 1,$$

no matter what the value of α_0 is. In addition, projection of v_n to ϕ' in Π_0 is zero since $v_n \in H^2_{\text{ev}}(\mathbb{R})$. As a result, the linearized iteration map (3.3.5) defines a contraction map if the maximal positive eigenvalue of $\mathcal{T}$ in $L^2(\mathbb{R})$ is smaller than 2. However,

$$\sigma\left(\mathcal{T}\Big|_{L^2}\right) - 1 \leq -2 \inf_{\|u\|_{L^2}=1} \left(u, (c - \partial_z^2 + \partial_z^4)^{-1}\phi(z)u\right). \tag{3.3.6}$$

If $\phi(z) \geq 0$ on $z \in \mathbb{R}$, the right-hand-side of (3.3.6) is zero. Otherwise, the right-hand-side of (3.3.6) is bounded from above by $\frac{2}{c}\left|\inf_{z\in\mathbb{R}} \phi(z)\right|$, which leads to the condition (3.3.4). □

Corollary 3.3.2 *Let $\phi(z)$ be a one-pulse solution of the ODE (3.1.2) with $c > 0$ defined by Theorem 3.2.1. Then, the iteration method (3.3.2)–(3.3.3) converges to $\phi(z)$ in a local neighborhood of ϕ in $H^2_{\text{ev}}(\mathbb{R})$ provided that the condition (3.3.4) is met.*

The condition (3.3.4) is satisfied for the positive exact solution (3.1.3) for $c = \frac{36}{169}$. Since the one-pulse solution is positive definite for $0 < c < \frac{1}{4}$ [5], it is also satisfied for

all values of $c \in \left(0, \frac{1}{4}\right)$. However, the solution is sign-indefinite for $c \geq \frac{1}{4}$, such that the condition (3.3.4) must be checked *a posteriori*, after a numerical approximation of the solution is obtained.

Besides the convergence criterion described in Theorem 3.3.1, there are additional factors in the numerical approximation of the one-pulse solution of the ODE (3.1.2) which comes from the discretization of the Fourier transform, truncation of the resulting Fourier series, and termination of iterations within the given tolerance bound. These three numerical factors are accounted by three numerical parameters:

(i) d - the half-period of the computational interval $z \in [-d, d]$ where the solution $\phi(z)$ is represented by the Fourier series for periodic functions;

(ii) N - the number of terms in the partial sum for the truncated Fourier series such that the grid size h of the discretization is $h = 2d/N$;

(iii) ε - the small tolerance distance that measures deviation of M_n from 1 and the distance between two successive approximations, such that the method can be terminated at the iteration n if

$$E_M \equiv |M_n - 1| < \varepsilon \qquad \text{and} \qquad E_\infty \equiv \|u_{n+1} - u_n\|_{L^\infty} < \varepsilon.$$

and $\tilde{\phi} \equiv u_n(z)$ can be taken as the numerical approximation of the solution $\phi(z)$.

The numerical approximation depends weakly of the three numerical parameters, provided (i) d is much larger than the half-width of the one-pulse solution, (ii) N is sufficiently large for convergence of the Fourier series, and (iii) ε is sufficiently small above the level of the round-off error. Indeed, the constraint (i) ensures that the truncation error is exponentially small when the one-pulse solution is replaced by the periodic sequence of one-pulse solutions in the trigonometric approximation [111]. The constraint (ii) ensures that the remainder of the Fourier partial sum is smaller than any inverse power of N (by Theorem 3.2.1(i), all derivatives of the function $\phi(z)$ are continuous) [119]. The constraint (iii) specifies the level of accuracy achieved when the iterations of the method (3.3.2)–(3.3.3) are terminated. While we do not proceed with formal analysis of the three numerical factors (see [40] for an example of this analysis), we illustrate the weak dependence of three numerical factors on the example of the numerical approximation $\tilde{\phi}(z)$ of the exact one-pulse solution (3.1.3), which exists for $c = \frac{36}{169}$. Numerical implementation of the iteration method (3.3.2)–(3.3.3) was performed in MATLAB according to a standard toolbox of the spectral methods [119].

Figure 3.1 displays the distance $E = \|\tilde{\phi} - \phi\|_{L^\infty}$ versus the three numerical factors d, h, and ε described above. The left panel shows that the error E converges to the numerical zero, which is $O(10^{-15})$ in MATLAB under the Windows platform, when the

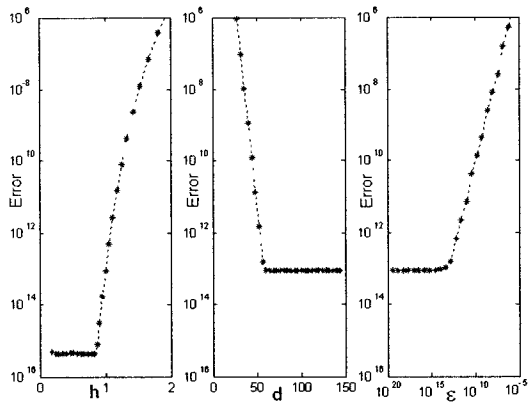

Figure 3.1: The distance $E = \|\tilde{\phi} - \phi\|_{L^\infty}$ for the ODE (3.1.2) with $c = \frac{36}{169}$ versus the half-period d of the computational interval, the step size h of the discretization, and the tolerance bound ε.

step size h is reduced, while $d = 50$ and $\varepsilon = 10^{-15}$ are fixed. The middle panel computed for $h = 1$ and $\varepsilon = 10^{-15}$ shows that the error E converges to the level $O(10^{-13})$ when the half-width d is enlarged. The numerical zero is not reached in this case, because the step size h is not sufficiently small. The right panel computed for $h = 1$ and $d = 50$ shows that the error E converges to the same level $O(10^{-13})$ as the tolerance bound ε is reduced. In all approximations that follow, we will specify $h = 0.01$, $d = 50$ and $\varepsilon = 10^{-15}$ to ensure that the error of the iteration method (3.3.2)–(3.3.3) for one-pulse solutions is on the level of the numerical zero $O(10^{-15})$.

Figure 3.2 (left) shows the numerical approximation of the one-pulse solutions for $c = 4$, where the small-amplitude oscillations of the exponentially decaying tail are visible. We check a posteriori the condition (3.3.4) for non-positive one-pulse solutions $|\inf_{z\in\mathbb{R}} \phi(z)| < 2$ for $c = 4$. *Figure 3.2* (right) displays convergence of the errors $E_M = |M_n - 1|$ and $E_\infty = \|u_{n+1} - u_n\|_{L^\infty}$ computed dynamically at each n as n increases. We can see that the error E_M converges to zero much faster than the error E_∞, in agreement with the decomposition of the linearized iterative map (3.3.5) into the one-dimensional projection α_n and the infinite-dimensional orthogonal compliment (see the proof of Theorem 3.3.1). In all further approximations, we will use the error E_∞ for termination of iterations and detecting its minimal values since E_∞ is more sensitive compared to E_M.

Figure 3.3 shows the dependence of $\tilde{P}(c) = \|\tilde{\phi}\|^2_{L^2(\mathbb{R})}$ on $c > 0$. Since the dependence of $\tilde{P}(c)$ is strictly increasing and the approximation error is controlled in the numerical method, the assumption of Theorem 2.1(iii) that $P'(c) > 0$ is verified.

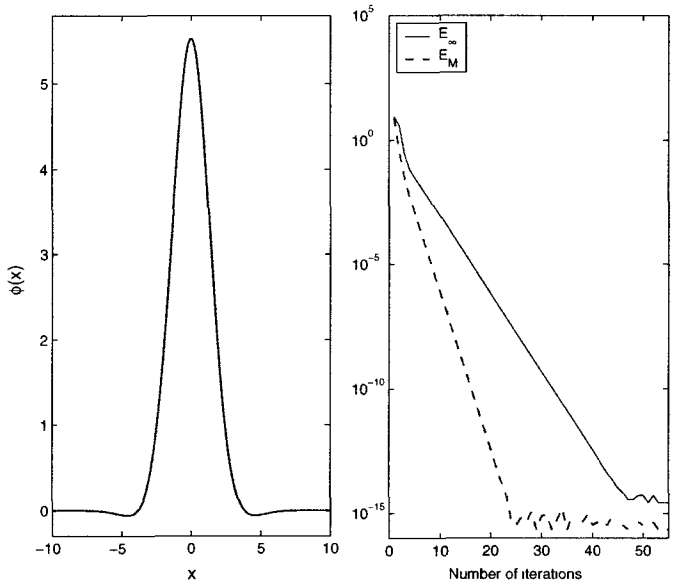

Figure 3.2: One-pulse solutions of the ODE (3.1.2) with $c = 4$ (left) and convergence of the errors E_M and E_∞ to zero versus the number of iterations n.

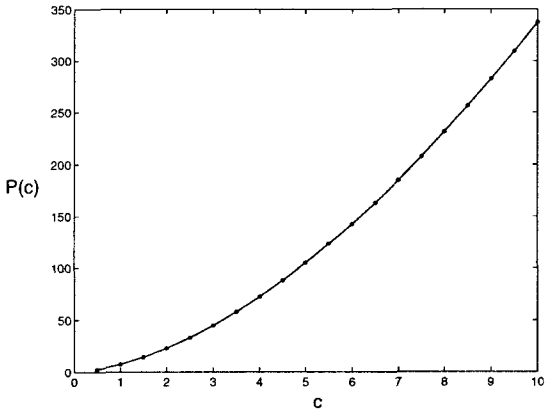

Figure 3.3: The squared L^2-norm of the one-pulse solutions of the ODE (3.1.2) versus c.

Since the numerical approximations $\tilde{\phi}(z)$ of one-pulse solutions can be computed for any value of $c > 0$, one can use $\tilde{\phi}(z)$ for a given c and compute the effective interaction potential (3.2.5), which defines the extremal values $\{L_n\}_{n\in\mathbb{N}}$. Theorem 3.2.3 guarantees that the two-pulse solution $\phi(z)$ consists of two copies of the one-pulse solutions separated by the distance L near the point L_n where $W'(L_n) = 0$ and $W''(L_n) \neq 0$. Table 1 shows the first four values of the sequence $\{L_n\}_{n=1}^{\infty}$ for $c = 1$ (where $s_n = L_n/2$ is the half-distance between the pulses). It also shows the corresponding values from the first four numerical approximations of two-pulse solutions $\phi(z)$ (obtained below) and the computational error computed from the difference of the two numerical approximations. We can see that the error decreases for larger indices n in the sequence $\{L_n\}_{n\in\mathbb{N}}$ since the Lyapunov–Schmidt reductions of Theorem 3.2.3 become more and more accurate in this limit.

solution	effective potential	root finding	error
$s = s_1$	5.058733328146916	5.079717398028492	0.02098406988158
$s = s_2$	8.196800619090793	8.196620796452045	$1.798226387474955 \cdot 10^{-4}$
$s = s_3$	11.338414567609066	11.338406246900558	$8.320708507980612 \cdot 10^{-6}$
$s = s_4$	14.479997655627219	14.479996635578457	$1.020048761901649 \cdot 10^{-6}$

Table 1: The first four members of the sequence of two-pulse solutions for $c = 1$.

By Theorem 3.2.3(ii), the Jacobian operator $\mathcal{H}$ associated with a two-pulse solution $\phi(z)$ has one finite negative eigenvalue in the space of even functions and one small eigenvalue which is either negative or positive depending on the sign of $W''(L_n)$. This small eigenvalue leads to either weak divergence or weak convergence of the Petviashvili method in a local neighborhood of ϕ in $H^2_{\text{ev}}(\mathbb{R})$. Even if the small eigenvalue is positive and the algorithm is weakly convergent, the truncation error from the numerical discretization may push the small eigenvalue to a negative value and lead thus to weak divergence of the iterations.

Figure 3.4 illustrates typical behaviors of the errors E_M and E_∞ versus n for the starting approximation

$$u_0(z) = U_0(z - s) + U_0(z + s), \tag{3.3.7}$$

where $U_0(z)$ is a starting approximation of a sequence $\{u_n(z)\}_{n\in\mathbb{N}}$ which converges to the one-pulse solution $\Phi(z)$ and s is a parameter defined near $L_n/2$ for the two-pulse solution $\phi(z)$. The left panel shows iterations for s near s_1 and the right panel shows iterations for s near s_2. Since $W''(L_1) > 0$ and $W''(L_2) < 0$, the iteration method (3.3.2)–(3.3.3) diverges weakly near the former solution, while it converges weakly near the latter solution.

At the initial stage of iterations, both errors E_M and E_∞ quickly drops to small values, since the starting iterations $U_0(z \mp s)$ converge to the one-pulse solutions $\Phi(z \mp s)$ while the contribution from the overlapping tails of $\Phi(z \mp s)$ is negligible. However, at

the later stage of iterations, both errors either start to grow (the left panel of *Figure 3.4*) or stop to decrease (the right panel). As it is explained above, this phenomenon is related to the presence of zero eigenvalue of $\mathcal{H}$ in the space of even functions which bifurcates to either positive or negative values due to overlapping tails of $\Phi(z \mp s)$ and due to the truncation error. At the final stage of iterations on the left panel of *Figure 3.4*, the numerical approximation $u_n(z)$ converges to the one-pulse solution $\Phi(z)$ centered at $z = 0$ and both errors quickly drop to the numerical zero, which occurs similarly to the right panel of *Figure 3.2*. No transformation of the solution shape occurs for large n on the right panel of *Figure 3.4*.

The following theorem defines an effective numerical algorithm, which enables us to compute the two-pulse solutions from the weakly divergent iterations of the Petviashvili's method (3.3.2)–(3.3.3).

Theorem 3.3.3 *Let $\phi(z)$ be the two-pulse solution of the ODE (3.1.2) defined by Theorems 3.2.2 and 3.2.3. There exists $s = s_*$ near $s = L_n/2$ such that the iteration method (3.3.2)–(3.3.3) with the starting approximation $u_0(z) = \Phi(z - s) + \Phi(z + s)$ converges to $\phi(z)$ in $H^2_{\rm ev}(\mathbb{R})$.*

Proof. The iteration operator (3.3.2)–(3.3.3) in a neighborhood of the two-pulse solution $\phi(z)$ in $H^2_{\rm ev}(\mathbb{R})$ can be represented into an abstract form

$$v_{n+1} = M(\epsilon)v_n + N(v_n, \epsilon), \qquad n \in \mathbb{N},$$

where the linear operator $M(\epsilon)$ has a unit eigenvalue at $\epsilon = 0$ and the nonlinear vector field $N(v_n, \epsilon)$ is C^∞ in $v_n \in H^2_{\rm ev}$ and $\epsilon \in \mathbb{R}$, such that $N(0,0) = D_v N(0,0) = 0$. Here v_n is a perturbation of u_n to the fixed point ϕ and ϵ is a small parameter for two-pulse solutions defined in Theorem 3.2.3. By the Center Manifold Reduction for quasi-linear discrete systems (Theorem 1 in [48]), there exists a one-dimensional smooth center manifold in a local neighborhood of ϕ in $H^2_{\rm ev}(\mathbb{R})$. Let ξ be a coordinate of the center manifold such that $\xi \in \mathbb{R}$, $\xi = 0$ corresponds to $v = 0$, and the dynamics on the center manifold is

$$\xi_{n+1} = \mu(\epsilon)\xi_n + f(\xi_n, \epsilon), \qquad n \in \mathbb{N},$$

where $\mu(\epsilon)$ satisfies $\mu(0) = 1$ and $f(\xi_n, \epsilon)$ is C^∞ in $\xi \in \mathbb{R}$ and $\epsilon \in \mathbb{R}$, such that $f(0,0) = \partial_\xi f(0,0) = 0$. Consider the one-parameter starting approximation $u_0(z) = \Phi(z - s) + \Phi(z + s)$ in a neighborhood of ϕ in $H^2_{\rm ev}(\mathbb{R})$, where s is close to the value $s = s_n$ defined in Theorem 3.2.3. By the time evolution of the hyperbolic component of v_n (see Lemma 2 in [48]), the sequence v_n approaches to the center manifold with the coordinate ξ_n. Iterations of ξ_n are sign-definite in a neighborhood of $\xi = 0$. Moreover, there exists $s_1 < s_n$ and $s_2 > s_n$, such that the sequences $\{\xi_n(s_1)\}_{n\in\mathbb{N}}$ and $\{\xi_n(s_2)\}_{n\in\mathbb{N}}$ are of opposite signs. By smoothness of v_n and ξ_n from parameter s, there exists a root s_* in between $s_1 < s_* < s_2$ such that $\xi_n(s_*) = 0$ for all $n \in \mathbb{N}$. □

Remark 3.3.4 The proof of Theorem 3.3.3 does not require that the root s_* be unique for the one-parameter starting approximation $u_0(z) = \Phi(z - s) + \Phi(z + s)$. Our numerical computations starting with a more general approximation (3.3.7) show, however, that the root s_* is unique near $s = s_n$.

To capture the two-pulse solutions according to Theorem 3.3.3, we compute the minimum of the error E_∞ for different values of s and find numerically a root $s = s_*$ of the function

$$f(s) = \min_{0 \le n \le n_0} (E_\infty),$$

where n_0 is the first iterations after which the value of E_{infty} increases (in case of the left panel of *Figure 3.4*) or remains unchanged (in case of the right panel of *Figure 3.4*). The numerical root $s = s_*$ is found by using the secant method:

$$s_k = \frac{s_{k-2} f(s_{k-1}) - s_{k-1} f(s_{k-2})}{f(s_{k-1}) - f(s_{k-2})}. \tag{3.3.8}$$

The Petviashvili method (3.3.2)–(3.3.3) with the starting approximation (3.3.7) where s is close to the root $s = s_*$ near the point $s = s_n$ converges to the two-pulse solution $\phi(z)$ within the accuracy of the round-off error.

Figure 3.5 shows the graph of $f(s)$ near the value $s = s_1$ for $c = 1$. (The graph of $f(s)$ near $s = s_2$ as well as other values of s_n look similar to *Figure 3.5*.) The left panel shows uniqueness of the root, while the right panel shows the linear behavior of $f(s)$ near $s = s_*$ which indicates that the root is simple. Numerical approximations for the first four values of the sequence $\{s_n\}_{n \in \mathbb{N}}$ obtained in this root finding algorithm are shown in Table 1. We note that the number of iterations N_{h} of the secant method (3.3.8) decreases with larger values of n, such that $N_{\text{h}} = 14$ for $n = 1$, $N_{\text{h}} = 12$ for $n = 2$, $N_{\text{h}} = 10$ for $n = 3$ and $N_{\text{h}} = 9$ for $n = 4$, while the number of iterations of the Petviashili method for each computation does not exceed 100 iterations.

Figure 3.6 shows numerical approximations of the two-pulse solutions for $c = 1$ and $c = 4$. We can see from the right panel that two-pulse solutions with $c = 4$ resemble the two copies of the one-pulse solutions from the left panel of *Figure 3.2*, separated by the small-amplitude oscillatory tails.

Finally, the three-pulse and multi-pulse solutions of the fixed-point problem (3.1.2) cannot be approximated numerically with the use of the Petviashili method (3.3.2). The Jacobian operator $\mathcal{H}$ associated with the three-pulse solution has two finite negative eigenvalues and one small eigenvalue in the space of even functions, while the stabilizing factor of Theorem 3.3.1 and the root finding algorithm of Theorem 3.3.3 can only be useful for one finite negative eigenvalue and one zero eigenvalue. The additional finite negative eigenvalue introduces a *strong* divergence of the iterative method (3.3.2) which leads to failure of numerical approximations for three-pulse solutions. This numerical problem remains open for further analysis.

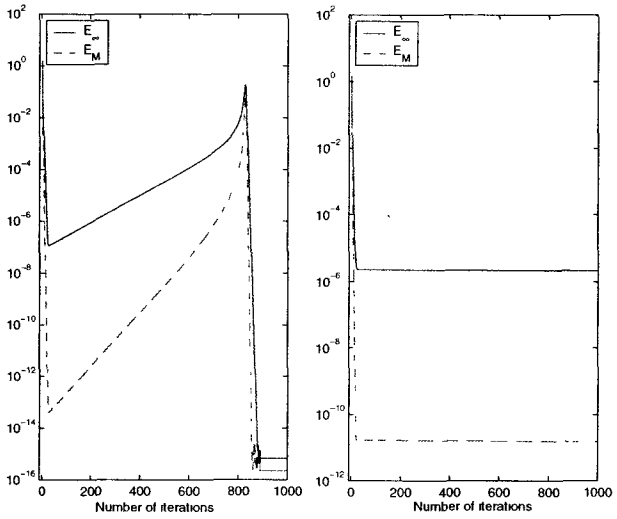

Figure 3.4: Errors E_M and E_∞ versus the number of iterations n for the starting approximation (3.3.7) with $s = 5.079$ (left panel) and $s = 8.190$ (right panel). The other parameters are: $c = 1$, $d = 50$, $h = 0.01$ and $\varepsilon = 10^{-15}$.

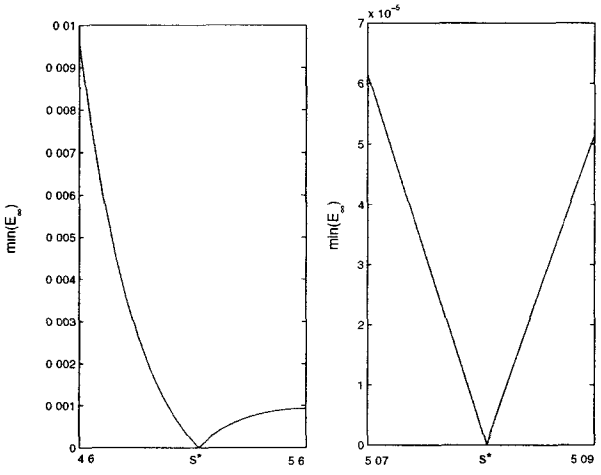

Figure 3.5: Minimal value of E_∞ versus s near $s_1 = 5.080$ (left panel) and the zoom of the graph, which shows the linear behavior of $f(s)$ near the root (right panel).

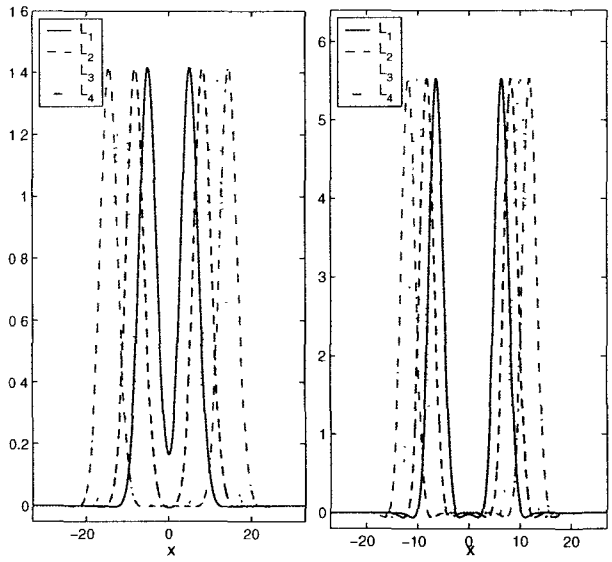

Figure 3.6: Numerical approximation of the first four two-pulse solutions of the ODE (3.1.2) for $c = 1$ (left) and $c = 4$ (right).

3.4 Application: KdV two-pulse solitons

We address spectral stability of the two-pulse solution by analyzing the linearized problem (3.1.5), where the operator $\mathcal{H} : H^4(\mathbb{R}) \mapsto L^2(\mathbb{R})$ is the Jacobian operator (3.1.4) evaluated at the two-pulse solution $\phi(z)$.

By Theorem 3.2.3(ii), operator $\mathcal{H}$ has two finite negative eigenvalue, a simple kernel and one small eigenvalue, which is negative when $W''(L_n) > 0$ and positive when $W''(L_n) < 0$. Persistence (structural stability) of these isolated eigenvalues beyond the leading order (3.2.7) is a standard property of perturbation theory of self-adjoint operators in Hilbert spaces (see Section IV.3.5 in [75]).

By Theorem 3.2.3(iii), operator $\partial_z \mathcal{H}$ has a pair of small eigenvalues, which are purely imaginary when $W''(L_n) > 0$ and real when $W''(L_n) < 0$. We first prove that no other eigenvalues may induce instability of two-pulse solutions (i.e. no other bifurcations of eigenvalues of $\partial_z \mathcal{H}$ with $\mathrm{Re}(\lambda) > 0$ may occur). We then prove persistence (structural stability) of the purely imaginary eigenvalues beyond the leading order (3.2.8). Combined together, these two results lead to the theorem on spectral stability of the two-pulse solution $\phi(z)$ that corresponds to L_n with $W''(L_n) > 0$.

Theorem 3.4.1 *Let $N_{\rm real}$ be the number of real positive eigenvalues of the linearized prob-*

lem (3.1.5), N_{comp} *be the number of complex eigenvalues in the first open quadrant, and* N_{imag}^{-} *be the number of simple positive imaginary eigenvalues with* $(\mathcal{H}v, v) \leq 0$*, where* $v(x)$ *is the corresponding eigenfunction for* $\lambda \in i\mathbb{R}_+$*. Assume that no multiple imaginary eigenvalues exist, the kernel of* $\mathcal{H}$ *is simple and* $P'(c) > 0$*, where* $P = \|\phi\|_{L^2}^2$*. Then,*

$$N_{\text{real}} + 2N_{\text{comp}} + 2N_{\text{imag}}^{-} = n(\mathcal{H}) - 1, \tag{3.4.1}$$

where $n(\mathcal{H})$ *is the number of negative eigenvalues of* $\mathcal{H}$*.*

Proof. The statement is equivalent to Theorem 6 in [29] in the case $(\mathcal{H}^{-1}\phi, \phi) = -(\partial_c \phi, \phi) = -\frac{1}{2}P'(c) < 0$. The result follows from the invariant subspace theorem in the Pontryagin space Π_κ, where $\kappa = n(\mathcal{H})$. □

Corollary 3.4.2 *Let* $\phi(z) \equiv \Phi(z)$ *be a one-pulse solution defined by Theorem 3.2.1. Then, it is a spectrally stable ground state in the sense that* $N_{\text{real}} = N_{\text{comp}} = N_{\text{imag}}^{-} = 0$*.*

Remark 3.4.3 Figure 3.3 confirms that $P'(c) > 0$ for the one-pulse solution. In addition, it is shown in Lemma 4.12 and Remark 4.14 in [29] that multiple imaginary eigenvalues may only occur if $(\mathcal{H}v, v) = 0$ such that $n(\mathcal{H}) \geq 2$ is a necessary condition for existence of multiple eigenvalues (with $P'(c) > 0$). No multiple imaginary eigenvalues exists for the one-pulse solution $\Phi(z)$.

Corollary 3.4.4 *Let* $\phi(z)$ *be a two-pulse solution defined by Theorem 3.2.3. Then,*

(i) the solution corresponding to L_n *with* $W''(L_n) < 0$ *is spectrally unstable in the sense that* $N_{\text{real}} = 1$ *and* $N_{\text{comp}} = N_{\text{imag}}^{-} = 0$ *for sufficiently large* L_n

(ii) the solution corresponding to L_n *with* $W''(L_n) > 0$ *satisfies* $N_{\text{real}} = 0$ *and* $N_{\text{comp}} + N_{\text{imag}}^{-} = 1$ *for sufficiently large* L_n*.*

Proof. It follows from Theorems 3.2.1 and 3.2.3 for sufficiently large L_n that the kernel of $\mathcal{H}$ is simple for $W''(L_n) \neq 0$ and the only pair of imaginary eigenvalues with $(\mathcal{H}v, v) < 0$ in the case $W_n''(L_n) > 0$ is simple. Therefore, assumptions of Theorem 3.4.1 are satisfied for the two-pulse solutions $\phi(z)$ with $W''(L_n) \neq 0$. By the count of Theorem 3.2.3(ii), $n(\mathcal{H}) = 3$ for $W''(L_n) > 0$ and $n(\mathcal{H}) = 2$ for $W''(L_n) < 0$. Furthermore, persistence (structural stability) of simple real eigenvalues of the operator $\partial_z \mathcal{H}$ follows from the perturbation theory of isolated eigenvalues of non-self-adjoint operators (see Section VIII.2.3 in [75]). □

There exists one uncertainty in Corollary 3.4.4(ii) since it is not clear if the eigenvalue of negative Krein signature in Theorem 3.2.3(iii) remains imaginary in N_{imag}^{-} or bifurcates to a complex eigenvalue in N_{comp}. This question is important for spectral stability

of the corresponding two-pulse solutions since the former case implies stability while the latter case implies instability of solutions. We will remove the uncertainty and prove that $N_{\text{imag}}^{-} = 1$ and $N_{\text{comp}} = 0$ for sufficiently large L_n. To do so, we rewrite the linearized problem (3.1.5) in the exponentially weighted space [96]:

$$L^2_\alpha = \left\{ v \in L^2_{\text{loc}}(\mathbb{R}) : \ e^{\alpha z} v(z) \in L^2(\mathbb{R}) \right\}. \tag{3.4.2}$$

The linearized operator $\partial_z \mathcal{H}$ transforms to the form

$$\mathcal{L}_\alpha = (\partial_z - \alpha)\left(c - (\partial_z - \alpha)^2 + (\partial_z - \alpha)^4 - 2\phi(z)\right), \tag{3.4.3}$$

which acts on the eigenfunction $v_\alpha(z) = e^{\alpha z} v(z) \in L^2(\mathbb{R})$. The absolute continuous part of the spectrum of $\mathcal{L}_\alpha$ is located at $\lambda = \lambda_\alpha(k)$, where

$$\lambda_\alpha(k) = (ik - \alpha)(c - (ik - \alpha)^2 + (ik - \alpha)^4), \qquad k \in \mathbb{R}. \tag{3.4.4}$$

A simple analysis shows that

$$\begin{aligned} \frac{d}{dk}\text{Re}(\lambda_\alpha(k)) &= -2\alpha k(10k^2 - 10\alpha^2 + 3), \\ \frac{d}{dk}\text{Im}(\lambda_\alpha(k)) &= c - 3\alpha^2 + 5\alpha^4 + 3k^2(1 - 10\alpha^2) + 5k^4. \end{aligned}$$

The following lemma gives a precise location of the dispersion relation $\lambda = \lambda_\alpha(k)$ on $\lambda \in \mathbb{C}$.

Lemma 3.4.5 *The dispersion relation $\lambda = \lambda_\alpha(k)$ is a simply-connected curve located in the left half-plane of $\lambda \in \mathbb{C}$ if*

$$0 < \alpha < \frac{1}{\sqrt{10}}, \qquad c > \frac{1}{4}. \tag{3.4.5}$$

Proof. The mapping $k \mapsto \text{Im}(\lambda_\alpha)$ is one-to-one provided that $c - 3\alpha^2 + 5\alpha^4 > 0$ and $1 - 10\alpha^2 > 0$. Since $c - 3\alpha^2 + 5\alpha^4$ reaches the minimum value on $\alpha \in \left[0, \frac{1}{\sqrt{10}}\right]$ at the right end $\alpha = \frac{1}{\sqrt{10}}$ and the minimum value is positive if $c > \frac{1}{4}$, the first inequality is satisfied under (3.4.5). The second inequality is obviously satisfied if $|\alpha| < \frac{1}{\sqrt{10}}$. The mapping $k \mapsto \text{Re}(\lambda_\alpha)$ has a single extremal point at $k = 0$ provided $3 - 10\alpha^2 > 0$, which is satisfied if $|\alpha| < \frac{1}{\sqrt{10}}$. The extremal point is the point of maximum and the entire curve is located in the left half-plane of $\lambda \in \mathbb{C}$ if $0 < \alpha < \frac{1}{\sqrt{10}}$. □

The following two lemmas postulate properties of eigenfunctions corresponding to embedded eigenvalues of negative Krein signature.

Lemma 3.4.6 *Let $v_0(z)$ be an eigenfunction of $\partial_z\mathcal{H}$ for a simple eigenvalue $\lambda_0 \in i\mathbb{R}_+$ in $L^2(\mathbb{R})$. Then, $\lambda_0 \in i\mathbb{R}_+$ is also an eigenvalue in $L^2_\alpha(\mathbb{R})$ for sufficiently small α.*

Proof. Let $k = k_0 \in \mathbb{R}$ be the unique real root of the dispersion relation $\lambda_0(k) = \lambda_0$ (with $\alpha = 0$) for a given eigenvalue $\lambda_0 \in i\mathbb{R}_+$. The other four roots $k = k_{1,2,3,4}$ for a given $\lambda_0 \in i\mathbb{R}_+$ are complex with $|\mathrm{Re}(k_j)| \geq \kappa_0 > 0$. By the Stable and Unstable Manifolds Theorem in linearized ODEs [31], the decaying eigenfunction $v_0(z) \in L^2(\mathbb{R})$ is exponentially decaying with the decay rate greater than $\kappa_0 > 0$ and it does not include the bounded term $e^{ik_0 z}$ as $z \to \pm\infty$. By construction, $v_\alpha(z) = e^{\alpha z}v_0(z)$ is also exponentially decaying as $z \to \pm\infty$ for sufficiently small $|\alpha| < \kappa_0$. Since $v_0 \in L^2(\mathbb{R})$ and due to the exponential decay of $v_\alpha(z)$ as $|z| \to \infty$, we have $v_\alpha \in L^2(\mathbb{R})$ for any small α. □

Lemma 3.4.7 *Let $v_0(z) \in H^2(\mathbb{R})$ be an eigenfunction of $\partial_z\mathcal{H}$ for a simple eigenvalue $\lambda_0 \in i\mathbb{R}_+$ with $(\mathcal{H}v_0, v_0) < 0$. Then, there exists $w_0 \in H^2(\mathbb{R})$, such that $v_0 = w_0'(x)$ and $w_0(z)$ is an eigenfunction of $\mathcal{H}\partial_z$ for the same eigenvalue λ_0. Moreover, $(w_0, v_0) \in i\mathbb{R}_+$.*

Proof. Since $\mathcal{H} : H^4(\mathbb{R}) \mapsto L^2(\mathbb{R})$, the eigenfunction $v_0(z)$ of the eigenvalue problem $\partial_z\mathcal{H}v_0 = \lambda_0 v_0$ for any $\lambda_0 \neq 0$ must satisfy the constraint $\int_{\mathbb{R}} v_0(z)dz = 0$. Let $v_0 = w_0'(z)$. Since $v_0(z)$ decays exponentially as $|z| \to \infty$ and $(1, v_0) = 0$, then $w_0(z)$ decays exponentially as $|z| \to \infty$, so that $w_0 \in H^2(\mathbb{R})$. By construction, $\mathcal{H}\partial_z w_0 = \mathcal{H}v_0 = \lambda_0 \int v_0(z)dz = \lambda w_0$. The values of (w_0, v_0) are purely imaginary as

$$\overline{(w_0, v_0)} = \int_{\mathbb{R}} \bar{w}_0 v_0 dz = \int_{\mathbb{R}} \bar{w}_0 \partial_z w_0 dz = -\int_{\mathbb{R}} w_0 \partial_z \bar{w}_0 dz = -\int_{\mathbb{R}} w_0 \bar{v}_0 dz = -(w_0, v_0).$$

Since $\mathcal{H}v_0 = \lambda_0 w_0$ with $\lambda_0 \in i\mathbb{R}_+$ and $(\mathcal{H}v_0, v_0) < 0$, we have (w_0, v_0) $= \lambda_0^{-1}(\mathcal{H}v_0, v_0) \in i\mathbb{R}_+$. □

The following theorem states that the embedded eigenvalues of negative Krein signature are structurally stable in the linearized problem (3.1.5).

Theorem 3.4.8 *Let $\lambda_0 \in i\mathbb{R}_+$ be a simple eigenvalue of $\partial_z\mathcal{H}$ with the eigenfunction $v_0 \in H^2(\mathbb{R})$ such that $(\mathcal{H}v_0, v_0) < 0$. Then, it is structurally stable to parameter continuations, e.g. for any $V \in L^\infty(\mathbb{R})$ and sufficiently small δ, there exists an eigenvalue $\lambda_\delta \in i\mathbb{R}_+$ of $\partial_z(\mathcal{H} + \delta V(z))$ in $H^2(\mathbb{R})$, such that $|\lambda_\delta - \lambda_0| \leq C\delta$ for some $C > 0$.*

Proof. By Lemma 3.4.6, λ_0 is also an eigenvalue of $\mathcal{L}_\alpha$ in $L^2(\mathbb{R})$ for sufficiently small α. Let α be fixed in the bound (3.4.5). There exists a small neighborhood of λ_0, which is isolated from the absolute continuous part of the spectrum of $\mathcal{L}_\alpha$. By the perturbation theory of isolated eigenvalues of non-self-adjoint operators (see Section VIII.2.3 in [75]), there exists a simple eigenvalue λ_δ of $\partial_z(\mathcal{H} + \delta V(z))$ in $L^2_\alpha(\mathbb{R})$ for the same value of α

and sufficiently small δ in a local neighborhood of λ_0, such that $|\lambda_\delta - \lambda_0| \leq C\delta$ for some $C > 0$.

It remains to show that the simple eigenvalue λ_δ is purely imaginary for the same value of $\alpha > 0$. Denote the eigenfunction of $\partial_z(\mathcal{H} + \delta V(z))$ in $H^2_\alpha(\mathbb{R})$ for the eigenvalue λ_δ by $v_\delta(z)$, such that $e^{\alpha z}v_\delta \in H^2(\mathbb{R})$. If $v_\delta \notin H^2(\mathbb{R})$, then the count of eigenvalues (3.4.1) is discontinuous at $\delta = 0$: the eigenvalue λ_0 in the number N^-_{imag} at $\delta = 0$ disappears from the count for $\delta \neq 0$. If $v_\delta \in H^2(\mathbb{R})$, then $(1, v_\delta) = 0$ and since $v_\delta(z)$ is exponentially decaying as $|z| \to \infty$, there exists $w_\delta(z) \in H^2(\mathbb{R})$ such that $v_\delta = w_\delta'(z)$. The 2-form (w_δ, v_δ) is invariant with respect to the weight α since if $e^{\alpha z}v_\delta(z)$ is an eigenfunction of $\partial_z(\mathcal{H}+\delta V(z))$ for the eigenvalue λ_δ (i.e. $v_\delta \in H^2_\alpha(\mathbb{R})$), then $e^{-\alpha z}w_\delta(z)$ is an eigenfunction of $(\mathcal{H} + \delta V(z))\partial_z$ for the same eigenvalue λ_δ (i.e. $w_\delta \in H^2_{-\alpha}(\mathbb{R})$). Computing (w_δ, v_δ) at $\alpha = 0$, we have

$$\lambda_\delta(w_\delta, v_\delta) = (\mathcal{H}v_\delta, v_\delta) \in \mathbb{R}.$$

Since (w_δ, v_δ) is continuous in δ and $(w_\delta, v_\delta) \in i\mathbb{R}$ by Lemma 3.4.7, then $\lambda_\delta \in i\mathbb{R}$ for any $\delta \neq 0$. □

Corollary 3.4.9 *Let $\phi(z)$ be a two-pulse solution defined by Theorem 3.2.3 that corresponds to L_n with $W''(L_n) > 0$. Then, it is spectrally stable in the sense that $N_{\text{real}} = N_{\text{comp}} = 0$ and $N^-_{\text{imag}} = 1$ for sufficiently large L_n.*

Remark 3.4.10 Using perturbation theory in exponentially weighted spaces for a fixed value $\alpha > 0$, one cannot a priori exclude the shift of eigenvalue λ_0 to λ_δ with $\text{Re}(\lambda_\delta) > 0$. Even if $v_0(z)$ for λ_0 contains no term $e^{ik_0 z}$ as $z \to -\infty$ (see Lemma 3.4.6), the eigenfunction $v_\delta(z)$ for λ_δ may contain the term $e^{ik_\delta z}$ as $z \to -\infty$ with $\text{Im}(k_\delta) < 0$ and $\lim_{\delta\to 0} k_\delta = k_0 \in \mathbb{R}$. However, when Theorem 3.4.8 holds (that is under the assumptions that $v_0 \in H^2(\mathbb{R})$ and $(\mathcal{H}v_0, v_0) < 0$), the eigenvalue λ_δ remains on $i\mathbb{R}$ and the eigenfunction $v_\delta(z)$ must have no term $e^{ik_\delta z}$ with $k_\delta \in \mathbb{R}$ as $z \to -\infty$ for any sufficiently small δ. The hypothetical bifurcation above can however occur if $v_0 \notin H^2(\mathbb{R})$ but $v_0 \in H^2_\alpha(\mathbb{R})$ with $\alpha > 0$. We do not know any example of such a bifurcation.

Remark 3.4.11 When the potential is symmetric (i.e. $\phi(-z) = \phi(z)$), the stability problem $\partial_z\mathcal{H}v = \lambda v$ admits a symmetry reduction: if $v(z)$ is an eigenfunction for λ, then $\overline{v(-z)}$ is the eigenfunction for $-\bar{\lambda}$. If $\lambda_0 \in i\mathbb{R}$ is a simple eigenvalue and $v_0 \in H^2_\alpha(\mathbb{R})$ with $\alpha \geq 0$, the above symmetry shows that $v_0 \in H^2_{-\alpha}(\mathbb{R})$ with $-\alpha \leq 0$. If $\text{Re}(\lambda_\delta) > 0$ and $v_\delta \in H^2_\alpha(\mathbb{R})$, then $-\overline{v_\delta(-z)} \in H^2_{-\alpha}(\mathbb{R})$ is an eigenfunction of the same operator for eigenvalue $\text{Re}(-\overline{\lambda_\delta}) = -\text{Re}(\lambda_\delta)$ and $\text{Im}(-\overline{\lambda_\delta}) = \text{Im}(\lambda_\delta)$. Thus, the hypothetical bifurcation in Remark 3.4.10 implies that the embedded eigenvalue $\lambda_0 \in i\mathbb{R}$ may split into two isolated eigenvalues λ_δ and $-\overline{\lambda_\delta}$ as $\delta \neq 0$. Theorem 3.4.8 shows that such splitting is impossible if $v_0 \in H^2(\mathbb{R})$ and $(\mathcal{H}v_0, v_0) < 0$.

We confirm results of Corollaries 3.4.4 and 3.4.9 with numerical computations of eigenvalues in the linearized problem (3.1.5). Throughout computations, we use the values $\alpha = 0.04$ and $c = 1$, which satisfy the constraint (3.4.5). The spectra of the operators $\mathcal{H}$ in $L^2(\mathbb{R})$ and $\partial_z\mathcal{H}$ in $L^2_\alpha(\mathbb{R})$ are computed by using the Fourier spectral method. This method is an obvious choice since the solution $\phi(z)$ is obtained by using the spectral approximations in the iterative scheme (3.3.2)–(3.3.3). As in the previous section, we use numerical parameters $d = 100$, $h = 0.01$ and $\varepsilon = 10^{-15}$ for the Petviashvili method (3.3.2)–(3.3.3).

Eigenvalues of the discretized versions of the operators $\mathcal{H}$ and $\mathcal{L}_\alpha$ are obtained with the MATLAB eigenvalue solver `eig`. The spectra are shown on *Figure 3.7* for the two-pulse solution $\phi_1(z)$ and on *Figure 3.8* for the two-pulse solution $\phi_2(z)$. The inserts show zoomed eigenvalues around the origin and the dotted line connects eigenvalues of the discretized operators that belong to the absolutely continuous part of the spectra. *Figures 3.7* and *3.8* clearly illustrate that the small eigenvalue of $\mathcal{H}$ is negative for $\phi_1(z)$ and positive for $\phi_2(z)$, while the pair of small eigenvalues of $\mathcal{L}_\alpha$ is purely imaginary for $\phi_1(z)$ and purely real for $\phi_2(z)$. This result is in agreement with Corollaries 3.4.4 and 3.4.9. We have observed the same alternation of small eigenvalues for two-pulse solutions $\phi_3(z)$ and $\phi_4(z)$, as well as for other values of parameters c and α.

The numerical discretization based on the Fourier spectral method shifts eigenvalues of the operators $\mathcal{H}$ and $\mathcal{L}_\alpha$. In order to measure the numerical error introduced by the discretization, we compute the numerical value for the "zero" eigenvalue corresponding to the simple kernel of $\mathcal{H}$ and the double zero eigenvalue of $\mathcal{L}_\alpha$. Table II shows numerical values for the "zero" and small eigenvalues for two-pulse solutions $\phi_n(z)$ with $n = 1, 2, 3, 4$. It is obvious from the numerical data that the small eigenvalues are still distinguished (several orders higher) than the numerical approximations for zero eigenvalues for $n = 1, 2, 3$ but they become comparable for higher-order two-pulse solutions $n \geq 4$. This behavior is understood from Theorem 3.2.3 since the small eigenvalues becomes exponentially small for larger values of s (larger n) in the two-pulse solution (3.2.4) and the exponentially small contribution is negligible compared to the numerical error of discretization.

	$\phi_1(z)$	$\phi_2(z)$	$\phi_3(z)$	$\phi_4(z)$
"Zero" EV of $\mathcal{H}$	$1.216 \cdot 10^{-9}$	$2.668 \cdot 10^{-9}$	$1.474 \cdot 10^{-9}$	$1.894 \cdot 10^{-9}$
Small EV of $\mathcal{H}$	$1.785 \cdot 10^{-2}$	$7.664 \cdot 10^{-5}$	$3.334 \cdot 10^{-7}$	$2.921 \cdot 10^{-9}$
"Zero" EVs of $\mathcal{L}_\alpha$	$0.365 \cdot 10^{-5}$	$0.532 \cdot 10^{-5}$	$0.783 \cdot 10^{-5}$	$1.237 \cdot 10^{-5}$
Re of small EVs of $\mathcal{L}_\alpha$	$4.529 \cdot 10^{-6}$	$3.285 \cdot 10^{-3}$	$6.326 \cdot 10^{-5}$	$1.652 \cdot 10^{-5}$
Im of small EVs of $\mathcal{L}_\alpha$	$0.502 \cdot 10^{-1}$	$1.152 \cdot 10^{-8}$	$2.167 \cdot 10^{-4}$	$5.444 \cdot 10^{-6}$

Table II: Numerical approximations of the zero and small eigenvalues (EVs) of operators $\mathcal{H}$ and $\mathcal{L}_\alpha$ for the first four two-pulse solutions with $c = 1$, $\alpha = 0.04$, $d = 100$, $h = 0.01$ and $\varepsilon = 10^{-15}$. The absolute values are shown.

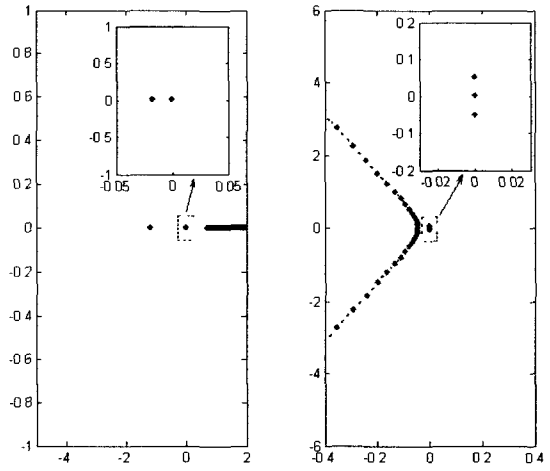

Figure 3.7: Numerical approximations of the spectra of operators $\mathcal{H}$ and $\mathcal{L}_\alpha$ for the two-pulse solution $\phi_1(z)$ with $c = 1$ and $\alpha = 0.04$. The insert shows zoom of small eigenvalues and the dotted curve connects eigenvalues of the continuous spectrum of $\mathcal{L}_\alpha$.

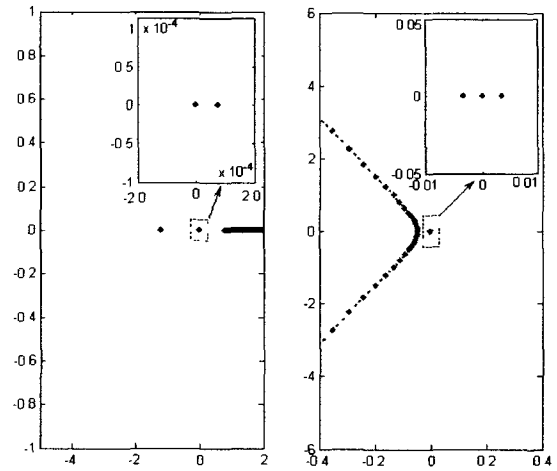

Figure 3.8: The same as Figure 3.7 but for the two-pulse solution $\phi_2(z)$.

We have confirmed numerically the analytical predictions that all two-pulse solutions corresponding to the points L_n with $W''(L_n) < 0$ (which are maxima of the effective interaction potential) are unstable with a simple real positive eigenvalue, while all two-pulse solutions corresponding to the points L_n with $W''(L_n) > 0$ (which are minima of the effective interaction potential) are spectrally stable. The stable two-pulse solutions are not however ground states since the corresponding linearized problem has a pair of eigenvalues of negative Krein signature.

3.5 Nonlinear dynamics of two-pulse solution

The Newton law (3.2.14) is a useful qualitative tool to understand the main results of this chapter. Existence of an infinite countable sequence of two-pulse solution $\{\phi_n(z)\}_{n\in\mathbb{N}}$ is related to existence of extremal points $\{L_n\}_{n\in\mathbb{N}}$ of the effective potential function $W(L)$, while alternation of stability and instability of the two-pulse solutions is related to the alternation of minima and maxima points of $W(L)$. It is natural to ask if the Newton law (3.2.14) extends beyond the existence and spectral stability analysis of two-pulse solutions in the fifth-order KdV equation (3.1.1). In particular, one can ask if the purely imaginary (embedded) eigenvalues of the linearized problem (3.1.5) lead to nonlinear asymptotic stability of two-pulse solutions or at least to their nonlinear stability in the sense of Lyapunov. From a more technical point of view, one can ask whether the Newton law (3.2.14) serves as the center manifold reduction for slow nonlinear dynamics of two-pulse solutions in the PDE (3.1.1) and whether solutions of the full problem are topologically equivalent to solutions of the Newton law. While we do not attempt to develop mathematical analysis of these questions, we illustrate nonlinear dynamics of two-pulse solutions with explicit numerical simulations.

The numerical pseudo-spectral method for solutions of the fifth-order KdV equation (3.1.1) is described in details in [89]. The main idea of this method is to compute analytically the linear part of the PDE (3.1.1) by using the Fourier transform and to compute numerically its nonlinear part by using an ODE solver. Let $\hat{u}(k,t)$ denote the Fourier transform of $u(x,t)$ and rewrite the PDE (3.1.1) in the Fourier domain (since the solution decays exponentially, the Fourier domain can be applied as a substitution for the unbounded domain):

$$\hat{u}_t = i(k^3 + k^5)\hat{u} - ik\widehat{u^2}. \tag{3.5.1}$$

In order to compute $\widehat{u^2}(k,t)$ we evaluate $u^2(x,t)$ on $x \in \mathbb{R}$ and apply the discrete Fourier transform. Substitution $\hat{u} = s(k,t)e^{i(k^3+k^5)t}$ transforms the evolution equation (3.5.1) to the form:

$$s_t = -ike^{-i(k^3+k^5)t}\widehat{u^2}(k,t). \tag{3.5.2}$$

The fourth-order Runge-Kutta method is used to integrate the evolution equation (3.5.2) in time with time step $\triangle t$. To avoid large variations of the exponent for large values of k and

t, the substitution above is updated after m time steps as follows:

$$\hat{u} = s_m(k,t)e^{i(k^3+k^5)(t-m\triangle t)}, \qquad m\triangle t \leq t \leq (m+1)\triangle t. \tag{3.5.3}$$

The greatest advantage of this numerical method is that no stability restriction arising from the linear part of (3.5.1) is posed on the timestep of numerical integration. On contrast, the standard explicit method for the fifth-order KdV equation (3.1.1) has a serious limitation on the timestep of the numerical integration since the fifth-order derivative term brings stiffness to the evolution problem. The small timestep would be an obstacle for the long time integration of the evolution problem due to accumulation of computational errors.

Numerical simulations of the PDE (3.5.1) are started with the initial condition:

$$u(x,0) = \Phi(x-s) + \Phi(x+s), \tag{3.5.4}$$

where $\Phi(x)$ is the one-pulse solution and $2s$ is the initial separation between the two pulses. The one-pulse solution $\Phi(x)$ is constructed with the iteration method (3.3.2)–(3.3.3) for $c = 4$. The numerical factors of the spectral approximation are $L = 100$, $N = 2^{12}$, $\varepsilon = 10^{-15}$, while the timestep is set to $\triangle t = 10^{-4}$.

Figure 3.9 shows six individual simulations of the initial-value problem (3.5.1) and (3.5.4) with $s = 2.3$, $s = 2.8$, $s = 3.6$, $s = 4.2$, $s = 4.5$ and $s = 4.7$. *Figure 3.10* brings these six individual simulations on the effective phase plane $(L, \dot{L})$ computed from the distance $L(t)$ between two local maxima (humps) of the two-pulse solutions.

When the initial distance ($s = 2.3$) is taken far to the left from the stable equilibrium point (which corresponds to the two-pulse solution $\phi_1(x)$), the two pulses repel and diverge from each other (trajectory 1). When the initial distance ($s = 2.8$) is taken close to the left from the stable equilibrium point, we observe small-amplitude oscillations of two pulses relative to each other (trajectory 2). When the initial distances ($s = 3.6$) and ($s = 4.2$) are taken to the right from the stable equilibrium point, we continue observing stable oscillations of larger amplitudes and larger period (trajectories 3 and 4). The oscillations are destroyed when the initial distances are taken close to the unstable equilibrium point (which corresponds to the two-pulse solution $\phi_2(x)$) from either left ($s = 4.5$) or right ($s = 4.7$). In either case, the two pulses repel and diverge from each other (trajectories 5 and 6). Ripples in the pictures are due to radiation effect and the numerical integration does not make sense after $t \approx 500$, because the ripples reach the left end of the computational interval and appear from the right end due to periodic boundary conditions.

The numerical simulations of the full PDE problem (3.1.1) indicate the validity of the Newton law (3.2.14). Due to the energy conservation, all equilibrium points in the Newton law are either centers or saddle points and the center points are surrounded by closed periodic orbits in the interior of homoclinic loops from the stable and unstable manifolds of the saddle points. Trajectories 2,3, and 4 are taken inside the homoclinic orbit from the saddle point corresponding to $\phi_2(x)$ and these trajectories represent periodic oscillations

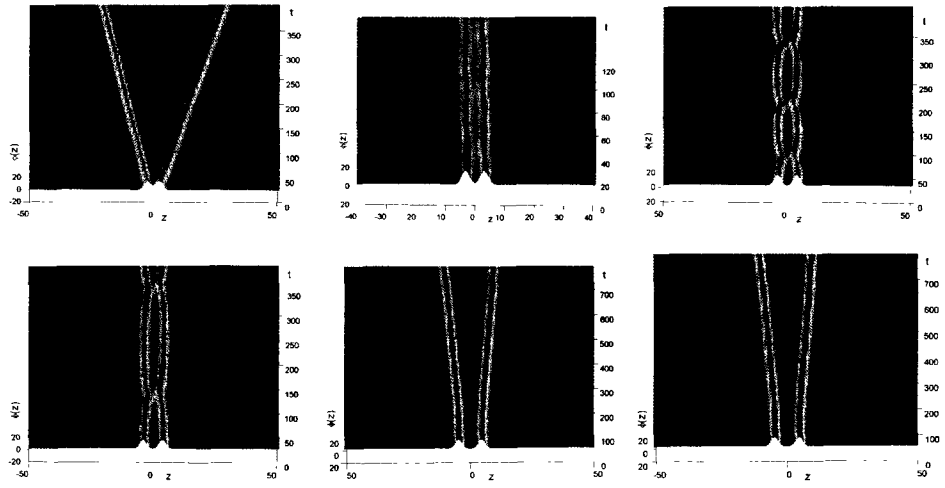

Figure 3.9: Individual simulations of the initial data (3.5.4) with $s = 2.3$ (top left), $s = 2.8$ (top right), $s = 3.6$ (middle left), $s = 4.2$ (middle right), $s = 4.5$ (bottom left) and 4.7 (bottom right).

of two-pulse solutions near the center point corresponding to $\phi_1(x)$. Trajectories 1 and 6 are taken outside the homoclinic orbit and correspond to unbounded dynamics of two-pulse solutions. The only exception from the Newton law (3.2.14) is trajectory 5, which is supposed to occur inside the homoclinic loop but turns out to occur outside the loop. This discrepancy can be explained by the fact that the Newton law (3.2.14) does not *exactly* represent the dynamics of the PDE (3.5.1) generated by the initial condition (3.5.4) but it corresponds to an *asymptotic* solution after the full solution is projected into the discrete and continuous parts and the projection equations are truncated (see details in [47] in the context of the NLS equations).

Summarizing, we have studied existence, spectral stability and nonlinear dynamics of two-pulse solutions of the fifth-order KdV equation. We have proved that the two-pulse solutions can be numerically approximated by the Petviashili method supplemented with a root finding algorithm. We have also proved structural stability of embedded eigenvalues with negative Krein signature and this result completes the proof of spectral stability of two-pulse solutions related to the minima points of the effective interaction potential. The validity of the Newton law is illustrated by the full numerical simulations of the fifth-order KdV equation (3.1.1).

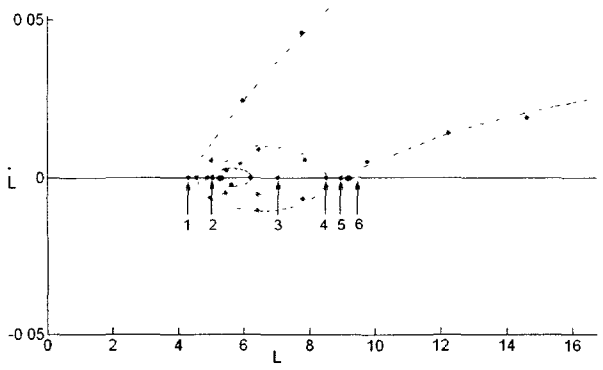

Figure 3.10: The effective phase plane $(L, \dot{L})$ for six simulations on Figure 3.9, where L is the distance between two pulses. The black dots denote stable and unstable equilibrium points which correspond to the two-pulse solutions $\phi_1(x)$ and $\phi_2(x)$.

CHAPTER 4

BLOCK DIAGONALIZATION OF THE COUPLED-MODE SYSTEM

4.1 Introduction

Various applications in nonlinear optics [118], photonics band-gap engineering [69] and atomic physics [34] call for systematic studies of the *coupled-mode system*, which is expressed by two first-order semi-linear PDEs in one space and one time dimensions. In nonlinear optics, the coupled-mode system describes counter-propagating light waves, which interact with a linear grating in an optical waveguide [117]. In photonics, the coupled-mode system is derived for coupled resonant waves in stop bands of a low-contrast three-dimensional photonic crystal [3]. In atomic physics, the coupled-mode system describes matter-wave Bose-Einstein condensates trapped in an optical lattice [102]. Existence, stability and nonlinear dynamics of *gap solitons*, which are localized solutions of the coupled-mode system, are fundamental problems for interest in the aforementioned physical disciplines.

In the context of spectral stability of gap solitons, it has been discovered that the linearized coupled-mode equations are equivalent to a four-by-four Dirac system with sign-indefinite metric, where numerical computations of eigenvalues represent a difficult numerical task. The pioneer work in [9, 10] showed that spurious unstable eigenvalues originate from the continuous spectrum in the Fourier basis decomposition and the Galerkin approximation. A delicate but time-consuming implementation of the continuous Newton method was developed to identify the "right" unstable eigenvalues from the spurious ones [9, 10]. Similar problems were discovered in the variational method [76, 77] and in the numerical finite-difference method [114, 115].

While some conclusions on instability bifurcations of gap solitons in the coupled-mode equations can be drawn on the basis of perturbation theory [9] and Evans function methods [73, 100], the numerical approximation of eigenvalues was an open problem until recently. A new progress was made with the use of exterior algebra in the numerical computations of the Evans function [41], when the same results on instability bifurcations of gap solitons as in [9] were recovered. Similar shooting method was also applied to gap solitons in a more general model of a nonlinear Schrödinger equation with a periodic potential [102].

Our work addresses the problem of numerical approximations of eigenvalues of the linearized coupled-mode system with a different objective. We will show that the linearized coupled-mode system with a symmetric potential function can be block-diagonalized into two coupled two-by-two Dirac systems. The two Dirac systems represent the linearized Hamiltonian of the coupled-mode equations and determine instability bifurcations and unstable eigenvalues of gap solitons.

The purpose of block-diagonalization is twofold. First, the number of unstable eigenvalues can be estimated analytically from the number of non-zero isolated eigenvalues of the linearized Hamiltonian. This analysis will be reported elsewhere. Second, a numerical algorithm can be developed to compute efficiently the entire spectrum of the linearized coupled-mode system. These numerical results are reported here for an example of symmetric quadric potential functions.

The chapter is organized as follows. *Section 4.2* describes the model and its symmetries. *Section 4.3* gives construction and properties of gap solitons in the nonlinear coupled-mode system. *Section 4.4* presents block-diagonalization of the linearized coupled-mode system. *Section 4.5* contains numerical computations of the spectrum of the block-diagonalized system. *Section 4.6* presents examples of gap solitons for various models.

4.2 Coupled-mode system

We consider the Hamiltonian coupled-mode system in the form:

$$\begin{cases} i(u_t + u_x) + v = \partial_{\bar{u}} W(u, \bar{u}, v, \bar{v}) \\ i(v_t - v_x) + u = \partial_{\bar{v}} W(u, \bar{u}, v, \bar{v}) \end{cases} \tag{4.2.1}$$

where $(u, v) \in \mathbb{C}^2$, $x \in \mathbb{R}$, $t \geq 0$, and $W(u, \bar{u}, v, \bar{v})$ is real-valued. We assume that the potential function satisfies the following three conditions:

(i) W is invariant with respect to the gauge transformation: $(u, v) \mapsto e^{i\alpha}(u, v)$, for all $\alpha \in \mathbb{R}$

(ii) W is symmetric with respect to the interchange: $(u, v) \mapsto (v, u)$

(iii) W is analytic in its variables near $u = v = 0$, such that $W = O(4)$.

The first property is justified by the standard derivation of the coupled-mode system (4.2.1) with an envelope approximation [3]. The second property defines a class of symmetric nonlinear potentials. Although it is somewhat restrictive, symmetric nonlinear potentials are commonly met in physical applications of the system (4.2.1). The third property is related to the normal form analysis [113], where the nonlinear functions are approximated by Taylor polynomials. Since the quadratic part of the potential function

is written in the left-hand-side of the system (4.2.1) and the cubic part violates the gauge transformation and analyticity assumptions, the Taylor polynomials of W start with quadric terms, denoted as $O(4)$.

We find a general representation of the function $W(u,\bar{u},v,\bar{v})$ that satisfies the conditions (1)-(3) and list all possible (four-parameter) quadric terms of W.

Lemma 4.2.1 *If $W \in \mathbb{C}$ and property (1) is satisfied, such that*

$$W(u,\bar{u},v,\bar{v}) = W\left(ue^{\imath\alpha},\bar{u}e^{-\imath\alpha},ve^{\imath\alpha},\bar{v}e^{-\imath\alpha}\right), \qquad \forall\alpha\in\mathbb{R}, \tag{4.2.2}$$

then $W = W(|u|^2,|v|^2,u\bar{v})$.

Proof. By differentiating (4.2.2) in α and setting $\alpha = 0$, we have the differential identity:

$$DW \equiv i\left(u\frac{\partial}{\partial u} - \bar{u}\frac{\partial}{\partial\bar{u}} + v\frac{\partial}{\partial v} - \bar{v}\frac{\partial}{\partial\bar{v}}\right)W(u,\bar{u},v,\bar{v}) = 0. \tag{4.2.3}$$

Consider the set of quadratic variables

$$z_1 = |u|^2, \quad z_2 = |v|^2, \quad z_3 = \bar{u}v, \quad z_4 = u^2,$$

which is independent for any $u \neq 0$ and $v \neq 0$ in the sense that the Jacobian is non-zero. It is clear that $Dz_{1,2,3} = 0$ and $Dz_4 = 2z_4$. Therefore, $DW = 2z_4\partial_{z_4}W = 0$, such that $W = W(z_1,z_2,z_3)$. □

Corollary 4.2.2 *If $W \in \mathbb{R}$ and property (1) is met, then*

$$W = W(|u|^2,|v|^2,u\bar{v}+v\bar{u}).$$

Lemma 4.2.3 *If $W \in \mathbb{R}$ and properies (1)-(3) are satisfied, then*

$$W = W(|u|^2+|v|^2,|u|^2|v|^2,u\bar{v}+v\bar{u}).$$

Proof. By Corollary 4.2.2 and property (2), we can re-order the arguments of W as $W = W(|u|+|v|,|u||v|,u\bar{v}+v\bar{u})$. By analyticity in property (3), W may depend only on $|u|^2$ and $|v|^2$ rather than on $|u|$ and $|v|$. □

Corollary 4.2.4 *If $W \in \mathbb{R}$ and properties (1)-(3) are satisfied, then*

$$\left(u\frac{\partial}{\partial u} + \bar{u}\frac{\partial}{\partial\bar{u}} - v\frac{\partial}{\partial v} - \bar{v}\frac{\partial}{\partial\bar{v}}\right)W(u,\bar{u},v,\bar{v})\Big|_{|u|^2=|v|^2} = 0 \tag{4.2.4}$$

Corollary 4.2.5 *The only quadric potential function $W \in \mathbb{R}$ that satisfies properties (1)-(3) is given by*

$$W = \frac{a_1}{2}(|u|^4 + |v|^4) + a_2|u|^2|v|^2 + a_3(|u|^2 + |v|^2)(v\bar{u} + \bar{v}u) + \frac{a_4}{2}(v\bar{u} + \bar{v}u)^2, \quad (4.2.5)$$

where (a_1, a_2, a_3, a_4) are real-valued parameters. It follows then that

$$\begin{cases} \partial_{\bar{u}} W = a_1|u|^2u + a_2u|v|^2 + a_3\left[(2|u|^2 + |v|^2)v + u^2\bar{v}\right] + a_4\left[v^2\bar{u} + |v|^2u\right] \\ \partial_{\bar{v}} W = a_1|v|^2v + a_2v|u|^2 + a_3\left[(2|v|^2 + |u|^2)u + v^2\bar{u}\right] + a_4\left[u^2\bar{v} + |u|^2v\right] \end{cases}$$

The potential function (4.2.5) with $a_1, a_2 \neq 0$ and $a_3 = a_4 = 0$ represents a standard coupled-mode system for a sub-harmonic resonance, e.g. in the context of optical gratings with constant Kerr nonlinearity [118]. When $a_1 = a_3 = a_4 = 0$, this system is integrable with inverse scattering and is referred to as the massive Thirring model [78]. When $a_1 = a_2 = 0$ and $a_3, a_4 \neq 0$, the coupled-mode system corresponds to an optical grating with varying, mean-zero Kerr nonlinearity, where a_3 is the Fourier coefficient of the resonant sub-harmonic and a_4 is the Fourier coefficient of the non-resonant harmonic [3] (see also [110]).

We rewrite the coupled-mode system (4.2.1) as a Hamiltonian system in complex-valued matrix-vector notations:

$$\frac{d\mathbf{u}}{dt} = J\nabla H(\mathbf{u}), \quad (4.2.6)$$

where $\mathbf{u} = (u, \bar{u}, v, \bar{v})^T$,

$$J = \begin{bmatrix} 0 & -i & 0 & 0 \\ i & 0 & 0 & 0 \\ 0 & 0 & 0 & -i \\ 0 & 0 & i & 0 \end{bmatrix} = -J^T,$$

and $H(u, \bar{u}, v, \bar{v}) = \int_{\mathbb{R}} h(u, \bar{u}, v, \bar{v})dx$ is the Hamiltonian functional with the density:

$$h = W(u, \bar{u}, v, \bar{v}) - (v\bar{u} + u\bar{v}) + \frac{i}{2}(u\bar{u}_x - u_x\bar{u}) - \frac{i}{2}(v\bar{v}_x - v_x\bar{v}).$$

The Hamiltonian $H(u, \bar{u}, v, \bar{v})$ is constant in time $t \geq 0$. Due to the gauge invariance, the coupled-mode system (4.2.1) has another constant of motion $Q(u, \bar{u}, v, \bar{v})$, where

$$Q = \int_{\mathbb{R}} \left(|u|^2 + |v|^2\right) dx. \quad (4.2.7)$$

Conservation of Q can be checked by direct computation:

$$\frac{\partial}{\partial t}(|u|^2 + |v|^2) + \frac{\partial}{\partial x}(|u|^2 - |v|^2) = DW = 0, \quad (4.2.8)$$

where the operator D is defined in (4.2.3). Due to the translational invariance, the coupled-mode system (4.2.1) has yet another constant of motion $P(u, \bar{u}, v, \bar{v})$, where

$$P = \frac{i}{2}\int_{\mathbb{R}} (u\bar{u}_x - u_x\bar{u} + v\bar{v}_x - v_x\bar{v})\, dx. \tag{4.2.9}$$

In applications, the quantities Q and P are referred to as the power and momentum of the coupled-mode system.

4.3 Existence of gap solitons

Stationary solutions of the coupled-mode system (4.2.1) take the form:

$$\begin{cases} u_{\rm st}(x,t) = u_0(x+s)e^{i\omega t+\imath\theta} \\ v_{\rm st}(x,t) = v_0(x+s)e^{i\omega t+\imath\theta} \end{cases} \tag{4.3.1}$$

where $(s, \theta) \in \mathbb{R}^2$ are arbitrary parameters, while the solution $(u_0, v_0) \in \mathbb{C}^2$ on $x \in \mathbb{R}$ and the domain for parameter $\omega \in \mathbb{R}$ are to be found from the nonlinear ODE system:

$$\begin{cases} iu_0' = \omega u_0 - v_0 + \partial_{\bar{u}_0} W(u_0, \bar{u}_0, v_0, \bar{v}_0) \\ -iv_0' = \omega v_0 - u_0 + \partial_{\bar{v}_0} W(u_0, \bar{u}_0, v_0, \bar{v}_0) \end{cases} \tag{4.3.2}$$

Stationary solutions are critical points of the Lyapunov functional:

$$\Lambda = H(u, \bar{u}, v, \bar{v}) + \omega Q(u, \bar{u}, v, \bar{v}), \tag{4.3.3}$$

such that variations of Λ produce the nonlinear ODE system (4.3.2).

Lemma 4.3.1 *Assume that there exists a decaying solution (u_0, v_0) of the system (4.3.2) on $x \in \mathbb{R}$. If $W \in \mathbb{R}$ satisfies properties (1)-(3), then $u_0 = \bar{v}_0$ (module to an arbitrary phase).*

Proof. It follows from the balance equation (4.2.8) for the stationary solutions (4.3.1) that

$$|u_0|^2 - |v_0|^2 = C_0 = 0, \qquad \forall x \in \mathbb{R},$$

where the constant $C_0 = 0$ is found from decaying conditions at infinity. Let us represent the solutions (u_0, v_0) in the form:

$$\begin{cases} u_0(x) = \sqrt{Q(x)}e^{\imath\Theta(x)+\imath\Phi(x)} \\ v_0(x) = \sqrt{Q(x)}e^{-\imath\Theta(x)+\imath\Phi(x)} \end{cases} \tag{4.3.4}$$

such that

$$\begin{cases} iQ' - 2Q(\Theta' + \Phi') = 2\omega Q - 2Qe^{-2\imath\Theta} + 2\bar{u}_0\partial_{\bar{u}_0} W(u_0, \bar{u}_0, v_0, \bar{v}_0) \\ -iQ' - 2Q(\Theta' - \Phi') = 2\omega Q - 2Qe^{2\imath\Theta} + 2\bar{v}_0\partial_{\bar{v}_0} W(u_0, \bar{u}_0, v_0, \bar{v}_0) \end{cases} \tag{4.3.5}$$

Separating the real parts, we obtain

$$\begin{cases} Q(\cos(2\Theta) - \omega - \Theta' - \Phi') = \mathrm{Re}\,[\bar{u}_0 \partial_{\bar{u}_0} W(u_0, \bar{u}_0, v_0, \bar{v}_0)] \\ Q(\cos(2\Theta) - \omega - \Theta' + \Phi') = \mathrm{Re}\,[\bar{v}_0 \partial_{\bar{v}_0} W(u_0, \bar{u}_0, v_0, \bar{v}_0)] \end{cases} \tag{4.3.6}$$

By Corollary 4.2.4, we have $\Phi' \equiv 0$, such that $\Phi(x) = \Phi_0$. □

Corollary 4.3.2 *Let $u_0 = \bar{v}_0$. The ODE system (4.3.2) reduces to the planar Hamiltonian form:*

$$\frac{d}{dx}\begin{pmatrix} p \\ q \end{pmatrix} = \begin{pmatrix} 0 & -1 \\ +1 & 0 \end{pmatrix} \nabla h(p, q), \tag{4.3.7}$$

where $p = 2\Theta$, $q = Q$, and

$$h = \tilde{W}(p, q) - 2q\cos p + 2\omega q, \qquad \tilde{W}(p, q) = W(u_0, \bar{u}_0, v_0, \bar{v}_0). \tag{4.3.8}$$

Proof. In variables (Q, Θ) defined by (4.3.4) with $\Phi(x) = \Phi_0 = 0$, we rewrite the ODE system (4.3.5) as follows:

$$\begin{cases} Q' = 2Q\sin(2\Theta) + 2\mathrm{Im}\,[\bar{u}_0 \partial_{\bar{u}_0} W(u_0, \bar{u}_0, v_0, \bar{v}_0)] \\ Q\Theta' = -\omega Q + Q\cos(2\Theta) - \mathrm{Re}\,[\bar{u}_0 \partial_{\bar{u}_0} W(u_0, \bar{u}_0, v_0, \bar{v}_0)] \end{cases} \tag{4.3.9}$$

The system (4.3.9) is equivalent to the Hamiltonian system (4.3.7) and (4.3.8) if

$$\begin{cases} \partial_p \tilde{W}(p, q) = i\,[u_0 \partial_{u_0} - \bar{u}_0 \partial_{\bar{u}_0}]\, W(u_0, \bar{u}_0, v_0, \bar{v}_0) \\ q\partial_q \tilde{W}(p, q) = [u_0 \partial_{u_0} + \bar{u}_0 \partial_{\bar{u}_0}]\, W(u_0, \bar{u}_0, v_0, \bar{v}_0) \end{cases} \tag{4.3.10}$$

The latter equations follows from (4.2.3), (4.2.4), and (4.3.4) with the chain rule. □

Corollary 4.3.3 *Let $u_0 = \bar{v}_0$. Then,*

$$\partial^2_{u_0\bar{u}_0} W = \partial^2_{v_0\bar{v}_0} W, \quad \partial^2_{\bar{u}_0^2} W = \partial^2_{v_0^2} W, \quad \partial^2_{u_0 v_0} W = \partial^2_{\bar{u}_0\bar{v}_0} W. \tag{4.3.11}$$

The only homogeneous potential function $W \in \mathbb{R}$ of the order $2n$ that satisfies properties (1)-(3) is given by:

$$W = \sum_{k=0}^{n} a_{k,0}[|u|^{2n-2k}|v|^{2k}] + \sum_{s=1}^{n-1}([u^s\bar{v}^s + \bar{u}^s v^s] \sum_{k=0}^{n-s} a_{k,s}[|u|^{2n-2k-2s}|v|^{2k}]) + A_n(u^n\bar{v}^n + \bar{u}^n v^n). \tag{4.3.12}$$

Where $(a_{k,s}, A_n)$ are real-valued coefficients which are subject to the symmetry conditions: $a_{k_1,s} = a_{k_2,s}$ if $k_1 + k_2 = n - s$ for $s = 0..n-1$.

Let's introduce new parameters ($s = 0, 1...n-1$):

$$A_s = \sum_{k=0}^{\frac{n-s-1}{2}} a_{k,s} \quad \text{if } n-s \text{ is odd}$$

$$A_s = \sum_{k=0}^{\frac{n-s-2}{2}} a_{k,s} + \frac{1}{2} a_{\frac{n-s}{2},s} \quad \text{if } n-s \text{ is even}$$

Using the variables (Q, Θ) defined in (4.3.4) with $\Phi(x) = \Phi_0 = 0$, we rewrite the ODE system (4.3.9) in the explicit form:

$$\begin{cases} Q' = 2Q\sin(2\Theta) - 4Q^n \sum_{s=0}^{n-1} sA_s \sin(2s\Theta) - 2nA_n Q^n \sin(2n\Theta) \\ \Theta' = -\omega + \cos(2\Theta) - nA_0 Q^{n-1} - 2Q^{n-1} n \sum_{s=1}^{n-1} A_s \cos(2s\Theta) - nA_n Q^{n-1} \cos(2n\Theta) \end{cases} \tag{4.3.13}$$

First integral

$$-\omega + \cos(2\Theta) - A_0 Q^{n-1} - 2Q^{n-1} \sum_{s=1}^{n-1} A_s \cos(2s\Theta) - A_n Q^{n-1} \cos(2n\Theta) = 0.$$

subject to the zero conditions $Q(x) \to 0$ as $|x| \to \infty$, reduces the second-order system to the first-order ODE

$$\Theta'(x) = (n-1)(\omega - \cos(2\Theta)), \tag{4.3.14}$$

while the function $Q(x)$ can be found from $\Theta(x)$ as follows:

$$Q^{n-1} = \frac{(\cos(2\Theta) - \omega)}{A_0 + 2\sum_{s=1}^{n-1} A_s \cos(2s\Theta) + A_n \cos(2n\Theta)}; \qquad Q \geq 0 \tag{4.3.15}$$

We introduce two auxiliary parameters:

$$\mu = \frac{1-\omega}{1+\omega}, \qquad \beta = \sqrt{1-\omega^2}, \tag{4.3.16}$$

such that $0 < \mu < \infty$ and $0 < \beta \leq 1$. In general case we will have two branches of solutions for $\Theta(x)$:

$$\cos(\Theta_+) = \frac{\cosh((n-1)\beta x)}{\sqrt{\cosh^2((n-1)\beta x) + \mu \sinh^2((n-1)\beta x)}}$$

$$\sin(\Theta_+) = \frac{-\sqrt{\mu}\sinh((n-1)\beta x)}{\sqrt{\cosh^2((n-1)\beta x) + \mu \sinh^2((n-1)\beta x)}}$$

and

$$\cos(\Theta_-) = \frac{\sinh((n-1)\beta x)}{\sqrt{\sinh^2((n-1)\beta x) + \mu\cosh^2((n-1)\beta x)}}$$

$$\sin(\Theta_-) = \frac{-\sqrt{\mu}\cosh((n-1)\beta x)}{\sqrt{\sinh^2((n-1)\beta x) + \mu\cosh^2((n-1)\beta x)}}$$

Choice of the branch depends on the condition $Q(x) \geq 0$.

In more general case for the non-homogeneous symmetric potential solutions of the ODE do not exist in the explicit form, because the elliptic integrals which will be naturally originated by the ODE system do not have explicit solutions in the general case.

We will illustrate decaying solutions of the system (4.3.2) for the quadric potential function (4.2.5). Decaying solutions may exist in the gap of continuous spectrum of the coupled-mode system (4.2.1) for $\omega \in (-1, 1)$. We will derive explicit conditions on existence of gap solitons for the general quadric potential function W given by (4.2.5). Using (4.3.14) and (4.3.15)for the case $n = 2$ we obtain:

$$\Theta'(x) = \omega - \cos(2\Theta), \tag{4.3.17}$$

$$Q = \frac{(t-\omega)}{\phi(t)}; \qquad Q \geq 0 \tag{4.3.18}$$

where

$$t = \cos(2\Theta), \qquad \phi(t) = a_4 t^2 + 2a_3 t + \frac{a_1 + a_2}{2},$$

such that $t \in [-1, 1]$. Let's consider two cases:

$$\begin{cases} t \geq \omega; & \phi(t) \geq 0 & \Rightarrow Q^+ \\ t \leq \omega; & \phi(t) \leq 0 & \Rightarrow Q^- \end{cases} \tag{4.3.19}$$

We can solve the first-order ODE (4.3.17) using the substitution $z = \tan(\Theta)$, such that

$$t = \frac{1-z^2}{1+z^2} \qquad z^2 = \frac{1-t}{1+t}.$$

After integration with the symmetry constraint $\Theta(0) = 0$, we obtain the solution

$$\left|\frac{(z-\sqrt{\mu})}{(z+\sqrt{\mu})}\right| = e^{2\beta x}, \tag{4.3.20}$$

where

$$\beta = \sqrt{1-\omega^2}, \qquad \mu = \frac{1-\omega}{1+\omega}$$

and $-1 < \omega < 1$. Two separate cases are considered:

$$|z| \leq \sqrt{\mu} \qquad z = -\sqrt{\mu}\frac{\sinh(\beta x)}{\cosh(\beta x)} \qquad t = \frac{\cosh^2(\beta x) - \mu\sinh^2(\beta x)}{\cosh^2(\beta x) + \mu\sinh^2(\beta x)}, \tag{4.3.21}$$

where $t \geq \omega$, and

$$|z| \geq \sqrt{\mu} \qquad z = -\sqrt{\mu}\frac{\cosh(\beta x)}{\sinh(\beta x)} \qquad t = \frac{\sinh^2(\beta x) - \mu\cosh^2(\beta x)}{\sinh^2(\beta x) + \mu\cosh^2(\beta x)}, \tag{4.3.22}$$

where $t \leq \omega$. Let's introduce new parameters

$$\begin{aligned} A &= -2a_3 + a_4 + \frac{a_1 + a_2}{2}, \\ B &= -2a_4 + a_1 + a_2, \\ C &= 2a_3 + a_4 + \frac{a_1 + a_2}{2}. \end{aligned} \tag{4.3.23}$$

It is clear that $A = \phi(-1)$ and $C = \phi(1)$. If $t \geq \omega$ and $\phi(t) \geq 0$, it follows from (4.3.19) and (4.3.21) that

$$Q^+(x) = \frac{(1-\omega)((\mu+1)\cosh^2(\beta x) - \mu)}{(A\mu^2 + B\mu + C)\cosh^4(\beta x) - (B\mu + 2A\mu^2)\cosh^2(\beta x) + A\mu^2}. \tag{4.3.24}$$

If $t \leq \omega$ and $\phi(t) \leq 0$, it follows from (4.3.19) and (4.3.22) that

$$Q^-(x) = \frac{(\omega-1)((\mu+1)\cosh^2(\beta x) - 1)}{(A\mu^2 + B\mu + C)\cosh^4(\beta x) - (B\mu + 2C)\cosh^2(\beta x) + C}. \tag{4.3.25}$$

The asymptotic behavior of the $Q(x)$ at infinity depends on the location of the zeros of the function $\psi(\mu) = A\mu^2 + B\mu + C$. The function $\psi(\mu)$ is related to the function $\phi(t)$, such that if $\psi(\mu) = 0$ then $\phi(\omega) = 0$.

Case: $A < 0, C > 0$

In this case the quadratic polynomial $\phi(t)$ has exactly one root $\phi(t_1) = 0$ such that $t_1 \in [-1, 1]$. We have two branches of decaying solutions with the positive amplitude $Q(x)$. One branch occurs for $t_1 < \omega \leq 1$ with $Q(x) = Q^+(x)$ and the other one occurs for $-1 \leq \omega < t_1$ with $Q(x) = Q^-(x)$. At the point $\omega = t_1$, the solution is bounded and decaying.

Case: $A > 0, C > 0$

In this case the quadratic polynomial $\phi(t)$ has no roots or has exactly two roots on $[-1, 1]$. We have a decaying solution with the positive amplitude $Q(x)$ for any $-1 < \omega < 1$ with $Q(x) = Q^+(x)$ if $\phi(t)$ does not have any roots on $[-1, 1]$. If $\phi(t)$ has two roots $\phi(t_1) = 0$ and $\phi(t_2) = 0$ such that $t_1, t_2 \in [-1, 1]$ then we have a decaying solution with

$Q(x) = Q^+(x)$ only on the interval $\max(t_1, t_2) < \omega \leq 1$. At the point $\omega = \max(t_1, t_2)$, the solution becomes unbounded.

Case: $A < 0, C < 0$

In this case the quadratic polynomial $\phi(t)$ has no roots or has exactly two roots on $[-1, 1]$. We have a decaying solution with the positive amplitude $Q(x)$ for any $-1 < \omega < 1$ with $Q(x) = Q^-(x)$ if $\phi(t)$ does not have any roots on $[-1, 1]$. If $\phi(t)$ has two roots $\phi(t_1) = 0$ and $\phi(t_2) = 0$ such that $t_1, t_2 \in [-1, 1]$ then we have a decaying solution with $Q(x) = Q^-(x)$ only on the interval $-1 \leq \omega < \min(t_1, t_2)$. At the point $\omega = \min(t_1, t_2)$, the solution becomes unbounded.

Case: $A > 0, C < 0$

In this case no decaying solutions with positive amplitude $Q(x)$ exist.

Other cases

Two special cases occur when $\phi(1) = 0$ or $\phi(-1) = 0$. If $\phi(1) = 0$, then $Q^+(x)$ has a singularity at $x = 0$ for any $-1 < \omega < 1$. If $\phi(-1) = 0$, then $Q^-(x)$ has a singularity at $x = 0$ for any $-1 < \omega < 1$.

4.4 Block-diagonalization of the linearized couple-mode system

Linearization of the coupled-mode system (4.2.1) at the stationary solutions (4.3.1) with $s = \theta = 0$ is defined as follows:

$$\begin{cases} u(x,t) = e^{i\omega t}\left(u_0(x) + U_1(x)e^{\lambda t}\right) \\ \bar{u}(x,t) = e^{-i\omega t}\left(\bar{u}_0(x) + U_2(x)e^{\lambda t}\right) \\ v(x,t) = e^{i\omega t}\left(v_0(x) + U_3(x)e^{\lambda t}\right) \\ \bar{v}(x,t) = e^{-i\omega t}\left(\bar{v}_0(x) + U_4(x)e^{\lambda t}\right) \end{cases} \tag{4.4.1}$$

where $v_0 = \bar{u}_0$, according to Lemma 4.3.1. Let $(\mathbf{f}, \mathbf{g})$ be a standard inner product for $\mathbf{f}, \mathbf{g} \in L^2(\mathbb{R}, \mathbb{C}^4)$. Expanding the Lyapunov functional (4.3.3) into Taylor series near $\mathbf{u}_0 = (u_0, \bar{u}_0, v_0, \bar{v}_0)^T$, we have:

$$\Lambda = \Lambda(\mathbf{u_0}) + (\mathbf{U}, \nabla\Lambda|_{\mathbf{u}_0}) + \frac{1}{2}(\mathbf{U}, H_\omega \mathbf{U}) + \ldots, \tag{4.4.2}$$

where $\mathbf{U} = (U_1, U_2, U_3, U_4)^T$ and H_ω is the the linearized energy operator in the explicit form

$$H_\omega = D(\partial_x) + V(x), \tag{4.4.3}$$

where

$$D = \begin{pmatrix} \omega - i\partial_x & 0 & -1 & 0 \\ 0 & \omega + i\partial_x & 0 & -1 \\ -1 & 0 & \omega + i\partial_x & 0 \\ 0 & -1 & 0 & \omega - i\partial_x \end{pmatrix} \tag{4.4.4}$$

and

$$V = \begin{pmatrix} \partial^2_{\bar{u}_0 u_0} & \partial^2_{u_0^2} & \partial^2_{\bar{u}_0 v_0} & \partial^2_{\bar{u}_0 \bar{v}_0} \\ \partial^2_{u_0^2} & \partial^2_{u_0 \bar{u}_0} & \partial^2_{u_0 v_0} & \partial^2_{u_0 \bar{v}_0} \\ \partial^2_{\bar{v}_0 u_0} & \partial^2_{\bar{v}_0 \bar{u}_0} & \partial^2_{\bar{v}_0 v_0} & \partial^2_{\bar{v}_0^2} \\ \partial^2_{v_0 u_0} & \partial^2_{v_0 \bar{u}_0} & \partial^2_{v_0^2} & \partial^2_{v_0 \bar{v}_0} \end{pmatrix} W(u_0, \bar{u}_0, v_0, \bar{v}_0). \tag{4.4.5}$$

The linearization (4.4.1) of the nonlinear coupled-mode system (4.2.1) results in the linearized coupled-mode system in the form:

$$H_\omega \mathbf{U} = i\lambda\sigma\mathbf{U}, \tag{4.4.6}$$

where σ is a diagonal matrix of $(1, -1, 1, -1)$. Due to the gauge and translational symmetries, the energy operator H_ω has a non-empty kernel which includes two eigenvectors:

$$\mathbf{U}_1 = \sigma\mathbf{u}_0(x), \qquad \mathbf{U}_2 = \mathbf{u}_0'(x). \tag{4.4.7}$$

The eigenvectors $\mathbf{U}_{1,2}$ represent derivatives of the stationary solutions (4.3.1) with respect to parameters (θ, s).

Due to the Hamiltonian structure, the linearized operator σH_ω has at least four-dimensional generalized kernel with the eigenvectors (4.4.7) and two generalized eigenvectors (see [97] for details). The eigenvectors of the linearized operator σH_ω satisfy the σ-orthogonality constraints:

$$(\mathbf{u}_0, \mathbf{U}) = \int_{\mathbb{R}} (\bar{u}_0 U_1 + u_0 U_2 + \bar{v}_0 U_3 + v_0 U_4)\, dx = 0, \tag{4.4.8}$$

$$(\mathbf{u}_0', \sigma\mathbf{U}) = \int_{\mathbb{R}} (\bar{u}_0' U_1 - u_0' U_2 + \bar{v}_0' U_3 - v_0' U_4)\, dx = 0. \tag{4.4.9}$$

The constraints (4.4.8) and (4.4.9) represent zero variations of the conserved quantities Q and P in (4.2.7) and (4.2.9) at the linearization (4.4.1).

It follows from the explicit form of H_ω and from Corollary 4.3.3 that the eigenvalue problem $H_\omega \mathbf{U} = \mu\mathbf{U}$ has two reductions:

$$(i)\ U_1 = U_4,\ U_2 = U_3, \qquad (ii)\ U_1 = -U_4,\ U_2 = -U_3. \tag{4.4.10}$$

Our main result on the block-diagonalization of the energy operator H_ω and the linearized coupled-mode system (4.4.6) is based on the reductions (4.4.10).

Theorem 4.4.1 *Let $W \in \mathbb{R}$ satisfy properties (1)-(3). Let (u_0, v_0) be a decaying solution of the system (4.3.2) on $x \in \mathbb{R}$, where $v_0 = \bar{u}_0$. There exists an orthogonal similarity transformation S, such that $S^{-1} = S^T$, where*

$$S = \frac{1}{\sqrt{2}} \begin{pmatrix} 1 & 0 & 1 & 0 \\ 0 & 1 & 0 & 1 \\ 0 & 1 & 0 & -1 \\ 1 & 0 & -1 & 0 \end{pmatrix},$$

that simultaneously block-diagonalizes the energy operator H_ω,

$$S^{-1}H_\omega S = \begin{pmatrix} H_+ & 0 \\ 0 & H_- \end{pmatrix} \equiv H, \tag{4.4.11}$$

and the linearized operator σH_ω

$$S^{-1}\sigma H_\omega S = \sigma \begin{pmatrix} 0 & H_- \\ H_+ & 0 \end{pmatrix} \equiv iL, \tag{4.4.12}$$

where $H_\pm$ are two-by-two Dirac operators:

$$H_\pm = \begin{pmatrix} \omega - i\partial_x & \mp 1 \\ \mp 1 & \omega + i\partial_x \end{pmatrix} + V_\pm(x), \tag{4.4.13}$$

and

$$V_\pm = \begin{pmatrix} \partial^2_{\bar{u}_0 u_0} \pm \partial^2_{\bar{u}_0 \bar{v}_0} & \partial^2_{\bar{u}_0^2} \pm \partial^2_{\bar{u}_0 v_0} \\ \partial^2_{u_0^2} \pm \partial^2_{u_0 \bar{v}_0} & \partial^2_{\bar{u}_0 u_0} \pm \partial^2_{u_0 v_0} \end{pmatrix} W(u_0, \bar{u}_0, v_0, \bar{v}_0). \tag{4.4.14}$$

Proof. Applying the similarity transformation to the operator $D(\partial_x)$ in (4.4.4), we have the first terms in Dirac operators $H_\pm$. Applying the same transformation to the potential $V(x)$ in (4.4.5) and using Corollary 4.3.3, we have the second term in the Dirac operators $H_\pm$. The same transformation is applied similarly to the linearized operator σH_ω with the result (4.4.12). □

Corollary 4.4.2 *The linearized coupled-mode system (4.4.6) is equivalent to the block-diagonalized eigenvalue problems*

$$\sigma_3 H_- \sigma_3 H_+ \mathbf{V}_1 = \gamma \mathbf{V}_1, \qquad \sigma_3 H_+ \sigma_3 H_- \mathbf{V}_2 = \gamma \mathbf{V}_2, \qquad \gamma = -\lambda^2, \tag{4.4.15}$$

where $\mathbf{V}_{1,2} \in \mathbb{C}^2$ and σ_3 is the Pauli's diagonal matrix of $(1, -1)$.

Corollary 4.4.3 *Let $\mathbf{u}_0 = (u_0, \bar{u}_0) \in \mathbb{C}^2$ and $(\mathbf{f}, \mathbf{g})$ be a standard inner product for $\mathbf{f}, \mathbf{g} \in L^2(\mathbb{R}, \mathbb{C}^2)$. Dirac operators $H_\pm$ have simple kernels with the eigenvectors*

$$H_+ \mathbf{u}_0' = 0, \qquad H_- \sigma_3 \mathbf{u}_0 = 0, \tag{4.4.16}$$

while the vectors $\mathbf{V}_{1,2}$ satisfy the constraints

$$(\mathbf{u}_0, \mathbf{V}_1) = 0, \qquad (\mathbf{u}_0', \sigma_3 \mathbf{V}_2) = 0. \tag{4.4.17}$$

Remark 4.4.4 *Block-diagonalization described in Theorem 4.4.1 has nothing in common with explicit diagonalization used in reduction (9.2) of [100] for the particular potential function (4.2.5) with $a_1 = a_2 = a_4 = 0$ and $a_3 = 1$. Moreover, the reduction (9.2) of [100] does not work for $\omega \neq 0$, while gap solitons do not exist in this particular model for $\omega = 0$.*

4.5 Numerical computations

Numerical discretization and truncation of the linearized coupled-mode system (4.4.6) leads to an eigenvalue problem for large matrices [108]. Parallel software libraries were recently developed for computations of large eigenvalue problems [54]. We shall use Scalapack library and distribute computations of eigenvalues of the system (4.4.6) for different parameter values between parallel processors of the SHARCnet cluster Idra using Message Passing Interface [30].

We implement a numerical discretization of the linearized coupled-mode system (4.4.6) using the Chebyshev interpolation method [109]. Given a function defined on the Chebyshev points $\nu_j = cos(j\pi/N), j = 0, 1...N$ we obtain a discrete first derivative as a multiplication by an $(N+1) \times (N+1)$ matrix, which we shell denote by $D_N^{(1)}$. Let's the rows and columns of the differentiation matrix $D_N^{(1)}$ be indexed from 0 to N. The entries of this matrix are:

$$(D_N^{(1)})_{00} = \frac{2N^2+1}{6}, \qquad (D_N^{(1)})_{NN} = -\frac{2N^2+1}{6},$$

$$(D_N^{(1)})_{jj} = \frac{-\nu_j}{2(1-\nu_j^2)}, \qquad j = 1, ..., N-1,$$

$$(D_N^{(1)})_{ij} = \frac{c_i}{c_j}\frac{(-1)^{i+j}}{(\nu_i - \nu_j)}, \quad i \neq j, \quad i, j = 0, ..., N,$$

where

$$c_0 = c_N = 2 \qquad and \qquad c_i = 1, \quad i = 1, ...N-1.$$

To transform the Chebyshev grid from $[-1, 1]$ to the infinite domain $[-\infty, +\infty]$ we will use the map $f(\nu) = L \tanh^{-1} \nu, x_i = f(\nu_i)$. This is the most efficient map for our case because the solitons decay exponentially. Decaying also implies the zero boundary conditions on the truncated interval. The constant L sets the length scale of the map. Differentiation in x is carried out using the chain rule so that

$$(\vec{u}_x) = \left[\left(\frac{\partial f^{-1}(x_i)}{\partial x} D_N^{(1)}\right) u(\nu_i)\right] \equiv D_{N+1}\vec{u}, \qquad i = 0...N.$$

Denote as I_{N+1} the identity matrix with $N+1$ elements. Finally we have a discretized eigenvalue problem for the operator H:

$$H_{\pm} = \begin{pmatrix} \omega I_{N+1} - iD_{N+1} & \mp I_{N+1} \\ \mp I_{N+1} & \omega I_{N+1} + iD_{N+1} \end{pmatrix} + diagV_{\pm}(x_i)$$

The main advantage of the Chebyshev grid is the clustering distribution of the grid points and for the $N = 2500$ this clustering prevents the appearance of spurious complex

eigenvalues from the discretized continuous spectrum up to the accuracy $\mathrm{Im}\,\lambda \leq 10^{-5}$ on the interval $[-2, 2]$.

Chebyshev points	$\inf \mathrm{Im}\,\lambda[-2,2]$	$\inf \mathrm{Im}\,\lambda[-10,10]$
100	0.085	0.75
200	0.0095	0.52
400	0.0053	0.21
800	$7.12 \cdot 10^-4$	0.12
1200	$2.34 \cdot 10^-4$	0.09
2500	$3.91 \cdot 10^-5$	0.06

In general, using higher number of polynomials the interval can be expanded although for the numerical analysis of the edge bifurcations of the continuous spectrum the number of Chebyshev polynomials mentioned above is sufficient.

If the eigenvector is analytic in a strip near the interpolation interval, the corresponding Chebyshev spectral derivatives converge geometrically, with an asymptotic convergence factor determined by the size of the largest ellipse in the domain of analyticity. [109]. As a result the accuracy of the numerical eigenvalues depends on the parameter ω and on the degree of the nonlinearity.

The continuous spectrum for the linearized coupled-mode system (4.4.6) can be found from the no-potential case $V(x) \equiv 0$. It consists of two pairs of symmetric branches on the imaginary axis $\lambda \in i\mathbb{R}$ for $|\mathrm{Im}(\lambda)| > 1 - \omega$ and $|\mathrm{Im}(\lambda)| > 1 + \omega$ [9, 41]. In the potential case $V(x) \neq 0$, the continuous spectrum does not move, but the discrete spectrum appears. The discrete spectrum is represented by symmetric pairs or quartets of isolated non-zero eigenvalues and zero eigenvalue of algebraic multiplicity four for the generalized kernel of σH_ω [9, 41]. We note that symmetries of the Chebyshev grid preserve symmetries of the linearized coupled-mode system (4.4.6).

We shall study eigenvalues of the energy operator H_ω, in connection to eigenvalues of the linearized operator σH_ω. It is well known [108, 109] that Hermitian matrices have condition number one, while non-Hermitian matrices may have large condition number. As a result, numerical computations for eigenvalues and eigenvectors have better accuracy and faster convergence for self-adjoint operators [108, 109]. We will use the block-diagonalizations (4.4.11) and (4.4.12) and compute eigenvalues of H_+, H_-, and L. The block-diagonalized matrix can be stored in a special compressed format which requires twice less memory than a full matrix and as it can be derived from the table below (cpu time is given in seconds) this representation accelerates computations of eigenvalues approximately in two times.

Chebyshev points	cpu time (full matrix)	cpu time (block-diag. matrix)
100	1.656	1.984
200	11.219	12.921
400	130.953	207.134
800	997.843	$1.583 \cdot 10^3$
1200	$3.608 \cdot 10^3$	$6.167 \cdot 10^3$
2500	$7.252 \cdot 10^3$	$12.723 \cdot 10^3$

4.6 Application: gap solitons

Example 1: gap solitons in nonlinear optics

In nonlinear optics, the coupled-mode system describes counter-propagating light waves. A pulse of light moving through a periodic medium consists of coupled backward and forward electric field components. A gap soliton emerges from the balance of the strong photonic band dispersion with the nonlinear effects present at sufficiently high intensities.

Define parameters as $a_1 = 1$, $a_2 = \rho$, and $a_3 = a_4 = 0$. We find the decaying solution $u_0(x)$ in the explicit form:

$$u_0 = \sqrt{\frac{2(1-\omega)}{1+\rho}} \frac{1}{(\cosh \beta x + i\sqrt{\mu} \sinh \beta x)}. \tag{4.6.1}$$

When $\omega \to 1$ (such that $\mu \to 0$ and $\beta \to 0$), the decaying solution (4.6.1) becomes small in absolute value and approaches the limit of sech-solutions $\mathrm{sech}(\beta x)$. When $\omega \to -1$ (such that $\mu \to \infty$ and $\beta \to 0$), the decaying solution (4.6.1) remains finite in absolute value and approaches the limit of the algebraically decaying solution:

$$u_0 = \frac{2}{\sqrt{1+\rho}(1+2ix)}.$$

Potential matrices $V_\pm(x)$ in the Dirac operators $H_\pm$ in (4.4.13)–(4.4.14) can be written in the explicit form:

$$V_+ = (1+\rho) \begin{pmatrix} 2|u_0|^2 & u_0^2 \\ \bar{u}_0^2 & 2|u_0|^2 \end{pmatrix}, \qquad V_- = \begin{pmatrix} 2|u_0|^2 & (1-\rho)u_0^2 \\ (1-\rho)\bar{u}_0^2 & 2|u_0|^2 \end{pmatrix}. \tag{4.6.2}$$

Figure 4.1 displays the pattern of eigenvalues and instability bifurcations for the symmetric quadric potential (4.2.5) with $a_1 = 1$ and $a_2 = a_3 = a_4 = 0$. The decaying solution $u_0(x)$ and the potential matrices $V_\pm(x)$ are given by (4.6.1) and (4.6.2) with $\rho = 0$. Parameter ω of the decaying solution $u_0(x)$ is defined in the interval $-1 < \omega < 1$. Six pictures of Fig. 4.1 shows the entire spectrum of L, H_+ and H_- for different values of ω.

When ω is close to 1 (the gap soliton is close to a small-amplitude sech-soliton), there exists a single non-zero eigenvalue for H_+ and H_- and a single pair of purely imaginary eigenvalues of L (see subplot (1) on Fig. 4.1). The first set of arrays on the subplot (1) indicates that the pair of eigenvalues of L becomes visible at the same value of ω as the eigenvalue of H_+. This correlation between eigenvalues of L and H_+ can be traced throughout the entire parameter domain on the subplots (1)–(6).

When ω decreases, the operator H_- acquires another non-zero eigenvalue by means of the edge bifurcation [73], with no changes in the number of isolated eigenvalues of L (see subplot (2)). The first complex instability occurs near $\omega \approx -0.18$, when the pair of purely imaginary eigenvalues of L collides with the continuous spectrum and emerge as a quartet of complex eigenvalues, with no changes in the number of isolated eigenvalues for H_+ and H_- (see subplot (3)).

The second complex instability occurs at $\omega \approx -0.54$, when the operator H_- acquires a third non-zero eigenvalue and the linearized operator L acquires another quartet of complex eigenvalues (see subplot (4)). The second set of arrays on the subplots (4)–(6) indicates a correlation between these eigenvalues of L and H_-.

When ω decreases further, the operators H_+ and H_- acquires one more isolated eigenvalue, with no change in the spectrum of L (see subplot (5)). Finally, when ω is close to -1 (the gap soliton is close to the large-amplitude algebraic soliton), the third complex instability occurs, correlated with another edge bifurcation in the operator H_- (see subplot (6)). The third set of arrays on subplot (6) indicates this correlation. The third complex instability was missed in the previous numerical studies of the example under consideration [9, 41]. In a narrow domain near $\omega = -1$, the operator H_+ has two non-zero eigenvalues, the operator H_- has five non-zero eigenvalues and the operator L has three quartets of complex eigenvalues.

Example 2: gap solitons in photonic crystals

In photonics, the coupled-mode system is derived for coupled resonant waves in stop bands of a low-contrast three-dimensional photonic crystal. Spatial soliton solutions is proved to exist in photonic crystal fibers. These guided localized nonlinear waves appear as a result of the balance between the linear and nonlinear diffraction properties of the inhomogeneous photonic crystal cladding.

Define the parameters as $a_1 = a_2 = 0, a_3 = 1$ and $a_4 = s$. The decaying solution $u_0(x)$ exists in two sub-domains: $\omega > 0$, $s > -1$ and $\omega < 0$, $s < 1$. When $\omega > 0$, $s > -1$, the solution takes the form:

$$u_0 = \sqrt{\frac{1-\omega}{2}} \frac{(\cosh \beta x - i\sqrt{\mu} \sinh \beta x)}{\sqrt{\Delta_+(x)}}, \tag{4.6.3}$$

where

$$\Delta_+ = [(s-1)\mu^2 - 2s\mu + (s+1)] \cosh^4(\beta x) + 2[s\mu - (s-1)\mu^2] \cosh^2(\beta x) + (s-1)\mu^2.$$

When $\omega < 0$, $s < 1$, the solution takes the form:

$$u_0 = \sqrt{\frac{1-\omega}{2}} \frac{(\sinh \beta x - i\sqrt{\mu} \cosh \beta x)}{\sqrt{\Delta_-(x)}}. \tag{4.6.4}$$

where

$$\Delta_- = [(s+1) - 2s\mu - (s-1)\mu^2] \cosh^4(\beta x) + 2[s+1-s\mu] \cosh^2(\beta x) - (s+1).$$

In both limits $\omega \to 1$ and $\omega \to -1$, the decaying solutions (4.6.3) and (4.6.4) approach the small-amplitude sech-solution $\mathrm{sech}(\beta x)$. In the limit $\omega \to 0$, the decaying solutions (4.6.3) and (4.6.4) degenerate into a non-decaying bounded solution with $|u_0(x)|^2 = \frac{1}{2}$.

The potential matrices $V_\pm(x)$ in the Dirac operators $H_\pm$ in (4.4.13)–(4.4.14) take the form:

$$V_+ = 3 \begin{pmatrix} u_0^2 + \bar{u}_0^2 & 2|u_0|^2 \\ 2|u_0|^2 & u_0^2 + \bar{u}_0^2 \end{pmatrix} + s \begin{pmatrix} 2|u_0|^2 & u_0^2 + 3\bar{u}_0^2 \\ \bar{u}_0^2 + 3u_0^2 & 2|u_0|^2 \end{pmatrix}, \tag{4.6.5}$$

$$V_- = \begin{pmatrix} u_0^2 + \bar{u}_0^2 & -2|u_0|^2 \\ -2|u_0|^2 & u_0^2 + \bar{u}_0^2 \end{pmatrix} + s \begin{pmatrix} 0 & -u_0^2 - \bar{u}_0^2 \\ -u_0^2 - \bar{u}_0^2 & 0 \end{pmatrix}. \tag{4.6.6}$$

Figure 4.2 displays the pattern of eigenvalues and instability bifurcations for the symmetric quadric potential (4.2.5) with $a_1 = a_2 = a_4 = 0$ and $a_3 = 1$. The decaying solution $u_0(x)$ and the potential matrices $V_\pm(x)$ are given by (4.6.3) and (4.6.5) with $\omega > 0$ and $s = 0$. Eigenvalues in the other case $\omega < 0$ can be found from those in the case $\omega > 0$ by reflections.

When ω is close to 1 (the gap soliton is close to a small-amplitude sech-soliton), there exists one non-zero eigenvalue of H_- and no non-zero eigenvalues of L and H_+ (see subplot (1) on Fig. 4.2). When ω increases, two more non-zero eigenvalues bifurcate in H_- from the left and right branches of the continuous spectrum, with no change in non-zero eigenvalues of L (see subplot (2)). The first complex bifurcation occurs at $\omega \approx 0.45$, when a quartet of complex eigenvalues occurs in L, in correlation with two symmetric edge bifurcations of H_+ from the left and right branches of the continuous spectrum (see subplot (3)). The first and only set of arrays on the subplots (3)-(6) indicates a correlation between eigenvalues of L and H_+, which is traced through the remaining parameter domain of ω. The inverse complex bifurcation occurs at $\omega \approx 0.15$, when the quartet of complex eigenvalues merge at the edge of the continuous spectrum into a pair of purely imaginary eigenvalues (see subplot (5)). No new eigenvalue emerge for smaller values of ω. When ω is close to 0 (the gap soliton is close to the non-decaying solution), the operator H_+ has two non-zero eigenvalues, the operator H_- has three non-zero eigenvalues and the operator L has one pair of purely imaginary eigenvalues (see subplot (6)).

We mention two other limiting cases of the symmetric quadric potential (4.2.5). When $a_1 = a_3 = a_4 = 0$ and $a_2 = 1$, the coupled-mode system is an integrable model

and no non-zero eigenvalues of L exist, according to the exact solution of the linearization problem [76, 77]. When $a_1 = a_2 = a_3 = 0$ and $a_4 = \pm 1$, one branch of decaying solutions $u_0(x)$ exists for either sign, according to (4.6.3) and (4.6.4). The pattern of eigenvalues and instability bifurcations repeats that of Fig. 4.2.

Example 3: gap solitons in relativity theory

Nuclear physics provides a unique laboratory for investigating the Dirac picture of vacuum. The basis for this is given by relativistic mean-field models. Within this approach nucleons are described by the Dirac equation coupled to scalar and vector meson fields. The potential function (4.2.5) with $a_1 = a_2 = a_3 = 0$, $a_4 = 1$ represents a standard nonlinear Dirac equation that is used as a model of vacuum. The existence of standing waves in the nonlinear Dirac equation was proved in [23].

We find the decaying solution $u_0(x)$ in the explicit form:

$$u_0 = \frac{(1-\omega)((\mu+1)\cosh^2(\beta x) - \mu)}{(\mu^2 - 2\mu + 1)\cosh^4(\beta x) - (-2\mu + 2\mu^2)\cosh^2 \beta x + \mu^2}. \tag{4.6.7}$$

When ω belongs to the interval $(-1, 0]$ the $Q(x)$ blows up to infinity in two symmetric points $\tanh^2 \beta x = \frac{1}{\mu}$. These two points are getting separated to plus and minus infinity and $Q(x)$ tends to $1/2\cosh(2x)$ as ω goes to 0 as a conclusion we do not have a soliton type solution for this interval of ω.

When ω belongs to the open interval $(0.5, 1)$ the $Q(x)$ is one pulse soliton solution with $\max(Q(x)) = 1 - \omega$ as ω goes to 1 the $Q(x)$ tends to 0.

When ω belongs to the interval $(0, 0.5)$ the $Q(x)$ is two pulse soliton solution with $\min(Q(x)) = 1 - \omega$ at the origin and $\max(Q(x)) = \frac{1}{4\omega}$ at two points $\cosh(2\beta x) = \frac{1-2\omega^2}{\omega}$ (see Fig. 4.3 (b)). In the limit ω goes to 0 the pulses are getting more and more separated and the amplitude of the pulses tends to infinity. The two pulse soliton solutions in the coupled mode system were also discovered but for the different type of the nonlinearity in the problem of the light propagation through deep nonlinear grating.

We can also find the exact analytical expression for the $\Theta(x)$ (4.3.4) as

$$\cos\Theta = \frac{\cosh \beta x}{\sqrt{\cosh^2 \beta x + \mu \sinh^2 \beta x}}, \qquad \sin(\Theta) = \frac{-\sqrt{\mu}\sinh(\beta x)}{\sqrt{\cosh^2 \beta x + \mu \sinh^2 \beta x}}.$$

This gives

$$\cos 2\Theta = \cos^2(\Theta) - \sin^2(\Theta) = \frac{(1+\omega)\cosh^2 \beta x - (1-\omega)\sinh^2 \beta x}{(1+\omega)\cosh^2 \beta x + (1-\omega)\sinh^2 \beta x} = \frac{1 + \omega\cosh(2\beta x)}{\cosh(2\beta x) + \omega}$$

The spectral stability of the gap solitons follows from the linearization (4.4.1) and diagonal blocks $H_\pm$ of the linearized energy operator (4.4.13) can be written as

$$H_- = \begin{bmatrix} \omega - i\partial_x & 1 - u_0^2 - \bar{u}_0^2 \\ 1 - u_0^2 - \bar{u}_0^2 & \omega + i\partial_x \end{bmatrix} \tag{4.6.8}$$

$$H_+ = \begin{bmatrix} \omega - i\partial_x + 2|u_0|^2 & u_0^2 + 3\bar{u}_0^2 - 1 \\ \bar{u}_0^2 + 3u_0^2 - 1 & \omega + i\partial_x + 2|u_0|^2 \end{bmatrix} = \tag{4.6.9}$$

The subspaces

$$X^+ = \begin{bmatrix} f(x) \\ \bar{f}(-x) \end{bmatrix}, \qquad X^- = \begin{bmatrix} f(x) \\ -\bar{f}(-x) \end{bmatrix}$$

are invariant under the action of $H_\pm$. So are the spaces

$$X_1 = \begin{bmatrix} f(x) \\ g(x) \end{bmatrix}, \quad \bar{f}(x) = f(-x), \quad \bar{g}(x) = g(-x);$$

$$X_2 = \begin{bmatrix} f(x) \\ g(x) \end{bmatrix}, \quad \bar{f}(x) = -f(-x), \quad \bar{g}(x) = -g(-x).$$

Denote

$$X_j^\pm = X^\pm \cap X_j, \qquad j = 1, 2.$$

The kernel of H_- is

$$\ker H_- = \operatorname{span}\left\langle \begin{bmatrix} \phi_1 - i\phi_2 \\ -\phi_1 - i\phi_2 \end{bmatrix} \right\rangle \subset X^-. \tag{4.6.10}$$

The kernel of H_+ is

$$\ker H_+ = \operatorname{span}\left\langle \begin{bmatrix} \phi_1 - i\phi_2 \\ \phi_1 + i\phi_2 \end{bmatrix} \right\rangle \subset X^+. \tag{4.6.11}$$

$$\begin{cases} -\partial_x\phi_2 = -\omega\phi_1 + g(\phi_1^2 - \phi_2^2)\phi_1 = \partial_{\phi_1} h(\phi), \\ \partial_x\phi_1 = -\omega\phi_2 - g(\phi_1^2 - \phi_2^2)\phi_2 = \partial_{\phi_2} h(\phi), \end{cases} \tag{4.6.12}$$

where

$$h(\phi) = -\frac{\omega}{2}(\phi_1^2 + \phi_2^2) + \frac{1}{2}G(\phi_1^2 - \phi_2^2). \tag{4.6.13}$$

This could be verified by taking the x-derivative of (4.6.12) and using the relations

$$\phi_1^2 = 2Q\cos^2\Theta = Q(1 + \cos 2\Theta), \qquad \phi_2^2 = 2Q\sin^2\Theta = Q(1 - \cos 2\Theta).$$

The essential spectrum of H_- consists of two intervals:

$$\sigma_{ess}(H_-) = (-\infty, -1 + \omega] \cup [1 + \omega, \infty).$$

Lemma 4.6.1 *The spectrum of H_- is symmetric with respect to $\lambda = \omega$. Moreover, If $\begin{bmatrix} f_1 \\ f_2 \end{bmatrix}$ is an eigenvector of H_- that corresponds to an eigenvalue λ, then $\begin{bmatrix} f_2 \\ -f_1 \end{bmatrix}$ is an eigenvector of H_- that corresponds to an eigenvalue $\lambda' = 2\omega - \lambda$.*

Proof. The relation $\lambda \begin{bmatrix} f_1 \\ f_2 \end{bmatrix} = H_- \begin{bmatrix} f_1 \\ f_2 \end{bmatrix}$ can be written as

$$\partial_x f_1 = -i(\omega - \lambda) f_1 + i\alpha(x) f_2, \qquad \partial_x f_2 = -i\alpha(x) f_1 + i(\omega - \lambda) f_2, \tag{4.6.14}$$

where $\alpha(x, \omega) = u_0^2 + \bar{u}_0^2 - 1 = 1 - \frac{2\omega}{\cos 2\Theta}$. We can rewrite these equations as

$$\partial_x f_2 = i(\omega - \lambda) f_2 + i\alpha(x)(-f_1), \qquad \partial_x(-f_1) = -i\alpha(x) f_2 - i(\omega - \lambda)(-f_1). \tag{4.6.15}$$

Taking into account that $\omega - \lambda = -(\omega - \lambda')$, we get:

$$\partial_x f_2 = -i(\omega - \lambda') f_2 + i\alpha(x)(-f_1), \qquad \partial_x(-f_1) = -i\alpha(x) f_2 + i(\omega - \lambda')(-f_1), \tag{4.6.16}$$

which finishes the proof. □

Corollary 4.6.2 *$2\omega \in \sigma_d(H_-)$, with the corresponding eigenvector $\begin{bmatrix} \phi_1 + i\phi_2 \\ \phi_1 - i\phi_2 \end{bmatrix}$.*

Lemma 4.6.3 *$\omega \notin \sigma_d(H_-)$.*

Proof. If ω were an eigenvalue with an eigenvector $\begin{bmatrix} f_1 \\ f_2 \end{bmatrix}$, then, by Lemma 4.6.1, the vector $\begin{bmatrix} f_2 \\ -f_1 \end{bmatrix}$ corresponds to the same eigenvalue, and so does the vector

$$\begin{bmatrix} f_1 \\ f_2 \end{bmatrix} + i \begin{bmatrix} f_2 \\ -f_1 \end{bmatrix} = \begin{bmatrix} f_1 + if_2 \\ f_2 - if_1 \end{bmatrix} = \begin{bmatrix} f_1 + if_2 \\ -i(f_1 + if_2) \end{bmatrix}.$$

Thus, we may assume that the eigenvector that corresponds to $\lambda = \omega$ has the form $\begin{bmatrix} f_1 \\ -if_1 \end{bmatrix}$. It follows that f_1 satisfies $\partial_x f_1 = (\xi(x) - 1) f_1$, hence $f_1(x) \sim c_\pm e^{-x}$ for $x \to \pm\infty$, which does not allow $f_1 \in L^2(\mathbb{R})$. □

The continuous spectrum for the linearized coupled-mode system can be found from the no-potential case $V(x) = 0$. It consists of two pairs of symmetric branches on the imaginary axis with positive and negative Krein signatures. The branches can be found analytically as $\lambda \in i\mathbb{R}$ for the $|\mathrm{Im}(\lambda)| > 1 + \omega$ and $|\mathrm{Im}(\lambda)| > 1 - \omega$. By perturbation theory in the nonzero potential case the continuous spectrum does not move but the additional

discrete spectrum appears. Eigenvalues of the operators L, H_+ and H_- are detected numerically for two values of the parameter ω by the Chebyshev interpolation method and are displayed in Figures 4.3(a) and 4.4. The ends of the branch of the continuous spectrum with the negative Krein signature I are $|\mathrm{Im}\,\lambda| = 1.2$ for $\omega = 0.2$ and $|\mathrm{Im}\,\lambda| = 1.7$ for $\omega = 0.7$, the zero eigenvalue II of the operator L is of the multiplicity 4 and for the $\omega = 0.2$ we can see a quadruplet of complex eigenvalues III. We can see a correlation to the discrete spectrum of the operators $H_\pm$ for the $\omega = 0.7$ the discrete spectrum of $H_\pm$ consist only of the kernel I and positive eigenvalue II, while for $\omega = 0.2$ the discrete spectrum of the operator H_+ has also two negative eigenvalues IV.

When ω is close to the double pulse bifurcation threshold ($\omega \approx 0.5$), the operator L has a four-dimensional kernel at $\lambda = 0$ and a quadruplet of small complex eigenvalues I bifurcating from the continuous spectrum of L with the correlation to the edge bifurcation of the operator H_+ at $\omega \approx 0.5$. The bifurcated eigenvalues of the operator L moves toward the origin and away from the real line as ω goes from 0.5 to 0 (see Fig: 4.5).

Within the numerical accuracy we can conclude that for the interval $\omega \in [0.5, 1)$ the one pulse soliton solution are spectrally stable while for the interval $\omega \in (0, 0.5)$ the double pulse soliton solutions are spectrally unstable, because of the oscillations related to small complex eigenvalues.

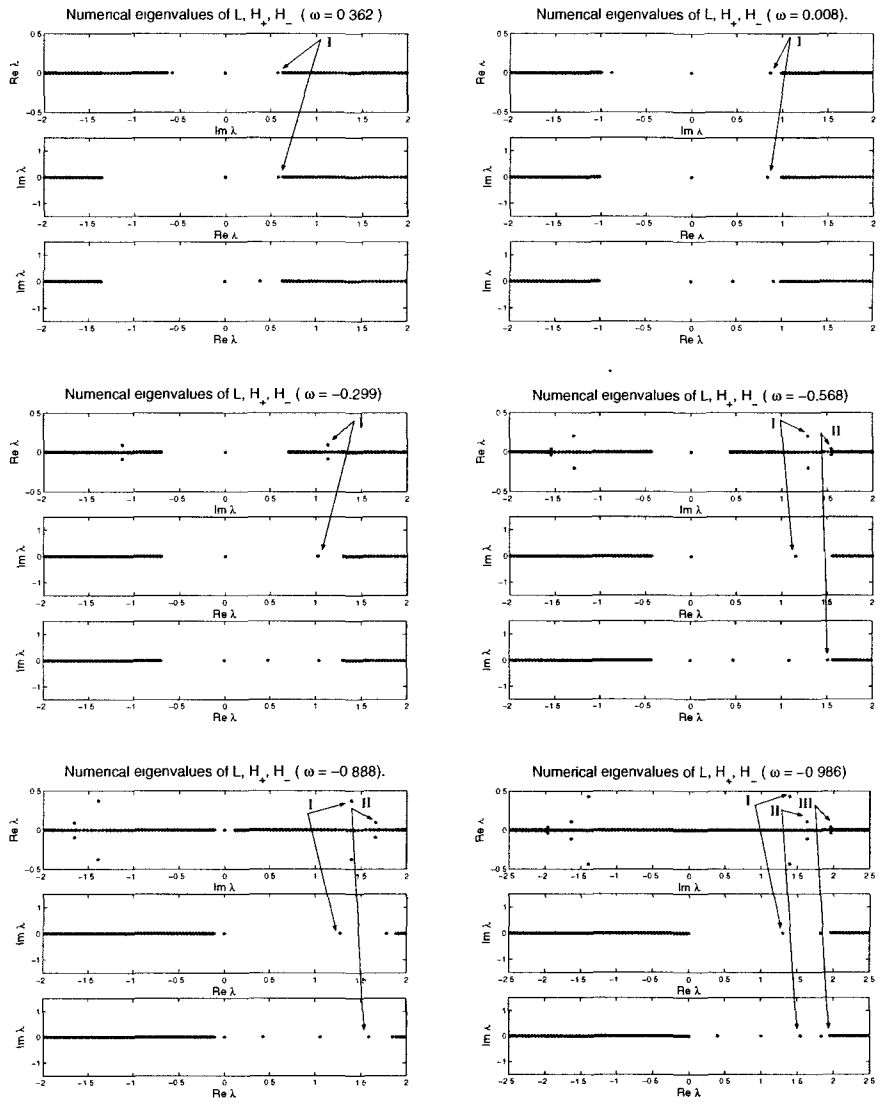

Figure 4.1: Eigenvalues and instability bifurcations for the symmetric quadric potential (4.2.5) with $a_1 = 1$ and $a_2 = a_3 = a_4 = 0$.

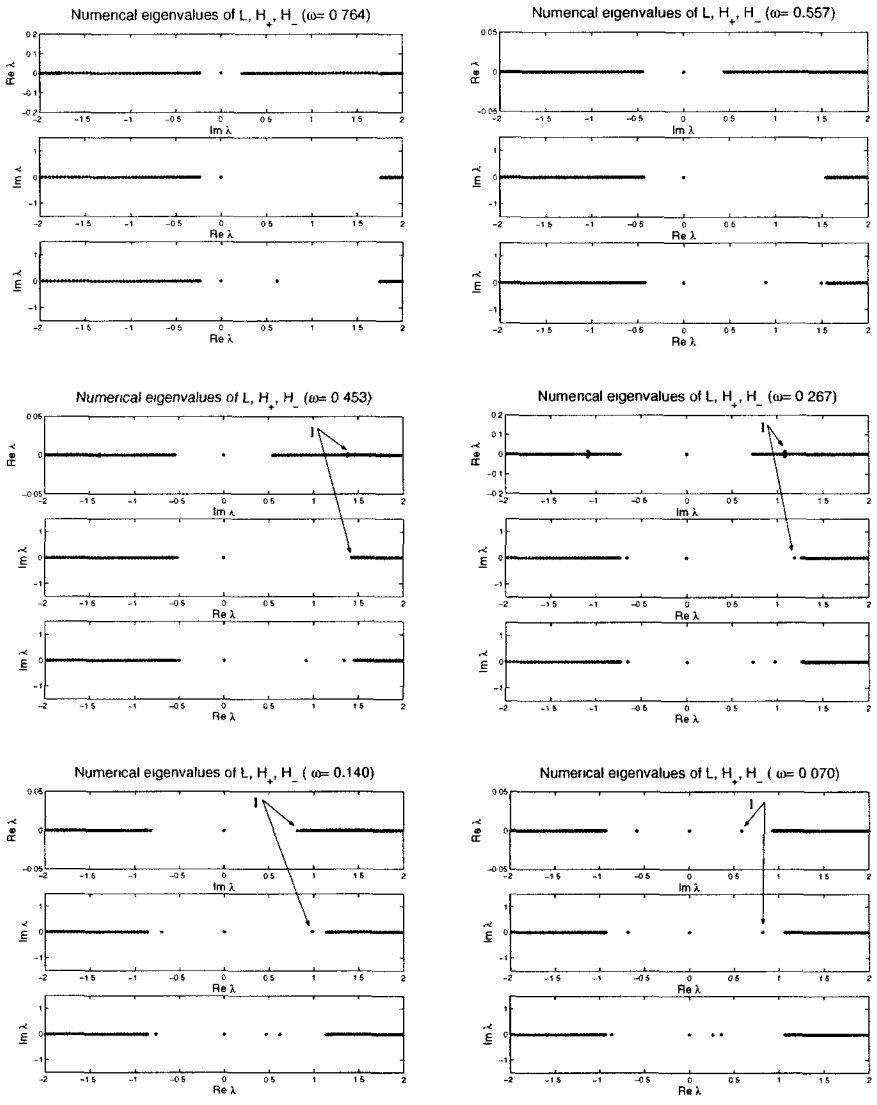

Figure 4.2: Eigenvalues and instability bifurcations for the symmetric quadric potential (4.2.5) with $a_3 = 1$ and $a_1 = a_2 = a_4 = 0$.

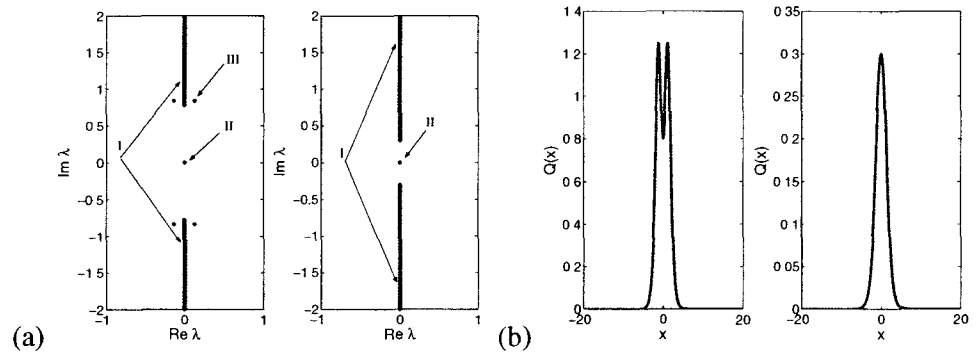

Figure 4.3: (a) $\sigma(L)$ at $\omega = 0.2$ and $\omega = 0.7$. (b) Plot of $Q(x)$ for $\omega = 0.2$ and $\omega = 0.7$.

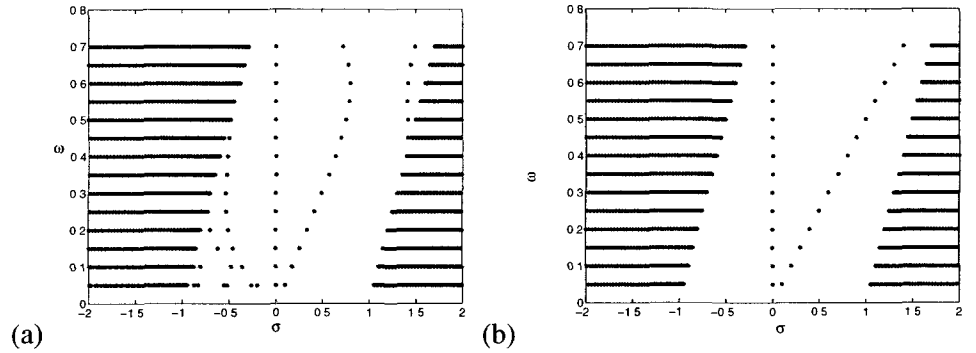

Figure 4.4: (a) Spectrum of the operator (H_+) versus ω and (b) spectrum of the operator (H_-) versus ω. (Dashed line is $\sigma = \omega$)

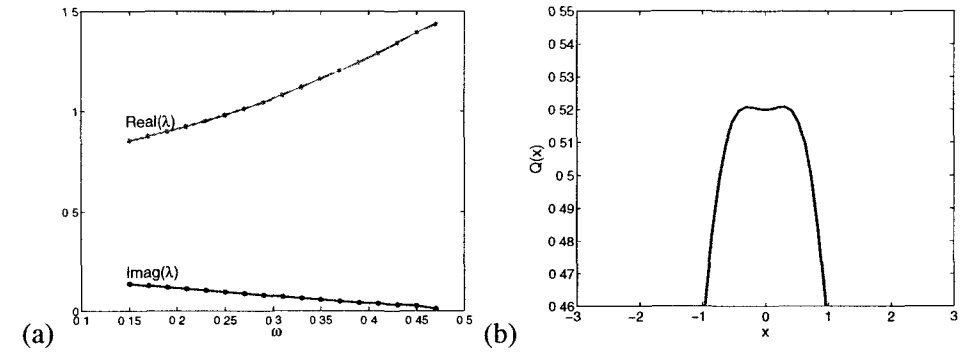

Figure 4.5: (a) Real and imaginary part of the bifurcated eigenvalue λ from the first quadrant versus ω. (b) The top part of the 2-hump $Q(x)$ for $\omega = 0.48$.

CHAPTER 5

SPECTRAL PROPERTIES OF THE NON-SELF-ADJOINT OPERATOR ASSOCIATED WITH THE PERIODIC HEAT EQUATION

5.1 Introduction

We address the Cauchy problem for the periodic heat equation

$$\begin{cases} \dot{h} = -h_\theta - \epsilon(\sin\theta h_\theta)_\theta, \quad t > 0, \\ h(0) = h_0, \end{cases} \tag{5.1.1}$$

subject to the periodic boundary conditions on $\theta \in [-\pi, \pi]$. This model was derived in the context of the dynamics of a thin viscous fluid film on the inside surface of a cylinder rotating around its axis in [11]. Extension of the model to the three-dimensional motion of the film was reported in [12].

The parameter ϵ is small for applications in fluid dynamics [11] and our main results correspond to the interval $|\epsilon| < 2$ in accordance to these applications. For any $\epsilon > 0$, the Cauchy problem for the heat equation (5.1.1) on the half-interval $\theta \in [0, \pi]$ is generally ill-posed [82] and it is naturally to expect that the Cauchy problem remains ill-posed on the entire interval $\theta \in [-\pi, \pi]$. The authors of the pioneer work [11] used a heuristic asymptotic solution to suggest that the growth of "explosive instabilities" might occur in the time evolution of the Cauchy problem (5.1.1).

Nevertheless, in a contradiction with the picture of explosive instabilities, only purely imaginary eigenvalues were discovered in the discrete spectrum of the associated linear operator

$$L = -\epsilon \frac{\partial}{\partial\theta}\left(\sin\theta \frac{\partial}{\partial\theta}\right) - \frac{\partial}{\partial\theta}, \tag{5.1.2}$$

acting on sufficiently smooth periodic functions $f(\theta)$ on $\theta \in [-\pi, \pi]$. Various approximations of eigenvalues were obtained in [11] by two asymptotic methods (expansions in powers of ϵ and the WKB method) and by three numerical methods (the Fourier series approximations, the pseudospectral method, and the Newton–Raphson iterations). The results of the pseudospectral method were checked independently in [120] (see pp. 124–125 and 406–408). It is seen both in [11] and [120] that the level sets of the resolvent $(\lambda - L)^{-1}$

form divergent curves to the left and right half-planes and, while true eigenvalues lie on the imaginary axis, eigenvalues of the truncated Fourier series may occur in the left and right half-planes of the spectral plane. This distinctive feature was interpreted in [11] towards the picture of growth of disturbances and the phenomenon of explosive instability.

One more question raised in [11] was about the validity of the series of eigenfunctions associated to the purely imaginary eigenvalues of the operator L for $\epsilon \neq 0$. Although various initial conditions h_0 were decomposed into a finite sum of eigenfunctions and the error decreased with a larger number of terms in the finite sum, the authors of [11] conjectured that the convergence of the series depended on the time variable and "even though the series converges at $t = 0$, it may diverge later". This conjecture would imply that the eigenfunctions of L for $\epsilon \neq 0$ do not form a basis of functions in the space $H^s([-\pi, \pi])$ with $s > \frac{1}{2}$ unlike the harmonics of the complex Fourier series associated with the operator L for $\epsilon = 0$.

In this chapter, we prove that the operator L is closed in $L^2_{\rm per}([-\pi, \pi])$ with a domain in $H^1_{\rm per}([-\pi, \pi])$ for $|\epsilon| < 2$, such that the spectrum of the eigenvalue problem

$$-\epsilon \frac{d}{d\theta}\left(\sin\theta \frac{df}{d\theta}\right) - \frac{df}{d\theta} = \lambda f, \qquad f \in H^1_{\rm per}([-\pi, \pi]), \tag{5.1.3}$$

is well-defined. Here and henceforth, we denote

$$H^1_{\rm per}([-\pi, \pi]) = \left\{ f \in H^1([-\pi, \pi]) : \quad f(\pi) = f(-\pi) \right\}. \tag{5.1.4}$$

Furthermore, we prove that the residual and continuous spectra of the spectral problem (5.1.3) are empty and the eigenvalues of the discrete spectrum accumulate at infinity along the imaginary axis. We further prove completeness of the series of eigenfunctions associated to all eigenvalues of the purely discrete spectrum of L in $L^2_{\rm per}([-\pi, \pi])$. Using the numerical approximations of eigenvalues and eigenfunctions of the spectral problem (5.1.3), we show that all eigenvalues of L are simple, located at the imaginary axis, and the angle between two subsequent eigenfunctions tends to zero for larger eigenvalues. As a result, the complete set of linearly independent eigenfunctions does not form a basis in $L^2_{\rm per}([-\pi, \pi])$ and hence it cannot be used to solve the Cauchy problem associated with the heat equation (5.1.1).

This chapter is structured as follows. Properties of the operator L are analyzed in *Section 5.2*. Eigenvalues of the operator L are characterized in *Section 5.3*. *Sections 5.4 – 5.5* present numerical approximations of eigenvalues and eigenfunctions of the spectral problem (5.1.3).

5.2 General properties of the linear operator L

It is obvious that the operator L is densely defined in $L^2_{\rm per}([-\pi, \pi])$ on the space of smooth functions with periodic boundary conditions. However, the operator L is not closed in

$L^2_{\rm per}([-\pi,\pi])$ if the functions are infinitely smooth. We therefore prove in Lemma 5.2.1 that the operator L admits a closure in $L^2_{\rm per}([-\pi,\pi])$ with a domain in $H^1_{\rm per}([-\pi,\pi])$. Eigenfunctions and eigenvalues of the spectral problem (5.1.3) are studied in Lemmas 5.2.4 and 3.4.7. The absence of the residual and continuous spectra of operator L is proved in Lemmas 5.2.6 and 5.2.7.

Lemma 5.2.1 *The operator L admits a closure in $L^2_{\rm per}([-\pi,\pi])$ for $|\epsilon|<2$ with* $\mathrm{Dom}(L)$ $\subset H^1_{\rm per}([-\pi,\pi])$.

Proof. According to Lemma 1.1.2 in [38], if an operator has a non-empty spectrum in a proper subset of a complex plane, then it must be closed. The operator L has a non-empty spectrum in $L^2_{\rm per}([-\pi,\pi])$ since $\lambda=0$ is an eigenvalue with the eigenfunction $f_0(\theta)=1\in L^2_{\rm per}([-\pi,\pi])$. We should show that there exists at least one regular point $\lambda_0\in\mathbb{C}$, such that

$$\forall f\in H^1_{\rm per}([-\pi,\pi]):\quad \|(L-\lambda_0 I)f\|_{L^2_{\rm per}([-\pi,\pi])}\geq k_0\|f\|_{L^2_{\rm per}([-\pi,\pi])} \tag{5.2.1}$$

for some $k_0>0$. In particular, we show that any $\lambda_0\in\mathbb{R}$ is a regular point of L in $H_0\subset H^1_{\rm per}([-\pi,\pi])$, where

$$H_0=\left\{f\in H^1_{\rm per}([-\pi,\pi]):\quad \int_{-\pi}^{\pi}f(\theta)d\theta=0\right\}. \tag{5.2.2}$$

By using straightforward computations, we obtain

$$(f',Lf)=-\int_{-\pi}^{\pi}(1+\epsilon\cos\theta)\,|f'|^2d\theta-\epsilon\int_{-\pi}^{\pi}\sin\theta\bar{f}'f''d\theta, \tag{5.2.3}$$

where $(g,f)=\int_{-\pi}^{\pi}\bar{g}(\theta)f(\theta)d\theta$ is a standard inner product in L^2. If $f\in H^1_{\rm per}([-\pi,\pi])$, then

$$\mathrm{Re}(f',f)=0,\qquad \mathrm{Re}(f',Lf)=-\int_{-\pi}^{\pi}\left(1+\frac{\epsilon}{2}\cos\theta\right)|f'|^2d\theta, \tag{5.2.4}$$

such that for any $\lambda_0\in\mathbb{R}$ it is true that

$$|\mathrm{Re}(f',(L-\lambda_0 I)f)|\geq\left(1-\frac{|\epsilon|}{2}\right)\|f'\|^2_{L^2_{\rm per}([-\pi,\pi])}.$$

By using the Cauchy–Schwarz inequality, we estimate the left-hand-side term from above

$$|\mathrm{Re}(f',(L-\lambda_0 I)f)|\leq|(f',(L-\lambda_0 I)f)|\leq\|f'\|_{L^2_{\rm per}([-\pi,\pi])}\|(L-\lambda_0 I)f\|_{L^2_{\rm per}([-\pi,\pi])},$$

such that

$$\|(L-\lambda_0 I)f\|_{L^2_{\rm per}([-\pi,\pi])}\geq\left(1-\frac{|\epsilon|}{2}\right)\|f'\|_{L^2_{\rm per}([-\pi,\pi])}. \tag{5.2.5}$$

According to the Neumann–Poincare inequality on $\theta \in [-\pi, \pi]$, we have

$$\|f\|^2_{L^2_{\rm per}([-\pi,\pi])} \leq 4\pi^2 \|f'\|^2_{L^2_{\rm per}([-\pi,\pi])} + \frac{1}{2\pi}\left(\int_{-\pi}^{\pi} f(\theta)d\theta\right)^2. \tag{5.2.6}$$

If $f \in H_0 \subset H^1_{\rm per}([-\pi, \pi])$, we continue the right-hand-side of the inequality (5.2.5) and recover the inequality (5.2.1) for any $\lambda_0 \in \mathbb{R}$ with

$$k_0 = \frac{1}{2\pi}\left(1 - \frac{|\epsilon|}{2}\right) > 0.$$

The estimate holds if $|\epsilon| < 2$. □

Corollary 5.2.2 *$\lambda \in \mathbb{R}\backslash\{0\}$ is not in the spectrum of L in $L^2_{\rm per}([-\pi, \pi])$.*

Remark 5.2.3 The formal adjoint of L in $L^2_{\rm per}([-\pi, \pi])$ is $L^* = -\epsilon\partial_\theta(\sin\theta\partial_\theta) + \partial_\theta$. According to Lemma 1.2.1 in [38], the operator L^* also admits a closure in $L^2_{\rm per}([-\pi, \pi])$ with $\mathrm{Dom}(L^*) \subset H^1_{\rm per}([-\pi, \pi])$ for $|\epsilon| < 2$.

Lemma 5.2.4 *Let λ be an eigenvalue of the spectral problem $Lf = \lambda f$ with an eigenfunction $f \in H^1_{\rm per}([-\pi, \pi])$. Then,*

(i) $-\lambda$, $\bar{\lambda}$ and $-\bar{\lambda}$ are also eigenvalues of the spectral problem $Lf = \lambda f$ with the eigenfunctions $f(-\theta)$, $\bar{f}(\theta)$ and $\bar{f}(-\theta)$ in $H^1_{\rm per}([-\pi, \pi])$.

(ii) λ is also an eigenvalue of the adjoint spectral problem $L^*f^* = \lambda f^*$ with the eigenfunction $f^* = f(\pi - \theta)$ in $H^1_{\rm per}([-\pi, \pi])$.

(iii) λ is a simple isolated eigenvalue of $Lf = \lambda f$ if and only if $(f^*, f) \neq 0$.

Proof. (i) Due to inversion $\theta \to -\theta$, the spectral problem (5.1.3) transforms to itself with the transformation $\lambda \to -\lambda$. Due to the complex conjugation, it transforms to itself with $\lambda \to \bar{\lambda}$. (ii) Due to the transformation $\theta \to \pi - \theta$, the spectral problem (5.1.3) transforms to the adjoint problem $L^*f = \lambda f$ with the same eigenvalue. (iii) The assertion follows by the Fredholm Alternative Theorem for isolated eigenvalues. □

Lemma 5.2.5 *Let λ be an eigenvalue of the spectral problem (5.1.3) with the eigenfunction $f \in H^1_{\rm per}([-\pi, \pi])$. Then,*

$$\mathrm{Re}(\lambda) = \epsilon\frac{(f', \sin\theta f')}{(f, f)}, \qquad i\mathrm{Im}(\lambda) = \frac{(f', f)}{(f, f)}, \tag{5.2.7}$$

and $\mathrm{Im}(\lambda) \neq 0$ except for a simple zero eigenvalue $\lambda = 0$.

Proof. By constructing the quadratic form for $f \in H^1_{\text{per}}([-\pi,\pi])$, we obtain

$$(f, Lf) = \epsilon \int_{-\pi}^{\pi} \sin\theta |f'|^2 d\theta - \int_{-\pi}^{\pi} \bar{f} f' d\theta, \tag{5.2.8}$$

where the second term is purely imaginary since

$$f \in H^1_{\text{per}}([-\pi,\pi]): \quad \int_{-\pi}^{\pi} \bar{f}' f d\theta = |f(\theta)|^2 |_{\theta=-\pi}^{\theta=\pi} - \int_{-\pi}^{\pi} \bar{f} f' d\theta = -\overline{\int_{-\pi}^{\pi} \bar{f}' f d\theta}. \tag{5.2.9}$$

Moreover, the equality (5.2.4) can be rewritten in the form

$$i\text{Im}(\lambda)(f', f) = \text{Re}(f', Lf) = -\int_{-\pi}^{\pi} \left(1 + \frac{\epsilon}{2}\cos\theta\right) |f'(\theta)|^2 d\theta \le -\left(1 - \frac{|\epsilon|}{2}\right) \|f'\|^2_{L^2}, \tag{5.2.10}$$

where the right-hand side is negative if $|\epsilon| < 2$ and $f(\theta)$ is not constant on $\theta \in [-\pi,\pi]$. Therefore, $(f', f) \neq 0$ and $\text{Im}(\lambda) \neq 0$. Finally, the constant eigenfunction $f(\theta) = 1$ corresponds to the eigenvalue $\lambda = 0$ and it is a simple eigenvalue since $(f^*, f) \neq 0$, where $f^*(\theta) = f(\pi - \theta) = 1$ is an eigenfunction of the adjoint operator L^* for the same eigenvalue $\lambda = 0$. □

Lemma 5.2.6 *The residual spectrum of the operator L is empty.*

Proof. By a contradiction, assume that λ belongs to the residual part of the spectrum of L such that $\text{Ker}(L - \lambda I) = \varnothing$ but $\text{Range}(L - \lambda I)$ is not dense in $L^2_{\text{per}}([-\pi,\pi])$. Let $g \in L^2_{\text{per}}([-\pi,\pi])$ be orthogonal to $\text{Range}(L - \lambda I)$, such that

$$\forall f \in L^2([-\pi,\pi]): \quad 0 = (g, (L - \lambda I)f) = ((L^* - \bar{\lambda} I)g, f).$$

Therefore, $(L^* - \bar{\lambda} I)g = 0$, that is $\bar{\lambda}$ is an eigenvalue of L^*. By Lemma 5.2.4(ii), $\bar{\lambda}$ is an eigenvalue of L and by Lemma 5.2.4(i), λ is also an eigenvalue of L. Hence λ can not be in the residual part of the spectrum of L. □

Lemma 5.2.7 *The continuous spectrum of the operator L is empty.*

Proof. According to Theorem 4 on p.1438 in [43], if L is a differential operator defined on the interval $\theta \in (-\pi,\pi) = (-\pi,0) \cup (0,\pi)$ and $L_\pm$ are restrictions of L on $\theta \in (-\pi,0)$ and $\theta \in (0,\pi)$, then $\sigma_c(L) = \sigma_c(L_+) \cup \sigma_c(L_-)$, where $\sigma_c(L)$ denotes the continuous spectrum of L. By the symmetry of the two intervals, it is sufficient to prove that the operator L_+ has no continuous spectrum on $\theta \in (0,\pi)$ (independently of the boundary conditions at $\theta = 0$ and $\theta = \pi$). It is also sufficient to carry out the proof for $\epsilon > 0$. Let $f_+(t) = f(\theta)$ on $\theta \in [0,\pi]$ and

$$\cos\theta = \tanh t, \quad \sin\theta = \text{sech} t, \qquad t \in \mathbb{R},$$

such that the interval $[0, \pi]$ for θ is mapped to the infinite line $\mathbb{R}$ for t. The function $f_+(t)$ satisfies the spectral problem

$$-\epsilon f_+''(t) + f_+'(t) = \lambda \text{sech} t \, f_+(t). \tag{5.2.11}$$

With a transformation $f_+(t) = e^{t/2\epsilon} g_+(t)$, the spectral problem (5.2.11) is written in the symmetric form

$$-\epsilon g_+''(t) + \frac{1}{4\epsilon} g_+(t) = \lambda \text{sech} t \, g_+(t). \tag{5.2.12}$$

Thus, our operator is extended to a symmetric operator with an exponentially decaying weight $\rho(t) = \text{sech}(t)$. According to Corollary 3 on p. 1437 in [43], if L is a symmetric operator on an open interval (a, b) and L_0 is a self-adjoint extension of L with respect to some boundary conditions at $x = a$ and $x = b$, then $\sigma_c(L) = \sigma_c(L_0)$. Here $a = -\infty$, $b = \infty$, and we need to show that the continuous spectrum of the symmetric problem (5.2.12) is empty in $L^2(\mathbb{R})$. This follows by Theorem 7 on p.93 in [51]: since the weight function $\rho(t)$ of the problem $-y''(t) - \lambda\rho(t)y(t) = 0$ on $t \in \mathbb{R}$ decays faster than $1/t^2$ as $|t| \to \infty$, the spectrum of $-y''(t) - \lambda\rho(t)y(t) = 0$ is purely discrete[1]. □

5.3 Eigenvalues of the linear operator L

By results of Lemmas 5.2.4, 5.2.5, 5.2.6, and 5.2.7, the spectral problem (5.1.3) for $|\epsilon| < 2$ may have only two types of eigenvalues in addition to the simple zero eigenvalue: either pairs of purely imaginary eigenvalues or quartets of symmetric complex eigenvalues. We prove in Lemmas 5.3.1 and 5.3.4 that there exists an infinite sequence of eigenvalues λ which accumulate to infinity along the imaginary axis. Furthermore, we prove in Theorem 5.3.6 that the eigenfunctions associated to all eigenvalues of the spectral problem (5.1.3) form a complete dense set in $L^2_{\text{per}}([-\pi, \pi])$. In the end of this section, Theorem 5.3.9 gives a necessary and sufficient condition that the set of eigenfunctions forms a basis in $L^2_{\text{per}}([-\pi, \pi])$.

Lemma 5.3.1 *Let $0 < \epsilon < 2$ and $\epsilon \neq \frac{1}{n}$, $n \in \mathbb{N}$. For $\lambda \in \mathbb{C}$, the spectral problem (5.1.3) admits three sets of two linearly independent solutions in the form of the Frobenius series*

$$-\pi < \theta < \pi: \quad f_1 = 1 + \sum_{n \in \mathbb{N}} c_n \theta^n, \quad f_2 = \theta^{-1/\epsilon} \left(1 + \sum_{n \in \mathbb{N}} d_n \theta^n \right), \tag{5.3.1}$$

[1] Although the spectral problem (5.2.12) has an additional term $Cy(t)$ with $C > 0$, this term only makes better the inequality (30) on p.93 in the proof of Theorem 7 of [51].

and

$$0 < \pm\theta < \pi: \quad f_1^{\pm} = 1 + \sum_{n\in\mathbb{N}} a_n^{\pm}(\pi \mp \theta)^n, \quad f_2^{\pm} = (\pi \mp \theta)^{1/\epsilon}\left(1 + \sum_{n\in\mathbb{N}} b_n^{\pm}(\pi \mp \theta)^n\right), \tag{5.3.2}$$

where all coefficients are uniquely defined. The solution $f_1(\theta)$ is an analytic function of $\lambda \in \mathbb{C}$ uniformly on $\theta \in [-\pi, \pi]$.

Proof. Existence of two linearly independent solutions on $-\pi < \theta < \pi$ in the form (5.3.1) and on $0 < \pm\theta < \pi$ in the form (5.3.2) follows by the ODE analysis near the regular singular points [31]. The difference between the two indices of the indicial equation is $\frac{1}{\epsilon}$ and it is non-integer for $\epsilon \neq \frac{1}{n}$, $n \in \mathbb{N}$[2]. Since the spectral problem (5.1.3) depends analytically on λ and the Frobenius series converges absolutely and uniformly in between two regular singular points, the solution $f_1(\theta)$ is analytic in $\lambda \in \mathbb{C}$ for any fixed $\theta \in (-\pi, \pi)$. Due to uniqueness of the solutions of the ODE (5.1.3), the solution $f_1(\theta)$ can be equivalently represented by the other solutions

$$f_1(\theta) = A^{\pm} f_1^{\pm}(\theta) + B^{\pm} f_2^{\pm}(\theta), \quad 0 < \pm\theta < \pi, \tag{5.3.3}$$

where $A^{\pm}$ and $B^{\pm}$ are some constants, while the functions $f_1^{\pm}(\theta)$ and $f_2^{\pm}(\theta)$ are analytic in $\lambda \in \mathbb{C}$ for any fixed $\pm\theta \in (0, \pi]$. By matching analytic solutions for any $\pm\theta \in (0, \pi)$, we find that $A^{\pm}$ and $B^{\pm}$ are analytic functions of $\lambda \in \mathbb{C}$, the Frobenius series for $f_1(\theta)$ converges absolutely and uniformly on $\theta \in [-\pi, \pi]$, and the solution $f_1(\theta)$ is an analytic function in $\lambda \in \mathbb{C}$ uniformly on $\theta \in [-\pi, \pi]$. □

Corollary 5.3.2 *There exists an analytic function $F_\epsilon(\lambda)$ on $\mathrm{Im}\lambda > 0$, roots of which give isolated eigenvalues of the spectral problem (5.1.3) with the account of their multiplicity. The only accumulation point of isolated eigenvalues in the λ-plane may occur at infinity.*

Proof. The function $f \in H^1([-\pi, \pi])$ satisfies the spectral problem (5.1.3) if and only if $f(\theta) = C_0 f_1(\theta)$ on $\theta \in [-\pi, \pi]$, where $C_0 = 1$ thanks to the scaling invariance of homogeneous equations. By using the representation (5.3.3), we can find that $A^{\pm} = \lim_{\theta\to\pm\pi} f_1(\theta)$ are uniquely defined analytic functions in $\lambda \in \mathbb{C}$. The function $F_\epsilon(\lambda) = A^+ - A^-$ is analytic function of $\lambda \in \mathbb{C}$ by construction and zeros of $F_\epsilon(\lambda)$ on $\mathrm{Im}\lambda > 0$ coincide with the eigenvalues λ of the spectral problem (5.1.3) with the account of their multiplicity. If $F_\epsilon(\lambda_0) = 0$ for some $\lambda_0 \in \mathbb{C}$, the corresponding eigenfunction $f(\theta)$ lies in $H^1_{\mathrm{per}}([-\pi, \pi])$, i.e. it satisfies the periodic boundary conditions $f(\pi) = f(-\pi)$. By analytic function theory, the sequence of roots of $F_\epsilon(\lambda)$ can not accumulate at a finite point on $\lambda \in \mathbb{C}$. □

[2] An additional logarithmic term $\log(\pi - \theta)$ may need to be included into the Frobeneus series if $\epsilon = \frac{1}{n}$, $n \in \mathbb{Z}$.

Remark 5.3.3 We will use the method involving the analytic function $F_\epsilon(\lambda)$ on $\lambda \in \mathbb{C}$ for a numerical shooting method which enables us to approximate eigenvalues of the spectral problem (5.1.3). This method involves less computations than the shooting method described in Appendix C of [11]. Nevertheless, it is essentially the same shooting method and it uses the ODE analysis near the regular singular point (Lemma 5.3.1), which repeats the arguments in Appendix B of [11].

Lemma 5.3.4 *Fix $0 < \epsilon < 2$ and let $\{\lambda_n\}_{n\in\mathbb{N}}$ be a set of eigenvalues of the spectral problem (5.1.3) with $\mathrm{Im}\lambda_n > 0$, ordered in the ascending order of $|\lambda_n|$. There exists a finite number $N \geq 1$, such that for all $n \geq N$, $\lambda_n = i\omega_n \in i\mathbb{R}_+$ and*

$$\omega_n = Cn^2 + \mathrm{o}(n^2) \ \ as \ \ n \to \infty, \tag{5.3.4}$$

for some $C > 0$.

Proof. We reduce the spectral problem (5.1.3) to two uncoupled Schroödinger equations on an infinite line. Let $f(\theta)$ be represented on two intervals $\pm\theta \in [0, \pi]$ by using the transformations

$$\cos\theta = \tanh t, \qquad \sin\theta = \pm \mathrm{sech} t, \tag{5.3.5}$$

where $t \in \mathbb{R}$. Then, the functions $f_\pm(t) = f(\theta)$ on $\pm\theta \in [0, \pi]$ satisfy the uncoupled spectral problems

$$-\epsilon f_\pm''(t) + f_\pm'(t) = \pm\lambda \mathrm{sech} t \ f_\pm(t), \quad t \in \mathbb{R}, \tag{5.3.6}$$

The normalization condition $f(0) = 1$ is equivalent to the condition $\lim\limits_{t\to\infty} f_\pm(t) = 1$. The periodic boundary condition $f(\pi) = f(-\pi)$ is equivalent to the condition $\lim\limits_{t\to-\infty} f_-(t) = \lim\limits_{t\to-\infty} f_+(t)$. The linear problems (5.3.6) are reformulated as the quadratic Ricatti equations by using the new variables

$$f_\pm(t) = e^{\int_\infty^t S_\pm(t')dt'} : \quad S_\pm - \epsilon(S_\pm' + S_\pm^2) = \pm\lambda \mathrm{sech} t. \tag{5.3.7}$$

We choose a negative root of the quadratic equation in the form

$$S_\pm(t) = \frac{1 - \sqrt{1 \mp 4\epsilon\lambda \mathrm{sech} t - 4\epsilon^2 R_\pm}}{2\epsilon}, \qquad R_\pm = S_\pm'(t). \tag{5.3.8}$$

The representation (5.3.8) becomes the chain fraction if the derivative of $S_\pm(t)$ is defined recursively from the same expression (5.3.8). By using the theory of chain fractions, we claim that $R_\pm = \mathrm{O}(\sqrt{|\lambda|})$ as $|\lambda| \to \infty$ uniformly on $t \in \mathbb{R}$. The function $F_\epsilon(\lambda)$ of Corollary 5.3.2 is now expressed by

$$F_\epsilon(\lambda) = \lim_{t\to-\infty} [f_+(t) - f_-(t)] = e^{\int_{-\infty}^{\infty} S_+(t)dt} - e^{\int_{-\infty}^{\infty} S_-(t)dt}. \tag{5.3.9}$$

Zeros of $F_\epsilon(\lambda)$ are equivalent to zeros of the infinite set of functions

$$G_n(\lambda) = \frac{1}{4\pi i\epsilon}\int_{-\infty}^{\infty}\left[\sqrt{1+4\epsilon\lambda\mathrm{sech}t-4\epsilon^2R_-(t)}-\sqrt{1-4\epsilon\lambda\mathrm{sech}t-4\epsilon^2R_+(t)}\right]dt-n, \tag{5.3.10}$$

where $n\in\mathbb{N}$. If $R_\pm(t)\equiv 0$, the function $\tilde{G}_n(\omega)=G(i\omega)$, $n\in\mathbb{N}$ is real-valued and strictly increasing on $\omega\in\mathbb{R}_+$ with $\tilde{G}_n(0)=-n$. By performing asymptotic analysis, we compute that

$$\begin{aligned}
&\frac{1}{4\pi i\epsilon}\int_{-\infty}^{\infty}\left[\sqrt{1+4i\epsilon\omega\mathrm{sech}t-4\epsilon^2R_-(t)}-\sqrt{1-4i\epsilon\omega\mathrm{sech}t-4\epsilon^2R_+(t)}\right]dt\\
&=\frac{1}{\pi i}\int_{-\infty}^{\infty}\frac{2i\omega\mathrm{sech}t+\epsilon(R_+-R_-)}{\sqrt{1+4i\epsilon\omega\mathrm{sech}t-4\epsilon^2R_-(t)}+\sqrt{1-4i\epsilon\omega\mathrm{sech}t-4\epsilon^2R_+(t)}}dt\\
&=\frac{\sqrt{\omega}}{\sqrt{2\epsilon\pi}}\int_{-\infty}^{\infty}\frac{dt}{\sqrt{\cosh t}}+\mathrm{o}\left(\sqrt{\omega}\right),
\end{aligned}\tag{5.3.11}$$

such that $\lim_{\omega\to\infty}\tilde{G}_n(\omega)=\infty$. Therefore, there exists exactly one root $\omega=\omega_n$ of $\tilde{G}_n(\omega)$ for each n. Since $R_-=\bar{R}_+$ for $\lambda=i\omega\in i\mathbb{R}$, each simple root of $\tilde{G}_n(\omega)$ persists for non-zero values of $R_\pm(t)=\mathrm{O}(\sqrt{\omega})$ uniformly on $t\in\mathbb{R}$ as $\omega\to\infty$. According to the asymptotic result (5.3.11), the roots ω_n of $\tilde{G}_n(\omega)$ satisfy the asymptotic distribution (5.3.4) with $C=\frac{2\epsilon\pi^2}{\left(\int_{-\infty}^{\infty}\frac{dt}{\sqrt{\cosh t}}\right)^2}$. □

Remark 5.3.5 Analysis of Lemma 5.3.4 extends the formal WKB approach proposed in Section 3 of [11]. In particular, the equation (5.3.10) with $R_\pm=0$ has been obtained in Eq. (3.11) of [11].

Theorem 5.3.6 *Let $\{f_n\}_{n\in\mathbb{N}}$ be the set of eigenfunctions corresponding to the set of eigenvalues $\{\lambda_n\}_{n\in\mathbb{N}}$ in Lemma 5.3.4 with $\mathrm{Im}\lambda_n>0$. The set of eigenfunctions is complete in $X_0\subset L^2_{\mathrm{per}}([-\pi,\pi])$, where*

$$X_0=\left\{f\in L^2_{\mathrm{per}}([-\pi,\pi]):\quad\int_{-\pi}^{\pi}f(\theta)d\theta=0\right\}.$$

Proof. By Corollary 5.3.2, eigenvalues of L with $\mathrm{Im}\lambda>0$ accumulate to infinity, such that the operator $M=L^{-1}$ acting on elements in X_0 is compact. By Lemma 5.3.4, there are infinitely many eigenvalues of L and large eigenvalues are all purely imaginary, such that $|\lambda_n|=\mathrm{O}(n^2)$ as $n\to\infty$. These two facts satisfy two sufficient conditions of the Lidskii's Completeness Theorem. According to Theorem 6.1 on p. 302 in [52], the set of

eigenvectors and generalized eigenvectors of a compact operator M in a Hilbert space X_0 is complete if there exists $p > 0$ such that

$$s_n(M) = o(n^{\frac{-1}{p}}), \quad \text{as } n \to \infty, \tag{5.3.12}$$

where s_n is a singular number of the operator M, and the set

$$W_M = \{(Mf, f): \quad f \in X_0, \quad \|f\|_{X_0} = 1\} \tag{5.3.13}$$

lies in a closed angle θ_M with vertex at 0 and opening $\frac{\pi}{p}$. Since the singular numbers s_n are eigenvalues of the positive self-adjoint operator $(MM^*)^{1/2}$ and the eigenvalues of L grow like $O(n^2)$ as $n \to \infty$, we have $s_n(M) = O(n^{-2})$ as $n \to \infty$, such that the first condition (5.3.12) is verified with $p = 1$. Since all $\mathrm{Im}\lambda_n > 0$ for the set of eigenvalues $\{\lambda_n\}_{n\in\mathbb{N}}$ of Lemma 5.3.4, the spectrum of M lies in the lower half plane, such that the second condition (5.3.13) is also verified with $p = 1$ ($\theta_M = \pi$). □

Corollary 5.3.7 *The set of eigenfunctions $\{f_n\}_{n\in\mathbb{Z}}$ with $f_0 = 1$ and $f_{-n} = \bar{f}_n$, $\forall n \in \mathbb{N}$ is complete in $L^2_{\mathrm{per}}([-\pi, \pi])$.*

Remark 5.3.8 Due to linear independence of eigenfunctions for distinct eigenvalues, the set of eigenfunctions $\{f_n\}_{n\in\mathbb{Z}}$ is also minimal if all eigenvalues are simple[3]. If the set $\{f_n\}_{n\in\mathbb{Z}}$ is complete and minimal, any function $f \in L^2_{\mathrm{per}}([-\pi, \pi])$ can be approximated by a finite linear combination $f_N = \sum_{n=-N}^{N} c_n f_n$ in the following sense: for any fixed $\varepsilon > 0$, there exists $N \geq 1$ and the set of coefficients $\{c_n\}_{-N\leq n\leq N}$, such that the inequality $\|f - f_N\|_{L^2_{\mathrm{per}}([-\pi,\pi])} < \epsilon$ holds. This approximation does not imply that the set $\{f_n\}_{n\in\mathbb{Z}}$ forms a Schauder basis in the Hilbert space $L^2_{\mathrm{per}}([-\pi, \pi])$, in which case there would exist a unique series representation $f = \sum_{n\in\mathbb{Z}} c_n f_n$ for any $f \in L^2_{\mathrm{per}}([-\pi, \pi])$.

Theorem 5.3.9 *Let $\{f_n\}_{n\in\mathbb{Z}}$ be a complete and minimal set of eigenfunctions of the spectral problem (5.1.3) for the set of eigenvalues $\{\lambda_n\}_{n\in\mathbb{Z}}$ in Theorem 5.3.6. The set of eigenfunctions forms a basis in Hilbert space $L^2_{\mathrm{per}}([-\pi, \pi])$ if and only if $\lim_{n\to\infty} \cos(\widehat{f_n, f_{n+1}}) < 1$.*

Proof. According to Theorem 2 on page 31 in [87], the complete and minimal set of eigenfunctions $\{f_n\}_{n\in\mathbb{Z}}$ forms a basis in Hilbert space $X = L^2_{\mathrm{per}}([-\pi, \pi])$ if and only if $\sup_N \|P_N\| < \infty$, where P_N is the projector of the linear span $\{f_n\}_{-N\leq n\leq N}$ in the direction of the linear span $\{f_n\}_{|n|\geq N+1}$. Since the Hilbert space X is a direct sum of the two linear spans above, the norm of the parallel projector P_N has the geometrical representation

[3]By Lemma 5.3.4, all eigenvalues are simple starting with some $n \geq N$.

$\|P_N\| = \frac{1}{\sin\alpha_N}$, where α_N is the angle between the two linear spans [4]. This implies that the set $\{f_n\}_{n\in\mathbb{Z}}$ is a basis in the Hilbert space X if and only if

$$\cos(\widehat{f_n, f_{n+1}}) = \frac{|(f_n, f_{n+1})|}{\|f_n\|\|f_{n+1}\|} < 1, \tag{5.3.14}$$

for sufficiently large $n \in \mathbb{Z}$ [53]. □

5.4 Numerical shooting method

We approximate isolated eigenvalues of the spectral problem (5.1.3) for $0 < \epsilon < 2$ numerically. In agreement with numerical results in [11], we show that all eigenvalues in the set $\{\lambda_n\}_{n\in\mathbb{Z}}$ are simple and purely imaginary. Therefore, the set $\{\lambda_n\}_{n\in\mathbb{Z}}$ can be ordered in the ascending order, such that $\lambda_0 = 0$, $\lambda_n = -\lambda_{-n}$, $\forall n \in \mathbb{N}$, $\mathrm{Im}\lambda_n < \mathrm{Im}\lambda_{n+1}$ and $\lim\limits_{n\to\infty} |\lambda_n| = \infty$. We also show that the angle between two subsequent eigenfunctions $f_n(\theta)$ and $f_{n+1}(\theta)$ in the set $\{f_n(\theta)\}_{n\in\mathbb{Z}}$ tends to zero as $n \to \infty$.

The numerical shooting method is based on the ODE formulation of the spectral problem (5.1.3). By Lemma 5.3.1 and Corollary 5.3.2, complex eigenvalues $\lambda \in \mathbb{C}$ are determined by roots of the analytic function $F_\epsilon(\lambda)$ in the λ-plane. The number of complex eigenvalues can be computed with the winding number theory. The number and location of purely imaginary eigenvalues can be found from real-valued roots of a scalar real-valued function.

Proposition 5.4.1 *Let the eigenfunction $f(\theta)$ of the spectral problem (5.1.3) for $0 < \epsilon < 2$ be normalized by the condition $f(0) = 1$. The eigenvalue λ is purely imaginary if and only if $f(\theta) = \overline{f}(-\theta)$ on $\theta \in [-\pi, \pi]$.*

Proof. If $\lambda \in i\mathbb{R}$ and $f(\theta)$ satisfies the second-order ODE (5.1.3) on $\theta \in [-\pi, \pi]$, then $\bar{f}(-\theta)$ satisfies the same ODE (5.1.3) on $\theta \in [-\pi, \pi]$. By Corollary 5.3.2, if $f \in H^1_{\rm per}([-\pi, \pi])$, $f(0) = 1$ and $0 < \epsilon < 2$, the solution $f(\theta)$ is uniquely defined. By uniqueness of solutions, $f(\theta) = \overline{f}(-\theta)$ on $\theta \in [-\pi, \pi]$.

If $f(\theta) = \overline{f}(-\theta)$ on $\theta \in [-\pi, \pi]$, then,

$$\int_{-\pi}^{\pi} \sin\theta |f'(\theta)|^2 d\theta = \int_0^{\pi} \sin\theta |f'(\theta)|^2 d\theta - \int_0^{\pi} \sin\theta |f'(-\theta)|^2 d\theta = 0,$$

such that $\mathrm{Re}\lambda = 0$ according to the equality (5.2.7) in Lemma 5.2.5. □

Corollary 5.4.2 *Let $f(\theta)$ be an eigenfunction of the spectral problem (5.1.3) for $\lambda \in i\mathbb{R}$, such that $f \in H^1_{\rm per}([-\pi, \pi])$ and $f(0) = 1$. Then, $f(\pi) = f(-\pi)$ is equivalent to $f(\pi) \in \mathbb{R}$. The eigenvalue $\lambda \in i\mathbb{R}$ is simple if and only if*

$$(f^*, f) = 2\mathrm{Re}\int_0^{\pi} f(\theta)\bar{f}(\pi - \theta)d\theta \neq 0. \tag{5.4.1}$$

Proof. The first assertion follows by the symmetry relation $f(\theta) = \bar{f}(-\theta)$ evaluated at $\theta = \pi$. The second asserion follows by Lemma 5.2.4 with the use of the symmetry $f^*(\theta) = f(\pi - \theta)$. □

By Lemma 5.3.1, the function $f(\theta)$ with $f(0) = 1$ is represented uniquely by the Frobenius series

$$f(\theta) = f_1(\theta) = 1 + \sum_{n\in\mathbb{N}} c_n \theta^n, \tag{5.4.2}$$

where the coefficients $\{c_n\}_{n\in\mathbb{N}}$ are uniquely defined by the recursion relation

$$c_n = -\frac{1}{n(1+\epsilon n)}\left(\lambda c_{n-1} + \epsilon n \sum_{m\in\mathbb{N}'} \frac{(-1)^{\frac{n-m}{2}} m}{(n-m+1)!} c_m\right), \quad n \in \mathbb{N}, \tag{5.4.3}$$

where $c_0 = 1$ and $\mathbb{N}'$ is a set of integers in the interval $[1, n-2]$ such that $n - m$ is even. For instance,

$$c_1 = -\frac{\lambda}{1+\epsilon}, \quad c_2 = \frac{\lambda^2}{2(1+\epsilon)(1+2\epsilon)}, \quad c_3 = -\frac{\lambda(\lambda^2 + \epsilon(1+2\epsilon))}{3!(1+\epsilon)(1+2\epsilon)(1+3\epsilon)},$$

and so on. We truncate the power series expansion on $N = 100$ terms and approximate the initial value $[f(\theta_0), f'(\theta_0)]$ at $\theta_0 = 10^{-8}$. By using the fourth-order Runge–Kutta ODE solver with time step $h = 10^{-4}$, we obtain a numerical approximation of $f \equiv f_+(\theta)$ on $\theta \in [\theta_0, \pi - \theta_0]$ for λ and $f \equiv f_-(\theta)$ on the same interval for $-\lambda$. By Lemma 5.2.4(i), the numerical approximation of the function $F_\epsilon(\lambda)$ of Corollary 5.3.2 is

$$\hat{F}_\epsilon(\lambda) = f_+(\pi - \theta_0) - f_-(\pi - \theta_0). \tag{5.4.4}$$

If $\lambda \in i\mathbb{R}$, the function $\hat{F}_\epsilon(\lambda)$ is simplified by using Corollary 5.4.2 as $\hat{F}_\epsilon(\lambda) = 2i\mathrm{Im} f_+(\pi - \theta_0)$. Table 1 represents the numerical approximations of the first four non-zero eigenvalues $\lambda \in i\mathbb{R}$ for $\epsilon = 0.5, 1.0, 1.5$[4] with the error computed from the residual

$$R = \left|\frac{(f, Lf)}{(f, f)} - \lambda\right|.$$

We can see from Table 1 that the accuracy drops with larger values of ϵ and for larger eigenvalues, but the eigenvalues persist inside the interval $|\epsilon| < 2$.

Figure 5.1 shows the profiles of eigenfunctions $f(\theta)$ on $\theta \in [0, \pi]$ for the first two eigenvalues $\lambda = i\omega_{1,2} \in i\mathbb{R}_+$ for $\epsilon = 0.5$ (left) and $\epsilon = 1.5$ (right). We can see from Fig.

[4]We note that the Frobenius series (5.4.2) is not affected by the logarithmic terms for $\epsilon = 0.5$ and $\epsilon = 1.0$, since 0 is the largest index of the indicial equation at $\theta = 0$.

1 that the derivative of $f(\theta)$ becomes singular as $\theta \to \pi^-$ for $\epsilon \geq 1$. We can also see that the real part of the eigenfunction $f(\theta)$ has one zero on $\theta \in (0, \pi)$ for the first eigenvalue and two zeros for the second eigenvalue, while the imaginary part of the eigenfunction $f(\theta)$ has a fewer number of zeros by one. The numerical approximations of the eigenvalue and eigenfunctions of the spectral problem (5.1.3) are structurally stable with respect to variations in θ_0, N and h.

Figure 5.2 shows the complex plane of $w = \hat{F}_\epsilon(\lambda)$ (left) and the argument of w (right) when λ traverses along the first quadrant of the complex plane $\lambda \in \Lambda_1 \cup \Lambda_2 \cup \Lambda_3$ for $\epsilon = 0.5$. Here $\Lambda_1 = x + ir$ with $x \in [r, R]$, $\Lambda_2 = Re^{i\varphi}$ with $\varphi \in [\varphi_0, \frac{\pi}{2} - \varphi_0]$ and $\lambda_3 = r + iy$ with $y \in [r, R]$, where $r = 0.1$, $R = 10$, and $\varphi_0 = \arctan(r/R)$. It is obvious that the winding number of $\hat{F}_\epsilon(\lambda)$ across the closed contour is zero. Therefore, no zeros of $\hat{F}_\epsilon(\lambda)$ occurs in the first quadrant of the complex plane $\lambda \in \mathbb{C}$. The numerical result is structurally stable with respect to variations in r, R and ϵ.

ϵ	ω_1	R_1	ω_2	R_2
0.5	1.167342	0.000051	2.968852	0.000405
1.0	1.449323	0.000837	4.319645	0.007069
1.5	1.757278	0.002691	5.719671	0.018412

ϵ	ω_3	R_3	ω_4	R_4
0.5	5.483680	0.001436	8.715534	0.003653
1.0	8.631474	0.024964	14.382886	0.061881
1.5	11.846709	0.054271	20.138824	0.113834

Table 1: Numerical approximations of the first four eigenvalues $\lambda = i\omega_n$ of the spectral problem (5.1.3) and the residuals $R = R_n$ for three values of ϵ.

5.5 Numerical spectral method

The numerical spectral method is based on the reformulation of the second-order ODE (5.1.3) as the second-order difference equation and the subsequent truncation of the difference eigenvalue problem. It is found in [119] that the truncation procedure lead to spurious complex eigenvalues which bifurcate off the imaginary axis.

Let $f \in H^1_{\text{per}}([-\pi, \pi])$ be an eigenfunction of the spectral problem (5.1.3). This eigenfunction is equivalently represented by the Fourier series

$$f(\theta) = \sum_{n \in \mathbb{Z}} f_n e^{-in\theta}, \qquad f_n = \frac{1}{2\pi} \int_{-\pi}^{\pi} f(\theta) e^{in\theta} d\theta, \tag{5.5.1}$$

where the infinite-dimensional vector $\mathbf{f} = (..., f_{-2}, f_{-1}, f_0, f_1, f_2, ...)$ is defined in $\mathbf{f} \in l^2_1(\mathbb{Z})$ equipped with the norm $\|\mathbf{f}\|^2_{l^2_1} = \sum_{n \in \mathbb{Z}} (1 + n^2)|f_n|^2 < \infty$. The spectral problem

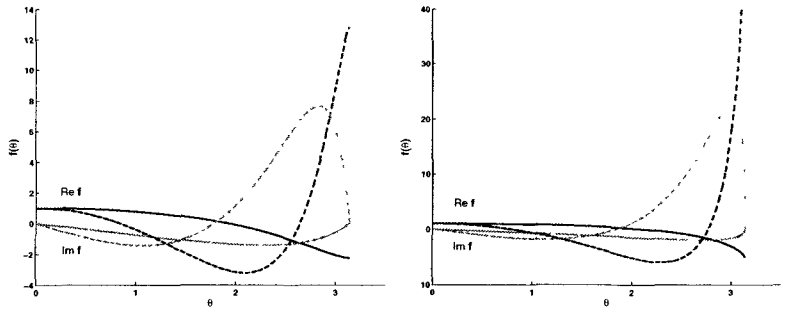

Figure 5.1: The real part (blue) and imaginary part (green) of the eigenfunction $f(\theta)$ on $\theta \in [0, \pi]$ for the first (solid) and second (dashed) eigenvalues $\lambda = i\omega_{1,2} \in i\mathbb{R}_+$ for $\epsilon = 0.5$ (left) and $\epsilon = 1.5$ (right).

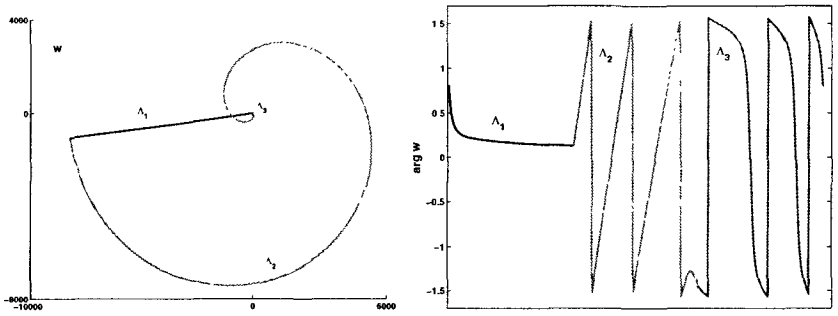

Figure 5.2: The image of the curve $w = \hat{F}_\epsilon(\lambda)$, when λ traverses along the contours Λ_1 (blue), Λ_2 (green) and Λ_3 (magenta) for $\epsilon = 0.5$: the image curve on the w-plane (left) and the argument of w (right).

(5.1.3) for $|\epsilon| < 2$ is equivalent to the difference eigenvalue problem

$$nf_n + \frac{\epsilon}{2} n\left[(n+1)f_{n+1} - (n-1)f_{n-1}\right] = -i\lambda f_n, \qquad n \in \mathbb{Z}. \tag{5.5.2}$$

The difference eigenvalue problem (5.5.2) splits into three parts

$$A\mathbf{f}_+ = -i\lambda \mathbf{f}_+, \qquad A\mathbf{f}_- = i\lambda \mathbf{f}_-, \qquad \lambda f_0 = 0, \tag{5.5.3}$$

where $\mathbf{f}_\pm = (f_{\pm 1}, f_{\pm 2}, ...)$ and A is an infinite-dimensional matrix

$$A = \begin{bmatrix} 1 & \epsilon & 0 & 0 & \cdots \\ -\epsilon & 2 & 3\epsilon & 0 & \cdots \\ 0 & -3\epsilon & 3 & 6\epsilon & \cdots \\ 0 & 0 & -6\epsilon & 4 & \cdots \\ \vdots & \vdots & \vdots & \vdots & \ddots \end{bmatrix} \tag{5.5.4}$$

Since $A = D - iS$, where D is a diagonal matrix and S is a self-adjoint tri-diagonal matrix, one can define the discrete counterpart of Lemma 5.2.5

$$\mathrm{Im}\lambda = \frac{(\mathbf{f}_+, D\mathbf{f}_+)}{(\mathbf{f}_+, \mathbf{f}_+)} = \frac{\sum_{n\in\mathbb{N}} n|f_n|^2}{\sum_{n\in\mathbb{N}} |f_n|^2}, \qquad \mathrm{Re}\lambda = \frac{(\mathbf{f}_+, S\mathbf{f}_+)}{(\mathbf{f}_+, \mathbf{f}_+)}.$$

where $\mathrm{Im}\lambda > 0$. The adjoint eigenfunction $f^*(\theta) = f(\pi - \theta)$ is recovered from the eigenvector $\mathbf{f}$ by $\mathbf{f}^* = J\mathbf{f}$, where

$$J = \begin{bmatrix} 0 & 0 & J_0 \\ 0 & 1 & 0 \\ J_0 & 0 & 0 \end{bmatrix}$$

and J_0 is a diagonal operator with entries $(-1, 1, -1, 1, ...)$.

According to Theorem 5.3.6, rewritten from the set of eigenfunctions $\{f_n\}_{n\in\mathbb{Z}}$ to the set of eigenvectors $\{\mathbf{f}_n\}_{n\in\mathbb{Z}}$, the inverse matrix operator A^{-1} is of the Hilbert-Schmidt type, and hence compact. Let $A_N^{-1} = P_N A^{-1} P_N$ denote the truncation of the matrix operator A^{-1} at the first N rows and columns, where P_N is an orthogonal projector from an infinite-dimensional vector to the N-dimensional vector of the first N components.

Proposition 5.5.1 *Operator sequence A_N^{-1} converges uniformly to the compact operator A^{-1} as $N \to \infty$. Eigenvalues of the matrices A_N^{-1} converge to the eigenvalues of the compact operator A^{-1} as $N \to \infty$.*

Proof. It follows from the Finite Rank Approximation Theorem that $P_N A^{-1}$ converges uniformly to the compact operator A^{-1}. Therefore, for any $\epsilon > 0$, there exists a number $N_1 \geq 1$ such that

$$\forall N > N_1 : \quad \|P_N A^{-1} - A^{-1}\| < \frac{\epsilon}{2}.$$

Because the adjoint operator is also compact and the orthogonal projector P_N is a self-adjoint operator, the sequence $P_N^* A^{-1*}$ is uniformly converges to A^{-1*}. Therefore, for any $\epsilon > 0$, there exists a number $N_2 \geq 1$ such that

$$\forall N > N_2 : \quad \|P_N^* A^{-1*} - A^{-1*}\| < \frac{\epsilon}{2}.$$

Let $N_0 = \max(N_1, N_2)$. For any $N > N_0$, we have

$$\begin{aligned} \|A^{-1} - P_N A^{-1} P_N\| &= \|(A^{-1} - P_N A^{-1}) + P_N (A^{-1*} - P_N^* A^{-1*})^*\| \\ &\leq \|(A^{-1} - P_N A^{-1})\| + \|P_N\| \|(A^{-1*} - P_N^* A^{-1*})^*\| \\ &\leq \|A^{-1} - P_N A^{-1} P_N\| + \|(A^{-1*} - P_N^* A^{-1*})\| \leq \epsilon. \end{aligned}$$

Therefore, $\lim_{N\to\infty} A_N^{-1} = A^{-1}$.

Let $\lambda_0 \neq 0$ belongs to the spectrum of the operator A^{-1}. Because all eigenvalues are isolated, there exists an open ball $D_0 \in \mathrm{Dom}(A^{-1})$ with the boundary ∂D_0 passing though regular points of operator A such that λ_0 is the only point of D_0 in the spectrum set of A^{-1}. It follows from the compactness of ∂D_0 that the set $\left\{(A_N^{-1} - \lambda I)^{-1} : \ \lambda \in \partial D_0\right\}$ is uniformly bounded by N and by λ. Therefore, the sequence of the Riesz projectors

$$R_N = -\frac{1}{2\pi i} \oint_{\Gamma_{D_0}} (A_N^{-1} - \lambda I)^{-1} d\lambda$$

strongly converges to the limiting projector

$$R = -\frac{1}{2\pi i} \oint_{\Gamma_{D_0}} (A^{-1} - \lambda I)^{-1} d\lambda.$$

If all $R_N = 0$, then the limiting projector $R = 0$. □

Remark 5.5.2 The distance between eigenvalues of A_N^{-1} and A^{-1} may not be small for fixed N, but it becomes small in the limit of large N. The convergence of eigenvalues is not uniform in λ.

The smallest eigenvalues of the truncated matrix A_N^{-1} are found with the parallel Krylov subspace iteration algorithm [46]. *Figure 5.3* shows the distance between eigenvalues of the shooting method and eigenvalues of the Krylov spectral method for $\epsilon = 0.1$. The

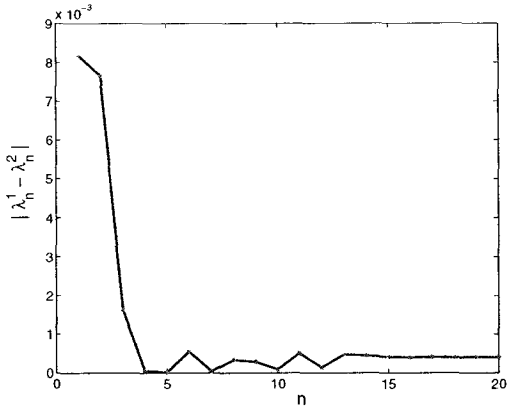

Figure 5.3: The distance between eigenvalues computed by the shooting and spectral methods for $\epsilon = 0.1$.

difference between two eigenvalues is small of the order $O(10^{-3})$ but the advantage of the parallel algorithm is that the calculating time of 20 largest eigenvalues of A_N^{-1} for $N = 10^6$ takes less than one minute on a network of 16 processors while finding the same set of eigenvalues by the shooting method with the time step $h = 10^{-5}$ takes about one hour.

Figure 5.4 shows symmetric pairs of eigenvalues of the matrix A_N for $\epsilon = 0.3$ at $N = 128$ (left) and $N = 1024$ (right). We confirm the numerical result of [119] that the truncation of the matrix operator A always produces splitting of large eigenvalues off the imaginary axis. Moreover, starting with some number n, the eigenvalues of A_N are real-valued. This feature is an artifact of the truncation, which contradicts to Lemmas 5.2.5 and 5.3.4 as well as to results of the shooting method. However, the larger is N, the more eigenvalues remain on the purely imaginary axis. Therefore, the corresponding eigenvectors can be used to compute the angle in Theorem 5.3.9.

Figure 5.5 (left) show the values of the cosine of the angle (5.3.14) for the first 20 purely imaginary eigenvalues for $\epsilon = 0.1$. As we can see from the figure, the angle between two eigenvectors tends to zero for larger eigenvalues up to the numerical accuracy. *Figure 5.5* (right) and Table 2 show that the angle drops to zero faster with larger values of the parameter ϵ.

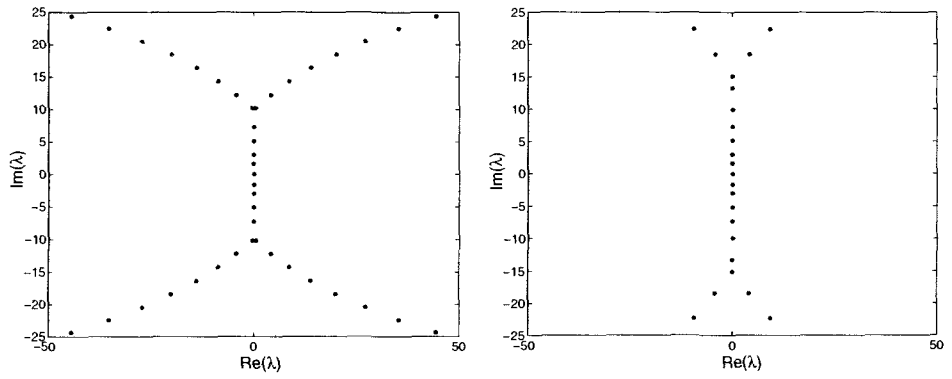

Figure 5.4: Spectrum of the truncated difference eigenvalue problem (5.5.2) for $\epsilon = 0.3$: $N = 128$ (left) and $N = 1024$ (right).

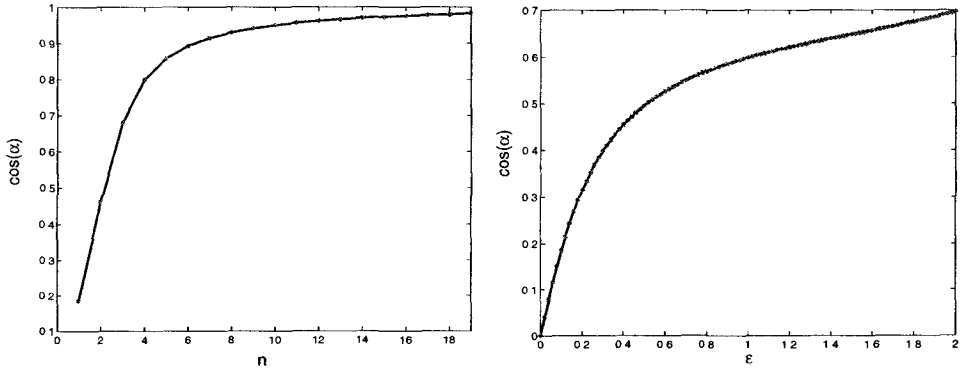

Figure 5.5: Left: the values of $\cos(\widehat{f_n, f_{n+1}})$ for the first 20 purely imaginary eigenvalues for $\epsilon = 0.1$. Right: the values of $\cos(\widehat{f_1, f_2})$ versus ϵ.

eigenvectors	$\epsilon = 0.1$	$\epsilon = 0.3$	$\epsilon = 0.5$
1-2	0.120166	0.325116	0.431987
2-3	0.461330	0.716192	0.780641
3-4	0.680709	0.838889	0.878055
4-5	0.799235	0.890440	0.914622
5-6	0.858944	0.921498	0.940306
6-7	0.892869	0.940395	0.955239
7-8	0.914745	0.953124	0.965235
8-9	0.930023	0.962120	0.972204
9-10	0.941262	0.968732	0.977265
10-11	0.949843	0.973741	0.981057
11-12	0.956580	0.977629	0.983988
12-13	0.961987	0.980702	0.986072
13-14	0.966407	0.983297	0.989617
14-15	0.970073	0.983459	0.990547
15-16	0.973153	0.995335	0.999101
16-17	0.975764	0.998749	0.999601

Table 2: Numerical values of $\cos(\widehat{f_n, f_{n+1}})$ for the first 16 purely imaginary eigenvalues for three values of ϵ.

The angle between two subsequent eigenvectors is closely related to the condition number [108]

$$\text{cond}(\lambda_n) = \frac{\|f_n\|\|f_n^*\|}{|(f_n, f_n^*)|}. \tag{5.5.5}$$

By Lemma 5.2.4(iii), the condition number is infinite for multiple eigenvalues since $(f_n, f_n^*) = 0$. From the point of numerical accuracy, the larger is the condition number, the poorer is the structural stability of the numerically obtained eigenvalues to the truncation and round-off errors.

Figure 5.6 shows the condition number (5.5.5) computed for the first 40 purely imaginary eigenvalues for $\epsilon = 0.001$ and $\epsilon = 0.002$. We can see that the condition number grows for larger eigenvalues which indicate their structural instability. Indeed, starting with some number n, all eigenvalues are no longer purely imaginary, according to the numerical approximations on *Figure 5.4*. The condition numbers become extremely large with larger values of ϵ.

We finally illustrate that all true eigenvalues of the spectral problem (5.1.3) are purely imaginary and simple. To do so, we construct numerically the sign-definite imaginary type function and obtain the interlacing property of eigenvalues of the spectral problem (5.1.3) for two values $\epsilon = \epsilon_0$ and $\epsilon = \epsilon_1$, where $|\epsilon_1 - \epsilon_0|$ is small. We say that the eigenvalues exhibit the interlacing property if there exists an eigenvalue for $\epsilon = \epsilon_1$ between each pair of eigenvalues for $\epsilon = \epsilon_0$ and vice verse.

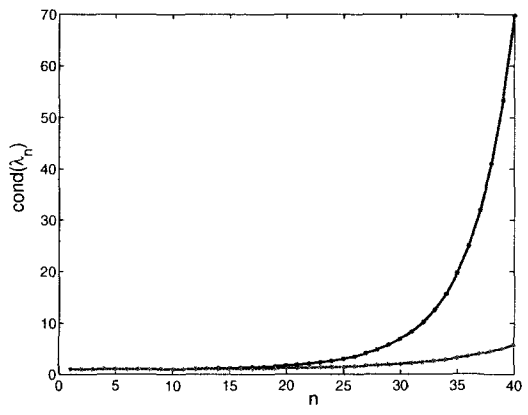

Figure 5.6: The condition number for the first 40 purely imaginary eigenvalues for $\epsilon = 0.001$ (red) and $\epsilon = 0.002$ (blue).

A meromorphic function $G(\lambda)$ is called a sign-definite imaginary type function if $\mathrm{Im}G(\lambda) \leq 0$ ($\mathrm{Im}G(\lambda) \geq 0$) on $\mathrm{Im}(\lambda) \leq 0$ ($\mathrm{Im}(\lambda) \geq 0$) [6]. We construct the meromorphic function $G(\omega)$ in the form $G(\lambda) = \frac{F_{\epsilon_0}(\lambda)}{F_{\epsilon_1}(\lambda)}$, where $F_\epsilon(\lambda)$ is an analytical function of Corollary 5.3.2. The numerical approximation of the meromorphic function $G(\lambda)$ is given by $\widehat{G}(\lambda) = \frac{\widehat{F}_{\epsilon_0}(\lambda)}{\widehat{F}_{\epsilon_1}(\lambda)}$. According to Theorems II.2.1 - II.3.1 on p. 437-439 in [6], the function $\widehat{G}(\lambda)$ is a meromorphic function of sign-definite imaginary type if and only if it has the form $\widehat{G}(\lambda) = \frac{P(\lambda)}{Q(\lambda)}$ where $P(\lambda)$ and $Q(\lambda)$ are polynomials with real coefficients, with real and simple zeros, which are interlacing.

Table 3 shows this interlacing property of eigenvalues for $\epsilon_0 = 0.48$ and $\epsilon_1 = 0.5$. The remainder term $R_\epsilon = \frac{\|Lf - \lambda f\|}{\|\lambda f\|}$ measures the numerical error of computations. We have also computed numerically the values of $\widehat{G}(\lambda)$ on the grid $0.1 < \mathrm{Im}\lambda < 100$ and $0.1 < \mathrm{Re}\lambda < 100$ with step size 0.1 in both directions (not shown). Based on the numerical data, we have confirmed that the function $\widehat{G}(\lambda)$ does indeed belongs to the class of sign-definite imaginary type functions while the eigenvalues $\{\lambda_n\}_{n\in\mathbb{Z}}$ exhibit the interlacing property. This computation gives a numerical verification that all eigenvalues of the spectral problem (5.1.3) are simple and purely imaginary.

$\mathrm{Im}\lambda_{\epsilon_0}$	R_{ϵ_0}	$\mathrm{Im}\lambda_{\epsilon_1}$	R_{ϵ_1}
1.063112	$2.3244e-10$	1.068314	$2.4073e-10$
2.970880	$2.1967e-10$	3.024428	$2.2531e-10$
5.414789	$2.2024e-10$	5.542829	$2.2683e-10$
8.471510	$2.0904e-10$	8.693066	$2.1572e-10$
12.312548	$2.0079e-10$	12.665485	$2.0601e-10$
16.816692	$1.9765e-10$	17.327038	$2.0288e-10$
22.014084	$1.9617e-10$	22.711070	$2.0197e-10$
27.899896	$1.9527e-10$	28.812177	$2.0157e-10$
34.474785	$1.9501e-10$	35.631088	$2.0190e-10$
41.738699	$1.9558e-10$	43.167733	$2.0313e-10$
49.691673	$1.9671e-10$	51.422281	$2.0476e-10$
58.333258	$1.9796e-10$	60.391382	$2.0623e-10$
67.665387	$1.9904e-10$	70.140636	$2.0725e-10$
77.957871	$1.9989e-10$	79.828287	$2.0782e-10$
89.484519	$2.6566e-10$	91.544035	$2.0821e-10$

Table 3: The interlacing property of the first 15 purely imaginary eigenvalues for $\epsilon = 0.48$ and $\epsilon = 0.5$.

CHAPTER 6

SUMMARY OF RESULTS AND OPEN QUESTIONS

The four main new results of my doctoral research are represented as separate chapters of the thesis.

The first result is a proof that spectral stability problems for Hamiltonian systems with semi-bounded energy can be reformulated in terms of self-adjoint operators acting on a space with indefinite metric. This allows deriving the criteria for stability and instability of solitons in terms of sign-definite invariant subspaces using Pontryagin space (Π_κ) decomposition method. Three major spectral theorems resulted from this approach : the number of unstable and potentially unstable eigenvalues equals the number of negative eigenvalues of the self-adjoint operator in Π_κ, the total number of isolated eigenvalues is bounded from above by the total number of isolated eigenvalues of the self-adjoint operator in Π_κ, the subspace that related to the absolute continuous spectrum is positive sign-definite. This decomposition method is used to determine the stability of solitary waves in various classes of nonlinear PDEs: the NLS, Klein - Gordon and KdV equations.

One of the interesting open questions is an extension of the Pontryagin subspace theorems to operators acting on exponentially weighted spaces. This is relevant for stability problems of multi-pulse solitary wave solutions in the 5-th order KdV equation. Potential applications for this research are magneto-acoustic waves in plasma and capillary-gravity water waves. It is also an open question how to apply indefinite metric space approach to spectral analysis of the quadratic pencils of the differential operators. This is relevant for the spectral stability problems associated with the linearized sine Gordon equation.

The second result is numerical calculations of two-pulse solutions for the fifth-order KdV equation. Two-pulse solutions are bound states of two solitary waves which travel together as a single coherent structure with a fixed peak-to-peak separation. We applied a new numerical method which is a modification of the Petviashvili method of successive iterations for numerical approximations of pulses. The successive iterations of the original Petviashvili method do not converge for two-pulse solutions. The iterative sequence with two pulses leads either to a single pulse or to a spurious solution with two pulses located at an arbitrary distance. This numerical problem arises due to the presence of small and negative eigenvalues of the linearized energy operator. We found that this nearly singular quasi-translational eigenmode does not create any serious problems for our numerical algorithm. Modification and a proof of the convergence of iterations in a neighborhood of two-pulse solutions are based on the Lyapunov–Schmidt reduction. It

is also shown that the embedded eigenvalues of negative Krein signature are structurally stable in a linearized KdV equation. Combined with stability analysis in Pontryagin spaces, this result completes the proof of spectral stability of the corresponding two-pulse solutions.

Although one-dimensional models are very useful for conceptual purposes the real world is not made that way. An open question is: can this method or its modification be applied in two or three dimensions ? Another question is to see if this algorithm can be used the $N-$pulse solutions with $N > 2$.

The third result is a construction of the canonical transformation of the linearized coupled-mode system to the block anti–diagonal form, when the spectral problem reduces to two coupled two-by-two Dirac systems. This block-diagonalization is used in numerical computations of eigenvalues that determine stability of gap solitons. This transformation is significant for numerical approximations of eigenvalues of the linearized Hamiltonian systems, because the block-diagonalized matrix can be stored in a special compressed format which requires twice less memory than a full matrix. Spectral analysis of Dirac systems can be done in terms of self-adjoint operators acting on Krein space (which is a generalization of Pontryagin space with index $\kappa = \infty$). Potential applications for this research are optical solitons in fibres and photonic crystals which provide an efficient (reliable and fast) means of long-distance communication.

The last new result is a proof that the operator L associated with the heat equation (5.1.1) admits a closure in $L^2_{\rm per}([-\pi,\pi])$ with a domain in $H^1_{\rm per}([-\pi,\pi])$ for $|\epsilon| < 2$. The spectrum of L consists of eigenvalues of finite multiplicities. Using the analytic function theory and the Fourier series, we have approximated eigenvalues numerically and showed that all eigenvalues of the spectral problem (5.1.3) are purely imaginary. Furthermore, we have proved with the assistance of numerical computations that the set of eigenfunctions of the spectral problem (5.1.3) is complete but does not form a basis in the Hilbert space $L^2_{\rm per}([-\pi,\pi])$.

We think that there is a relation between these properties of the linear operator L and ill-posedness of the Cauchy problem for the periodic heat equation (5.1.1). According to the Hille–Yosida Theorem (see Section IX.7 in [125]), if L is a linear operator with a dense domain in a Banach space X and the resolvent operator $(I - \lambda^{-1}L)^{-1}$ exists for any $\mathrm{Re}\lambda > 0$, then L is the infinitesimal generator of a strongly continuous semigroup if and only if

$$\|(I - \lambda^{-1}L)^{-1}\|_{X\mapsto X} \leq C, \tag{6.0.1}$$

for some $C > 0$ uniformly in $\mathrm{Re}\lambda > 0$. Moreover, if $C \leq 1$, then the semi-group is a contraction. When the conditions of the Hille–Yosida Theorem are satisfied, the Cauchy problem associated with the operator L is well-posed, whereas it is ill-posed if these conditions are not met.

According to the numerical results on pseudo-spectra in [11] and [119], the level

set of the resolvent norm

$$R(\lambda) = \|(\lambda I - L)^{-1}\|_{L^2_{\rm per}([-\pi,\pi])\mapsto L^2_{\rm per}([-\pi,\pi])}$$

extends to the right half-plane, such that $R(\lambda)$ does not decay along the level set curves with $\mathrm{Re}\lambda > 0$. This numerical fact serves as an indication that the conditions of the Hille–Yosida Theorem are not satisfied and the Cauchy problem for the heat equation is ill-posed. Furthermore, our work in progress is to prove that the ill-posedness of the periodic heat equation (5.1.1) follows from the fact that the set of eigenfunctions of the operator L does not form a basis in the Hilbert space $X = L^2_{\rm per}([-\pi,\pi])$.

Although the series of eigenfunctions of operator L can not be used to solve the Cauchy problem for the periodic heat equation, conditional convergence of the series of eigenfunctions can sometimes be achieved at least for finite times, as illustrated in [12]. Therefore, more detailed studies of applicability of the series of eigenfunctions and its dependence from the initial data h_0 are opened for further work.

Bibliography

[1] M.J. Ablowitz, D.J. Kaup, A.C. Newell and H. Segur, "The inverse scattering transform - Fourier analysis for nonlinear problems" Stud. Appl. Math. **53**, 249–336 (1974).

[2] M.J. Ablowitz and H. Segur, "Solitons and Inverse Scattering Transform" SIAM, Philadelphia (1981).

[3] D. Agueev and D. Pelinovsky, "Modeling of wave resonances in low-contrast photonic crystals", SIAM J. Appl. Math. **65**, 1101–1129 (2005).

[4] N.I. Akhiezer and I.M. Glazman, "Theory of Linear Operators in Hilbert Space", Frederic Ungar Publishing Co, New York, (1963).

[5] C.J. Amick and J.F. Toland, "Global uniqueness of homoclinic orbits for a class of 4th order equations", Z. Angew. Math. Phys. **43**, 591–597 (1992).

[6] F.V. Atkinson, "Discrete and Continuous Boundary Problems", Academic Press, London, (1964).

[7] T. Azizov and M. Chugunova, "Pontryagin's Theorem and analysis of spectral stability of solitons", preprint (2007).

[8] T. Azizov and I.S. Iohvidov, "Elements of the theory of linear operators in spaces with indefinite metric", Moscow, Nauka, (1986).

[9] I.V. Barashenkov, D.E. Pelinovsky, and E.V. Zemlyanaya, "Vibrations and oscillatory instabilities of gap solitons", Phys. Rev. Lett. **80**, 5117–5120 (1998)

[10] I.V. Barashenkov and E.V. Zemlyanaya, "Oscillatory instabilities of gap solitons: a numerical study", Comp. Phys. Comm. **126**, 22–27 (2000)

[11] E.S. Benilov, S.B.G. O'Brien, and I.A. Sazonov, "A new type of instability: explosive disturbances in a liquid fild inside a rotating horizontal cylinder", J. Fluid Mech. **497**, 201–224 (2003)

[12] E.S. Benilov, "Explosive instability in a linear system with neutrally stable eigenmodes. Part 2. Multi-dimensional disturbances", J. Fluid Mech. **501**, 105–124 (2004)

[13] J.L. Bona, P.E. Souganidis, and W.A. Strauss, "Stability and instability of solitary waves of Korteweg–de Vries type", Proc. Roy. Soc. Lond. A **411**, 395–412 (1987).

[14] J. P. Boyd, "Solitons from sine waves: analytical and numerical methods for non-integrable solitary and cnoidal waves", Physica D., **21**, 227–246 (1986).

[15] J. P. Boyd, "Numerical computations of a nearly singular nonlinear equation: weakly nonlocal bound states of solitons for the fifth-order Korteweg–de Vries equation", J. Comp. Phys., **124**, 55–70 (1996).

[16] T.J. Bridges and G. Derks, "Linear instability of solitary wave solutions of the Kawahara equation and its generalizations", SIAM J. Math. Anal. **33** 1356–1378 (2002).

[17] T.J. Bridges, G. Derks, and G. Gottwald, "Stability and instability of solitary waves of the fifth-order KdV equation: a numerical framework", Physica D **172** 190–216 (2002).

[18] B. Buffoni, "Infinitely many large amplitude homoclinic orbits for a class of autonomous Hamiltonian systems", J. Diff. Eqs. **121**, 109–120 (1995).

[19] B. Buffoni and E. Sere, "A global condition for quasi-random behaviour in a class of conservative systems", Commun. Pure Appl. Math. **49**, 285–305 (1996).

[20] A.V. Buryak and A.R. Champneys, "On the stability of solitary wave solutions of the fifth-order KdV equation", Phys. Lett. A **233**, 58–62 (1997).

[21] V.S. Buslaev and G.S. Perelman, "Scattering for the nonlinear Schrödinger equation: states close to a soliton", St. Peterburg Math. J. **4**, 1111-1142 (1993).

[22] C. Canuto, M. Hussaini , A. Quarteroni, and T.A. Zang "Spectral Methods in Fluid Dynamics", Springer-Verlag, Berlin, Germany (1988).

[23] T. Cazenave, L. Vazquez, "Existence of localized solutions for a classical nonlinear Dirac field", Comm. Math. Phys. **105:1** 35-47 (1986).

[24] A.R. Champneys, "Homoclinic orbits in reversible systems and their applications in mechanics, fluids and optics", Physica D **112**, 158–186 (1998)

[25] A.R. Champneys and M.D. Groves, "A global investigation of solitary-wave solutions to a two-parameter model for water waves", J. Fluid Mech. **342**, 199–229 (1997).

[26] A.R. Champneys and A. Spence, "Hunting for homoclinic orbits in reversible systems: a shooting technique", Adv. Comp. Math. **1**, 81–108 (1993)

[27] P.J. Channel and C. Scovel, "Symplectic integration of Hamiltonian systems", Nonlinearity **3**, 231–259 (1990)

[28] F. Chardard, F. Dias and T. J. Bridges, "Fast computation of the Maslov index for hyperbolic linear systems with periodic coefficients", J. Phys. A., **39**, 14545–14557 (2006).

[29] M. Chugunova and D. Pelinovsky, "Count of eigenvalues in the generalized eigenvalue problem", preprint (2006)

[30] Cluser Idra is a part of the SHARCnet network of parallel processors distributed between eight universities in Southern Ontario, including McMaster University.

[31] E.A. Coddington and N. Levinson, "Theory of ordinary differential equations", McGraw–Hill, New York, (1955).

[32] A. Comech, S. Cuccagna, and D. Pelinovsky, "Nonlinear instability of a critical traveling wave in the generalized Korteweg - de Vries equation", SIMA **39:1**, 1–33 (2007).

[33] A. Comech and D. Pelinovsky, "Purely nonlinear instability of standing waves with minimal energy", Comm. Pure Appl. Math. **56**, 1565–1607 (2003).

[34] E. Cornell and C. Wieman, "Bose–Einstein condensation in a dilute gas, the first 70 years and some recent experiments", Rev. Mod. Phys. **74**, 875–893 (2002).

[35] W. Craig, M. Groves, "Hamiltonian long-wave scaling limits of the water-wave problem ", Wave Motion **19**, 367–389 (1994).

[36] S. Cuccagna, "On asymptotic stability of ground states of nonlinear Schrödinger equations", Rev. Math. Phys. **15**, 877–903 (2003).

[37] S.Cuccagna, D. Pelinovsky, and V. Vougalter, Spectra of positive and negative energies in the linearized NLS problem, Comm. Pure Appl. Math. **58**, 1-29 (2005).

[38] E.B. Davies, "Spectral Theory and Differential Operators", Cambridge University Press, (1995).

[39] E.B. Davies, "An indefinite convection–diffusion operator", preprint (February, 2007).

[40] L. Demanet and W. Schlag, "Numerical verification of a gap condition for a linearized NLS equation", Nonlinearity **19**, 829-852 (2006).

[41] G. Derks and G.A. Gottwald, "A robust numerical method to study oscillatory instability of gap solitary waves", SIAM J. Appl. Dyn. Syst. **4**, 140–158 (2005).

[42] F. Dias and E.A. Kuznetsov, "Nonlinear stability of solitons in the fifth-order KdV equation", Phys. Lett. A **263**, 98–104 (1999).

[43] N. Dunford and J.T. Schwartz, "Linear Operators. Part II: Spectral Theory", John Wiley & Sons, New York, (1963).

[44] B. Fornberg, "A Practical Guide to Pseudo Spectral Methods", Cambridge University Press , New York, NY (1996).

[45] D. Funaro, "Polynomial Approximation of Differential Equations", Springer-Verlag, Berlin, Germany (1992).

[46] V. Hernandez, J.E. Roman and V. Vidal, "A Scalable and Flexible Toolkit for the Solution of Eigenvalue Problems " Vol. **31**, ACM Transactions on Mathematical Software, (2005).

[47] B.L.G. Jonsson, J. Fröhlich, S. Gustafson, and I.M. Sigal, "Long time dynamics of NLS solitary waves in a confining potential", Ann. Henri Poincare **23**, 621–660 (2006).

[48] G. James, "Centre manifold reduction for quasilinear discrete systems", J. Nonlin. Sci. **13**, 27–63 (2003).

[49] F.P. Gantmacher and M.G. Krein, "Oscillation matrices and kernels and small vibrations of mechanical systems", AMS Chelsea Publishing, AMS, Providence, (2002).

[50] I.M. Gelfand, "Lectures on linear algebra", Dover Publications, New York, (1961).

[51] I.M. Glazman, "Direct Methods of Qualitative Spectral Analysis of Singular Differential Operators", Israel Program for Scientific Translations Ltd., (1965).

[52] I. Gohberg, S. Goldberg, M.A. Kaashoek, "Classes of Linear Operators", Vol. **1** Birkhauser Verlag, Basel, (1990).

[53] I. Gohberg and M.G. Krein, "Introduction to the Theory of Linear Non-selfadjoint Operators", Vol. **18**, AMS Translations, Providence, (1969).

[54] G.H. Golub, H.A. Van der Vorst,"Eigenvalue computation in the 20th century", J. of Comp. and Appl. Math, **123**, 35–65 (2000)

[55] M. Golubitsky and D.G. Schaeffer, "Singularities and Groups in Bifurcation Theory", vol. 1, Springer-Verlag, New York, (1985).

[56] K.A. Gorshkov and L.A. Ostrovsky, "Interactions of solitons in nonintegrable systems: Direct perturbation method and applications", Physica D **3**, 428-438 (1981)

[57] K.A. Gorshkov, L.A. Ostrovsky, and V.V. Papko, "Hamiltonian and non-Hamiltonian models for water waves", Lecture Notes in Physics **195**, Springer, Berlin, 273–290 (1984).

[58] D. Gottlieb, N.Y. Hussaini, and S.A. Orszag, "Theory and applications of spectral methods", Springer-Verlag, Berlin, Germany (1984).

[59] M. Grillakis, J. Shatah, W. Strauss, "Stability theory of solitary waves in the presence of symmetry. I", J. Funct. Anal. **74**, 160–197 (1987).

[60] M. Grillakis, J. Shatah, W. Strauss, "Stability theory of solitary waves in the presence of symmetry. II", J. Funct. Anal. **94**, 308–348 (1990).

[61] M. Grillakis, "Linearized instability for nonlinear Schrödinger and Klein–Gordon equations", Comm. Pure Appl. Math. **41**, 747–774 (1988).

[62] M. Grillakis, "Analysis of the linearization around a critical point of an infinite dimensional Hamiltonian system", Comm. Pure Appl. Math. **43**, 299–333 (1990).

[63] M.D. Groves, "Solitary-wave solutions to a class of fifth-order model equations", Nonlinearity **11**, 341–353 (1998).

[64] K.F. Gurski, R. Kollar, and R.L. Pego, "Slow damping of internal waves in a stably stratified fluid", Proc. R. Soc. Lond. **460**, 977–994 (2004).

[65] J. Hunter and J. Scheurle, "Existence of perturbed solitary wave solutions to a model equation for water waves", Physica D **32**, 253–268 (1988).

[66] A.T. Illichev and A.Y. Semenov, "Stability of solitary waves in dispersive media described by a fifth-order evolution equation", Theor. Comp. Fluid Dyn. **3**, 307–326 (1992).

[67] I.S. Iohvidov, M.G. Krein, and H. Langer, "Introduction to the spectral theory of operators in spaces with an indefinite metric", Mathematische Forschung, Berlin, (1982).

[68] S. Kichenassamy, "Existence of solitary waves for water-wave models", Nonlinearity **10**, 1 (1997).

[69] Yu. S. Kivshar and G.P. Agrawal, "Optical Solitons: ¿From Fibers to Photonic Crystals", Academic Press, San Diego, (2003).

[70] T. Kapitula, P. Kevrekidis, and B. Sandstede, "Counting eigenvalues via the Krein signature in infinite-dimensional Hamiltonian systems", Physica D **195**, **3-4**, 263–282 (2004); Addendum: Physica D **201**, 199–201 (2005).

[71] T. Kapitula and P.G. Kevrekidis, "Linear stability of perturbed Hamiltonian systems: theory and a case example", J. Phys. A: Math. Gen. **37**, 7509-7526 (2004).

[72] T. Kapitula and P.G. Kevrekidis, "Three is a crowd: Solitary waves in photorefractive media with three potential wells", SIAM J. Appl. Dyn. Sys. **5:4** 598–633 (2006).

[73] T. Kapitula and B. Sandstede, "Edge bifurcations for near integrable systems via Evans function techniques", SIAM J. Math. Anal. **33**, 1117–1143 (2002)

[74] T. Kapitula and B. Sandstede, "Eigenvalues and resonances using the Evans function", Discr. Cont. Dyn. Syst. **B 10**, 857–869 (2004).

[75] T. Kato: *Perturbation theory for linear operators*, Springer-Verlag (1976)

[76] D.J. Kaup and T.I. Lakoba, "The squared eigenfunctions of the massive Thirring model in laboratory coordinates", J. Math. Phys. **37**, 308–323 (1996)

[77] D.J. Kaup and T.I. Lakoba, "Variational method: How it can generate false instabilities", J. Math. Phys. **37**, 3442–3462 (1996)

[78] D.J. Kaup and A.C. Newell, "On the Coleman correspondence and the solution of the Massive Thirring model", Lett. Nuovo Cimento **20**, 325–331 (1977).

[79] Y. Kodama and D. Pelinovsky, Spectral stability and time evolution of N solitons in KdV hierarchy, J. Phys. A: Math. Gen. **38**, 6129–6140 (2005)

[80] J. Krieger and W. Schlag, "Stable manifolds for all monic supercristical NLS in one dimension", J. of the Amer. Math. Soc. **19:4**, 815–920 (2006).

[81] S. Lafortune and J. Lega, "Spectral stability of local deformations of an elastic rod: Hamiltonian formalism", SIAM J. Math. Anal. **36**, 1726–1741 (2005).

[82] M. Lavrentjev and L. Saveljev, "Linear Operators and Ill-Posed Problems", Consultants Bureau, New York, (1995).

[83] P.D. Lax, "Integrals of nonlinear equations of evolution and solitary waves", Comm. Pure. Appl. Math., **21**, 467–490 (1968).

[84] S.P. Levandovsky, "A stability analysis for fifth-order water-wave models", Physica D **125**, 222–240 (1999).

[85] X.B. Lin, "Using Melnikov's method to solve Silnikov's problems", Proc. Roy. Soc. Edinburgh **116A**, 295–325 (1990).

[86] R.S. MacKay, "Stability of equilibria of Hamiltonian systems", in *"Hamiltonian Dynamical Systems"* (R.S. MacKay and J. Meiss, eds.) Adam Hilger, 137–153 (1987).

[87] J.T. Marti, "Introduction to the Theory of Bases", Springer-Verlag, New York, (1969).

[88] K. McLeod, "Uniqueness of positive radial solutions of $\Delta u + f(u) = 0$ in R^n", Trans. Amer. Math. Soc. **339**, 495–505 (1993).

[89] P.A Milewski and J.-M. Vanden-Broeck, "Time dependent gravity-capillary flows past an obstacle", Wave Motion **29**, 63–79 (1999).

[90] L.F. Mollenauer, R.H. Stolen, J.P. Gordon, Phys.Rev.Lett **45** 1095–1098 (1980).

[91] S.P. Novikov, S.V. Manakov, L.P. Pitaevskii and V.E. Zakharov, "Theory of solitons. The inverse scattering method," Plenum, New York (1984).

[92] B.E. Oldeman, A.R. Champneys, and B. Krauskopf, "Homoclinic branch switching: a numerical implementation of Lin's method", Internat. J. Bifur. Chaos Appl. Sci. Engrg. **13**, 2977–2999 (2003).

[93] J.A. Pava, "On the instability of solitary wave solutions for fifth-order water wave models", Electr. J. Diff. Eqs. **2003**, 6, 1–18 (2003).

[94] R.L. Pego and H.A. Warchall, "Spectrally stable encapsulated vortices for nonlinear Schrödinger equations", J. Nonlinear Sci. **12**, 347–394 (2002).

[95] R.L. Pego and M.I. Weinstein, "Eigenvalues, and instabilities of solitary waves", Philos. Trans. Roy. Soc. London A **340**, 47–94 (1992).

[96] R.L. Pego and M.I. Weinstein, "Asymptotic stability of solitary waves", Comm. Math. Phys. **164**, 305–349 (1994).

[97] D.E. Pelinovsky, "Inertia law for spectral stability of solitary waves in coupled nonlinear Schrödinger equations", Proc. Roy. Soc. Lond. A, **461** 783–812 (2005).

[98] D.E. Pelinovsky, P.G. Kevrekidis, and D.J. Frantzeskakis, "Stability of discrete solitons in nonlinear Schrödinger lattices", Physica D **212**, 1–19 (2005).

[99] D.E. Pelinovsky, P.G. Kevrekidis, and D.J. Frantzeskakis, "Persistence and stability of discrete vortices in nonlinear Schrödinger lattices", Physica D **212**, 20–53 (2005).

[100] D.E. Pelinovsky and A. Scheel, "Spectral analysis of stationary light transmission in nonlinear photonic structures", J. Nonlin. Science, **13**, 347-396 (2003).

[101] D.E. Pelinovsky and Yu.A. Stepanyants, "Convergence of Petviashvili's iteration method for numerical approximation of stationary solutions of nonlinear wave equations", SIAM J. Numer. Anal. **42**, 1110–1127 (2004).

[102] D.E. Pelinovsky, A.A. Sukhorukov, and Yu. S. Kivshar, "Bifurcations and stability of gap solitons in periodic potentials", Phys. Rev. E 70 036618 (2004).

[103] D.E. Pelinovsky and J. Yang, Instabilities of multihump vector solitons in coupled nonlinear Schrodinger equations, Stud. Appl. Math. **115**, 109–137 (2005).

[104] G. Perelman, "On the formation of singularities in solutions of the critical nonlinear Schrödinger equation", An. Henri Poincare **2**, 605–673 (2001).

[105] G. Perelman, "Asymptotic stability of multi-soliton solutions for nonlinear Schrdinger equations", Comm. Partial Differential Equations **29**, 1051–1095 (2004).

[106] L.S. Pontryagin, "Hermitian operators in spaces with indefinite metric", Izv. Akad. Nauk SSSR Ser. Mat. **8**, 243–280 (1944).

[107] I. Rodnianski, W. Schlag, and A. Soffer, "Dispersive analysis of charge transfer models", Comm. Pure Appl. Math. **58**, 149–216 (2005).

[108] Y. Saad, "Numerical methods for large eigenvalue problems", Manchester University Press, 60–101 (1992).

[109] Y. Saad "Chebyshev techniques for solving nonsymmetric eigenvalue problem", Mathematics of Computation **42**, 567–588 (1984).

[110] B. Sandstede, "Stability of multiple-pulse solutions", Trans. Am. Math. Soc. **350**, 429–472 (1998).

[111] B. Sandstede and A. Scheel, "Absolute and convective instabilities of waves on unbounded and large bounded domains", Physica D **145**, 233–277 (2000).

[112] W. Schlag, "Stable manifolds for an orbitally unstable NLS", J. of the Amer. Math. Soc. **19:4**, 815–920 (2006).

[113] G. Schneider and H. Uecker, "Existence and stability of modulating pulse solutions in Maxwell's equations describing nonlinear optics", Z. Angew. Math. Phys. **54**, 677–712 (2003).

[114] J. Schollmann, "On the stability of gap solitons", Physica A **288**, 218–224 (2000).

[115] J. Schollmann and A. P. Mayer, "Stability analysis for extended models of gap solitary waves", Phys. Rev. E **61**, 5830–5838 (2000).

[116] P.E. Souganidis and W.A. Strauss, "Instability of a class of dispersive solitary waves", Proc. Roy. Soc. Edin. A **114**, 195–212 (1990).

[117] C.M. de Sterke, D.G. Salinas, and J.E. Sipe, "Coupled-mode theory for light propagation through deep nonlinear gratings", Phys. Rev. E **54**, 1969–1989 (1996).

[118] C.M. de Sterke and J.E. Sipe, "Gap solitons", Progress in Optics, **33**, 203 (1994).

[119] L.N. Trefethen, "Spectral Methods in Matlab", SIAM, Philadelphia, (2000).

[120] L.N. Trefethen and M. Embree, "Spectra and Pseudospectra. The Behavior of Nonnormal Matrices and Operators", Princeton University Press, Princeton, NJ, (2005).

[121] J.A.C. Weidman, B.M. Herst, "Split-step methods for the solution of the NLS equation", SIAM. J. Numer.Anal, **23**, 485 – 507 (1986).

[122] M.I. Weinstein, "Existence and dynamic stability of solitary wave solutions of equations arising in long wave propagation", Comm. PDEs **12**, 1133–1173 (1987).

[123] J. D. Wright and A. Scheel, "Solitary waves and their linear stability in weakly coupled KdV equations", ZAMP, preprint, (2007).

[124] A.C. Yew, B. Sandstede, and C.K.R.T. Jones, "Instability of multiple pulses in coupled nonlinear Schrdinger equations", Phys. Rev. E **61**, 5886–5892 (2000).

[125] K. Yosida, "Functional Analysis", Springer–Verlag, New York, (1968).

[126] N.J. Zabusky, M.D. Kruskal, "Interaction of solitons in a collisionless plasma and recurrence of initial states", Phys.Rev.Lett., **15**, 240–243 (1965).

[127] V. Zakharov, A.B. Shabat, "Interaction between solitons in a stable medium", Soviet Phys, JETR **34**, 62–69 (1972).

[128] J.A. Zufiria, "Symmetry breaking in periodic and solitary gravity–capillary waves on water of finite depth", J. Fluid Mech. **184**, 183–206 (1987).